HOST-MEDIATED RESPONSES TO MALARIA INFECTION AND THEIR IMPACT ON PREGNANCY OUTCOME

by

ALICER K. ANDREW

(Under the Direction of JULIE M. MOORE)

ABSTRACT

Plasmodium falciparum malaria impacts 100,000+ pregnancies annually, leading to pregnancy loss, preterm delivery, and infant low birth weight attributed to placental malaria (PM). PM is initiated by parasitized erythrocyte binding, precipitating pathogenesis via dysregulated maternal inflammatory and coagulation responses. In Chapter 2, I hypothesized that these pathogenic processes are interconnected and that reducing one pathway will alleviate the other, improving pregnancy outcomes. My approach tests this hypothesis genetically and therapeutically using a mouse model that simulates human PM. Previous work showed that ablation of the inflammatory mediator, tumor necrosis factor (TNF), improves pregnancy outcomes in the mouse model; my work with infected TNF null mutant ($TNF^{-/-}$) mice corroborates that finding. Transcript analysis of infected $TNF^{-/-}$ mouse embryos reveals reduced expression of a critical molecular link between coagulation and inflammation, protease-activated receptor 2 (*F2rl1*). Simultaneously, endothelial protein C receptor (*Procr*) transcripts are elevated, suggesting suppressed coagulation. Prior studies in tissue factor deficient and anticoagulant treated infected wild-type mice showed improved pregnancy outcomes; my

studies indicate that anticoagulant treatment may operate by targeting related pathways, since embryonic transcripts for *Ifng, Tnf, Il10, Il1b,* and *Ccl2* are significantly downregulated. Plasma cytokine concentration corroborated the transcript data; IFNγ and IL-10 were significantly decreased by anticoagulant treatment. Antioxidant transcripts such as *Nfe2l2* (*Nrf2*), *Sod1*, and *Sod3* are also considerably reduced, and *Procr* transcript expression mirrored results obtained in $TNF^{-/-}$ studies. In Chapter 3, I hypothesized that therapeutic targeting of malaria-induced oxidative stress would improve pregnancy outcomes. Deferoxamine treatment, directed at heme/iron-induced oxidative stress, reduced parasitemia and successfully improved pregnancy outcomes. Other treatments directed toward lipid peroxides that promote the cell death modality, ferroptosis, and mitochondrial oxidative stress, were unsuccessful at improving pregnancy outcomes. Finally, Chapter 4 presents recently published work describing a novel murine model of malaria-induced preterm delivery. The research presented in this dissertation advances our understanding of the relationships between two pathogenic responses to PM and describes the limitations of antioxidant therapy in improving pregnancy outcomes in a murine model. These data hold clues that may inform future investigations of therapeutic interventions that can circumvent adverse pregnancy outcomes due to malaria infection.

INDEX WORDS: Placental malaria; inflammation-coagulation cycle; anticoagulant treatment; oxidative stress; antioxidant treatment; *Plasmodium chabaudi chabaudi* AS; mouse models of placental malaria

HOST-MEDIATED RESPONSES TO MALARIA INFECTION AND THEIR IMPACT ON PREGNANCY OUTCOME

by

ALICER K. ANDREW

BS, University of Georgia, 2015

A Dissertation Submitted to the Graduate Faculty of The University of Georgia in Partial Fulfillment of the Requirements for the Degree

DOCTOR OF PHILOSOPHY

ATHENS, GEORGIA

2022

HOST-MEDIATED RESPONSES TO MALARIA INFECTION AND THEIR IMPACT ON PREGNANCY OUTCOMES

by

ALICER K. ANDREW

Major Professor:	Julie M. Moore
Committee:	David S. Peterson
	Maria B. Cassera
	Balázs Rada
	Shelley Hooks

Electronic Version Approved:

Ron Walcott
Vice Provost for Graduate Education and Dean of the Graduate School
The University of Georgia
August 2022

DEDICATION

I dedicate this work to my parents, who have sacrificed so much for my academic and personal success. Martina Alie and Augustus Mansfield James. I love you; rest in peace. Dr. Vernie Andrew and Philmore Andrew. I love you. Thank you for everything.

ACKNOWLEDGEMENTS

This work would not be possible if it were not for the guidance, training, resources, advice, and emotional/professional support I received over the past six years. First, I want to thank my research advisor and mentor, Dr. Julie Moore, and all current and previous members of Dr. Moore's research team, including Dr. Demba Sarr, Dr. Catherine Morffy Smith, Dr. Simon Owino, Dr. Marta Reguera Gomez, Caitlin Cooper, Taylor Gonzalvo, and Brittany Russ – thank you all for sharing your expertise and helping with my training and completion of experiments. Thank you to the Department of Infectious Diseases at UGA and its Graduate Coordinator, Dr. David Peterson, for supporting me as an off-campus student. Likewise, thank you to the Department of Infectious Diseases and Immunology at UF for embracing me as a visiting student. Thank you to my Ph.D. advisory committee, who provided valuable feedback as my research projects evolved. Special thanks to the scholars of GRADS (Graduate Research Assistants Diversifying STEM) at UGA and BGSO (Black Graduate Student Organization) at UF, who were instrumental in my professional development and provided the social connections I needed to survive graduate school. To my talented and loyal friends, Dr. Krishna Latha, Dr. Kimberly Oliva, and Nicole-Lisa Williams – you made graduate school bearable; thank you! To my mom, Dr. Vernie Andrew, and my sister, Dr. Cyrielle Andrew, who inspire me to persevere through life's challenges – thank you, and I love you! Finally, I want to thank my family and friends in Antigua and across the globe for your prayers, support, and well-wishes. I hope I have made you proud.

TABLE OF CONTENTS

Page

LIST OF TABLES

Page

LIST OF FIGURES

Page

CHAPTER 1

INTRODUCTION & LITERATURE REVIEW

Introduction

Malaria is a global parasitic disease caused by several human-infective Plasmodial species, with *Plasmodium falciparum* causing the most severe disease. Young children, immunocompromised individuals, and pregnant women are especially prone to severe organ-specific manifestations of *P. falciparum* infection, such as cerebral and placental malaria (PM). PM is characterized by parasitized red blood cell adherence in the placenta, which triggers robust maternal inflammatory responses, immune cell infiltration, massive fibrin deposition and dysregulated hemostasis, and hemozoin accumulation in the placenta. These characteristics are associated with poor maternal-fetal health outcomes, including maternal anemia, preterm delivery, infant low birth weight, and pregnancy loss. Despite a growing body of research on severe malaria pathogenesis and antimalarial drug development, malaria remains a leading cause of morbidity and mortality worldwide, especially in susceptible populations. Thus, efforts to continue advancing our knowledge of how maternal responses meant to protect against PM can exacerbate disease and be detrimental to maternal-fetal health are imperative. By identifying more host-directed therapeutic strategies that shift the maternal inflammatory and coagulation responses from pathogenic to protective, we will be better equipped to

protect women and children from the poor consequences of PM and circumvent the emerging challenge of parasite resistance antimalarial drugs.

Rodent models of malaria have been instrumental to our current understanding of PM, but more work is required to address the remaining gaps in knowledge. Thus, continued work with these models is essential to make progress on identifying new modalities to combat the severe consequences of malaria infection during pregnancy. To recapitulate the pathogenic features of PM-induced pregnancy loss, which include enhanced maternal inflammatory and hypercoagulative states, Dr. Julie Moore's research group has developed a mouse model of malaria infection during pregnancy using the murine-infective Plasmodial species, *Plasmodium chaubaudi chaubaudi* AS (*Pcc*AS) and the standard laboratory C57BL/6J (B6) mouse. This model has advanced our understanding of how maternal inflammation and coagulation contribute to pregnancy compromise and provided evidence that targeting oxidative stress responses in the placenta may represent a therapeutic approach to preventing PM-associated poor pregnancy outcomes. Thus, my research seeks to define the crosstalk between inflammation, coagulation, and oxidative stress responses within this murine model of PM. The following specific aims outline my approach to achieving this goal.

Specific Aims

AIM 1: Describe the connections between tumor necrosis factor-driven inflammation, coagulation, and placental oxidative stress. In this research, the activity of the major pro-inflammatory cytokine, tumor necrosis factor (TNF), was used as a proxy for malaria-induced maternal inflammation. In mouse and human studies, malaria-

induced TNF production has consistently been associated with poor pregnancy outcomes [1–7]. Malaria-associated hemostatic dysfunction has also been well-documented in cases of severe disease [8–11]. Given the well-characterized relationship between inflammation and coagulation (the inflammation-coagulation cycle) in other disease systems [8,12–15], my work sought to investigate the relationship between TNF-driven inflammation and tissue factor (TF) mediated coagulation during maternal malaria infection. Using a murine model, my goal was to elucidate the extent to which the relationship between inflammation and coagulation drives pregnancy outcomes. *My first hypothesis for this aim is that TNF-driven inflammation influences coagulation in a manner that worsens pregnancy outcomes.* Additional studies of the pathophysiology of pregnancy loss in mice and humans with PM have highlighted the potential for oxidative stress as a driver of poor pregnancy outcomes [16–19]. Recently published data from Dr. Moore's laboratory identifies placental oxidative stress as a therapeutic target for PM [18]; thus, *my second hypothesis is that placental oxidative stress contributes to adverse pregnancy outcomes in PM due to dysregulated inflammation and coagulation.*

AIM 2: Investigate the role of maternal tissue factor in promoting inflammation and malaria-induced pregnancy loss. In this work, elevated TF expression was used as the first indicator of malaria-induced activation of the coagulation process. Given TF's central role in the inflammation-coagulation cycle [14,20,21], disruption of malaria-induced TF expression might impact TNF-driven inflammatory responses in PM. Recent work from Dr. Moore's group has demonstrated that TF is a potent driver of midgestational pregnancy loss; however, TF's impact on inflammatory responses in this

model has not been characterized. I sought to address this gap in knowledge by investigating the hypothesis that *reducing TF expression in malaria-infected pregnant animals will reduce the expression of inflammatory mediators and be associated with improved pregnancy outcomes*.

Literature Review

Despite concerted efforts to reduce the global malaria burden, the World Health Organization estimates that 241 million cases of malaria occurred in 2020, resulting in approximately 627,000 deaths [22]. Malaria is a parasitic disease caused by five human-infectious Plasmodial species: *Plasmodium falciparum, P. vivax, P. ovale*, *P. malariae*, and *P. knowlesi*, which until recently was thought to only infect long-tailed and pig-tailed macaques [23,24]. Historically, *P. falciparum* was considered the most dangerous human malaria parasite; however, *P. vivax* is becoming increasingly more recognized as a significant contributor to malaria morbidity in endemic regions [25].

Malaria infection is broadly categorized into two states, uncomplicated and complicated or severe malaria, reflecting the wide variety of symptoms associated with the disease. Uncomplicated malaria is commonly described as intermittent febrile illness accompanied by "flu-like" symptoms such as chills, sweats, body aches, nausea, and vomiting. According to the Centers for Disease Control and Prevention (CDC), uncomplicated malarial episodes can be further categorized into three stages that last about 6-10 hours. Stage one is called the cold stage, where the infected individual experiences bouts of cold sweats and shivers. The second stage is the hot stage, characterized by fever, headaches, and vomiting. The final stage is the sweating stage,

where body temperature returns to normal. For infections with *P. falciparum*, *P. vivax,* and *P. ovale*, these symptoms are repeated every two days, every three days for *P. malariae*, and every 24 hours for *P. knowlesi* infection. Complicated malaria is mainly associated with *P. falciparum* infection. It is linked to the development of organ-specific syndromes attributed to the sequestration of parasitized red blood cells within the vasculature of various organs [26]. Specifically, pregnant women experience a manifestation of complicated disease known as placental malaria due to the adherence of mature parasite forms within the placenta [27].

Plasmodium life cycle

Malaria parasites are transmitted to humans through the bite of female *Anopheles* sp. mosquitos. As an infected mosquito takes a blood meal, it injects parasitic forms known as sporozoites into the skin, where they enter the bloodstream and migrate to the liver to invade hepatocytes and begin the exo-erythrocytic stage of the life cycle [28]. The exo-erythrocytic stage is associated with asymptomatic infection and persists for about 7-16 days. At this stage, parasites undergo asexual replication before inducing the destruction of hepatocytes to facilitate the release of thousands of merozoites into the bloodstream. Once in the blood, merozoites begin the erythrocytic cycle by infecting red blood cells (RBCs). They undergo asexual transformation from the ring stage to trophozoite and then mature into schizonts. As the parasite undergoes these morphological changes, it metabolizes hemoglobin and produces an insoluble crystalline byproduct known as hemozoin (Hz). Once schizogony is obtained, new daughter merozoites burst out of the RBC, leading to the direct destruction of the host cell and

giving rise to the clinical symptoms of the disease. The erythrocytic stage lasts approximately 48 hours in *P. falciparum* infection, corresponding directly with the two-day recurrence of clinical symptoms in patients [29]. Upon egress, a maximum of roughly 36 merozoites per RBC [30] are released into the blood, where the majority continue the erythrocytic cycle by infecting fresh RBCs, while a subset differentiates into the parasite's sexual forms known as gametocytes. Immature male and female gametocytes sequester in the bone marrow [31], where they undergo maturation for approximately ten days before re-entering the peripheral circulation to await transmission to a mosquito. When a mosquito consumes a blood meal, ingested gametocytes undergo sexual development in the mosquito's midgut and eventually develop into sporozoites that migrate to the mosquitos' salivary glands and await subsequent transmission to a human host [28,29]. This sexual stage development within the mosquito can take up to three weeks and depends on the temperature of the mosquito's environment [32].

Placental malaria

Of the Plasmodial species known to reliably infect humans, *P. falciparum* is notorious for causing the most severe clinical symptoms, especially in sub-Saharan Africa, where it is widely abundant. The likelihood of severe manifestations of *P. falciparum* malaria is often dictated by transmission stability in endemic regions, prior immune exposure of the infected individual, and the availability of effective antimalarials. Immunocompromised individuals are especially prone to severe malaria, including children under age five, infants, HIV/AIDS patients, and pregnant women [33]. Generally, immunocompetent individuals living in regions of stable malaria transmission

develop partial immunity to severe disease over time [34]. However, primigravid women exposed to malaria are at an exceptionally high risk of developing the organ-specific disease syndrome known as placental malaria (PM) [33,34]. PM is characterized by the sequestration of infected red blood cells (iRBCs) in the intervillous space (IVS) of the placenta [35] and adherence to the syncytiotrophoblast [36], which is the terminally differentiated multi-nucleated epithelial cell that lines the IVS and regulates gas and nutrient exchange between the mother and developing fetus. Massive maternal inflammatory cell infiltration associated with robust proinflammatory cytokine release into the placenta is another common characteristic of PM [37,38]. These maternal responses are associated with increased syncytial knotting and fibrin deposition, basal membrane thickening, and placental insufficiency, which causes intrauterine growth restriction (IUGR) [33,38]. PM is also characterized by hemozoin (Hz) deposition in fibrin and accumulation in maternal immune cells in the placenta [38,39]. The clinical consequences of PM include poor maternal-fetal health outcomes through severe maternal anemia, pregnancy loss, preterm delivery, and infant low birth weight, which is associated with IUGR and neonatal mortality [33].

The characteristic cytoadherence of iRBCs to the syncytiotrophoblast in PM is mediated by a low sulfated glycosaminoglycan receptor abundantly expressed on the placenta, known as chondroitin sulfate A (CSA) [40–42]. CSA acts as a receptor for the parasite-derived ligand expressed by iRBCs known as VAR2CSA. VAR2CSA belongs to the *P. falciparum* erythrocyte membrane protein (*Pf*EMP1) family of high molecular weight proteins encoded by a diverse group of approximately 60 *var* genes [43]. Specifically, VAR2CSA is expressed on electron-dense protrusions termed “knobs” that

are abundant on the iRBC surface during the trophozoite and schizont stages [43]. In areas of high malaria transmission, pregnant women are three times more likely to experience complicated malaria and mortality due to infection than their non-pregnant counterparts [44]. This elevated susceptibility is particularly evident in first-time mothers, whose immune systems lack prior exposure to VAR2CSA expressing parasites, which cannot establish infection in non-pregnant hosts [45,46]. Over successive pregnancies, women with high antenatal exposure to malaria develop antibodies specific for VAR2CSA variants. These antibodies are associated with a reduced risk of developing PM, more asymptomatic infections, and better control of parasite burden [34,45–48].

Antigenic diversity VAR2CSA has been identified as an essential immune escape mechanism and mediator of poor pregnancy outcomes, even in multigravida women [49]. Due to VAR2CSA's high binding affinity for placental CSA [40], VAR2CSA-expressing parasites are exclusively isolated from pregnant women, avoiding clearance by the spleen and sequestering within the placenta, facilitating chronic infection [49]. In contrast, parasites isolated from non-pregnant individuals have a high affinity for other host-derived molecules that aid in their evasion of splenic clearance. One such molecule is CD36, which is abundantly expressed on the vascular endothelium of many tissues and is associated with uncomplicated malaria [50]. Intracellular adhesion molecule 1 (ICAM-1) and hyaluronic acid are two other targets for iRBC adherence in non-pregnant individuals [51,52]. Intriguingly, women living in areas of unstable malaria transmission are equally susceptible to PM development and its adverse outcomes regardless of gravidity [46,53].

Current interventions for placental malaria

Although the WHO reports a significant decrease in global malaria incidence over the past decade, more than 33 million women live at risk of malaria infection during pregnancy [22]. Malaria elimination programs have been established since the mid-1950s; however, successful eradication has only been achieved in some countries, leaving sub-Saharan Africa and southeast Asia with the highest malaria burdens. In fact, approximately 96% of malaria cases reported worldwide in 2021 occurred in the WHO African Region [22]. Several challenges have stalled the progress of malaria eradication, including drug and insecticide resistance, asymptomatic infections and their contribution to continual parasite transmission, poverty and conflict in endemic regions, unpredictable funding, and disruptions due to the COVID-19 pandemic [22,54]. However, malaria infection in pregnant women represents a unique challenge to disease eradication, as pregnant women experience higher parasite burdens and more asymptomatic infections in general, making them a reservoir for parasite transmission [55,56]. Additionally, mosquitos are reportedly more attracted to pregnant women than to their non-pregnant counterparts [57,58].

The WHO has established healthcare guidelines for protecting pregnant women from the adverse consequences of infection. Among the most widely used interventions is the administration of intermittent preventative treatment using antimalarial drugs sulfadoxine and pyrimethamine (IPTp-SP). IPTp-SP is a prophylactic treatment that reduces maternal and fetal anemia, spikes in maternal parasitemia episodes, the birth of LBW infants, and lowers the risk of neonatal mortality [59]. It is recommended for pregnant women living in high to moderate malaria transmission areas during routine

antenatal care visits. According to WHO guidelines, pregnant women should begin receiving IPTp-SP treatment early in their second trimester and receive at least three doses throughout their pregnancy. IPTp-SP has had a protective effect on maternal-fetal health outcomes during infection; however, suboptimal treatment coverage has limited the reach of this intervention, with only 32% of eligible women receiving three doses of the treatment in 2020 [22].

Another essential tool to protect pregnant women in malaria-endemic regions is the insecticide-treated bed net (ITN). ITNs have been important for malaria control efforts because of their cost-effective and relatively long-lasting (up to three years) insecticidal effect in high-transmission areas. However, despite these positive attributes, recent studies suggest that ITNs may be losing efficacy due to changes in mosquito behaviors and emerging mosquito resistance to the main insecticidal compound used in ITNs known as pyrethroids [60–62]. Alternatively, some publications emphasize increasing the use and durability of bednets instead of their insecticidal efficacy as a strategy that will establish long-term prevention of malaria transmission [63,64]. Another study argues that mosquito resistance to insecticides is not related to increased malaria incidence when bednets are consistently and appropriately used [65].

Widespread multi-drug resistance and decreased sensitivity of *P. falciparum* to frontline antimalarials have been reported worldwide [22,66]. Growing parasite resistance to sulfadoxine-pyrimethamine also raises concerns about the future effectiveness of IPTp-SP treatment [67–70]. Additionally, insecticide resistance is a growing primary concern in malaria-endemic regions, as mosquito resistance to many insecticides has already been reported [62,71,72]. This pattern of resistance is particularly

concerning as cases of mosquito migration from endemic to nonendemic regions have been reported [73,74].

The lack of an effective malaria vaccine approved for use in pregnant women undermines global malaria control and eradication efforts. Although two vaccine candidates for pregnant women have demonstrated promising safety and immunogenic profiles, they did not elicit cross-reactivity against a wide range of VAR2CSA variants [75–77]. Unsuccessful vaccine design attempts can be partly attributed to the antigenic diversity of the gene that encodes VAR2CSA across different parasite isolates. This feature facilitates immune evasion of the parasite and makes it challenging to develop a vaccine that induces broadly protective immunity prior to infection during pregnancy.

More broadly, antigenic variation of the surface proteins expressed by iRBCs poses a similar challenge for vaccine design in other vulnerable groups. Of the approximately 60 available *var* genes in the parasite's genome, only one gene is actively translated into protein during the intraerythrocytic cycle, and it is this variant that is eventually expressed on the iRBC surface [43,78]. Due to epigenetic modifications [79–81], the activity of a variety of genetic elements [82,83], and other signals that remain unknown [84], daughter merozoites, upon re-invasion of a new RBC, can express a *var* gene that is antigenically distinct from the *var* gene previously expressed in their parent parasite [43,79]. Thus, studies that identify reliable ways to circumvent the parasite's immune escape strategies will improve vaccine design efforts and may boost the longevity of the recently approved malaria vaccine, RTS,S (Mosquirix), which is currently intended for use in children only.

Mouse models of malaria during pregnancy

For decades, murine models of PM have been used as an inexpensive, convenient, genetically-tractable, and informative tool to draw parallels between pathogenesis and poor pregnancy outcomes associated with human disease. Given the ethical and logistical limitations of studying malaria infection in pregnant women, murine models provide the added benefit of having shorter gestational periods, comparable placental function and structure [85], and shared pathology and pregnancy outcomes to humans malaria [86]. *Plasmodium berghei* and *P. chabaudi* are murine-infective Plasmodial species commonly used to study pregnant and nonpregnant animals with various immune statuses. Although there is no perfect mouse model of human malaria, different combinations of mouse strains with different parasite isolates recapitulate various aspects of human disease and can give useful insights into how *P. falciparum* malaria causes disease and pregnancy demise [87].

P. berghei is a lethal malaria parasite because infection in pregnant and non-pregnant mice is fatal without antimalarial drug treatment [86,87]. Additionally, infection studies done in naive pregnant mice must be initiated at mid-late gestation (embryonic day (E) 10.5 through 13.5) to avoid maternal mortality[1]. Neres et al. characterized many similarities between mouse and human PM through the use of BALB/c mice infected with 10^6 *P. berghei* ANKA (*Pb*A)-iRBCs intravenously between E11-13 [88]. The course of infection in these mice typically mimics complications consistent with human malaria infection during pregnancy, including IUGR, the birth of LBW pups, and postnatal

[1] Published nomenclature to describe gestational age in murine models of PM vary between gestational day (GD) and embryonic day (E). All gestational time points in this document will be referred to with E for consistency.

growth impairment. Additionally, mononuclear cell infiltration of placental tissues and accumulation of iRBCs in the intervillous space are also commonly shared characteristics between humans and *P. berghei*-induced malaria [88]. In these studies, gestational age was determined through the detection of a vaginal plug in females mated with males overnight. Day zero of gestation and successful pregnancy were confirmed 10 and 13 days post-plug, based on steady weight gain. Within this model, pregnancy status severely exacerbated the course of infection, with infected pregnant (IP) mice experiencing more significant parasite burdens, reduced maternal survival, placental dysfunction and inflammation, and signs of intrauterine growth restriction and fetal loss relative to uninfected pregnant (UP) controls. Placentas from IP mice shared common characteristics with placentas from infected humans, including the accumulation of iRBCs and Hz, basal membrane thickening, fibrinoid necrosis, and inflammatory cell infiltration of the tissue [88]. Additionally, ex-vivo adhesion assays provided evidence that *Pb*A-infected RBCs can bind to CSA in mouse placentas, consistent with the VAR2CSA binding phenotype of *P. falciparum*. Thus, *Pb*A adhesion through CSA may be involved in the placental pathology and iRBC accumulation described in IP mouse placentas [88,89]. However, a major drawback of this model includes the high dosage of iRBCs that must be delivered to produce the abovementioned phenotypes. A 10^6 dosage could make it more likely that the host's defensive response to infection has insufficient time to develop, potentially making it more difficult to discern between natural and artificial host-parasite interactions, which may be generalizable across murine Plasmodium species [90]. An additional drawback to this model is the mode of infection. Natural malaria infection is initiated with sporozoites delivered through a mosquito bite

that proceed to the exo-erythrocytic cycle before RBC invasion; however, these critical stages of the lifecycle are bypassed entirely when iRBCs are introduced directly into the bloodstream.

Alternatively, Van Zon et al. and several others have studied *P. berghei* infection during pregnancy after pre-exposure to the same parasite, by immunizing mice prior to mating [91,92]. They infected virgin mice and subsequently treated them with immunosuppressive drugs to circumvent the guaranteed fatality associated with *P. berghei* infections. This approach provided a model for malaria infection in women who had been previously exposed to malaria before pregnancy, a feature that is common amongst women living in regions of stable malaria transmission. They found that non-pregnant mice with preexisting immunity to *P. berghei* experienced partial immunity to reinfection, with no clinical symptoms and low-level parasitemia observed. On the other hand, when these mice were mated, a considerable proportion developed pregnancy-associated recrudescence, which they attributed to pregnancy-related depression of the immune system. Intriguingly, other studies demonstrated that the severity of the clinical symptoms associated with pregnancy-induced recrudescence was parity dependent and directly correlated with the level of circulating pregnancy-specific IgG antibodies that recognized variant surface proteins selectively expressed on iRBCs [93,94]. Moreover, pregnancy-specific antibodies accumulated over subsequent pregnancies and protected mice from poor birth outcomes. Although this model is attractive for its incorporation of preexisting immunity to malaria prior to pregnancy, one major drawback is that it only considers outcomes associated with recrudescence from a primary infection but not the outcomes related to re-infection in early or late gestation. Another drawback to this

model is that mice were only exposed to the parasite once before pregnancy, which does not reflect the frequency of malaria exposure that women in highly endemic regions experience prior to their first pregnancies.

An example of how different host-parasite combinations can recreate very specific aspects of human disease in mouse models was published by Rodrigues-Duarte et al., who performed experiments in mid-late gestation using *P. berghei* isolates ANKAΔpm4, NK65, and K173 in C57BL/6 mice [89]. Each strain induced pathological features relevant to human PM, such as elevated parasite burden in pregnant versus non-pregnant hosts, basal membrane thickening, fibrinoid necrosis, thrombosis in the placenta, and overall placental disorganization. ANKAΔpm4 was associated with a robust innate immune response through elevated gene expression of key inflammatory mediators such as tumor necrosis factor (TNF), monocyte chemoattractant protein 1 (MCP-1), or CCL2, and macrophage inflammatory protein 1-α (MIP1-α) also known as CCL3. K173 parasites displayed increased growth kinetics but induced fewer inflammatory responses in the placenta. NK65 showed growth kinetics similar to ANKAΔpm4 and had a less reactive inflammatory response like K173, but resulted in the most severe pregnancy outcomes, including LBW pups, dysfunctional placenta, and a higher incidence of fetal loss. These differences in disease characteristics during pregnancy based on parasite isolates used in the mouse model allow researchers to focus on specific aspects of PM pathogenesis and their impact on pregnancy outcomes. One drawback to this model is that a high parasite inocula must be used to produce these distinct phenotypes.

As stated before, *Plasmodium chabaudi* is also commonly used in mice to study malaria-induced pregnancy outcomes [95]. An important feature of *P. chabaudi* is that

infection in rodents using this strain recapitulates several characteristics of *P. falciparum* infection in semi-immune individuals. *P. chabaudi*, like *P. falciparum*, preferentially infects erythrocytes [96], while *P. berghei* infects reticulocytes similar to *P. vivax* [97,98]. Additionally, *P. chabaudi* causes non-lethal infection in wildtype C57BL/6 mice [99], similar to what is observed in *P. falciparum* infection. Using two isolates of *P. chabaudi* known as *P. chabaudi chabaudi* CB (*Pcc*CB) and *P. chabaudi chabaudi* AS (*Pcc*AS), Sharma et al. developed a mouse model of heterologous reinfection and recrudescence in malaria-experienced dams [100]. The authors demonstrated that *Pcc*CB, the more virulent of the two isolates, causes severe anemia and recrudescent infection in C57BL/6 mice. For recrudescence studies, the authors infected mice intravenously with 2000 *Pcc*CB sporozoites and then mated them 35 days post-infection. They found that pregnant mice experienced parasite recrudescence by E14 but did not suffer adverse pregnancy outcomes or succumb to infection. Additionally, their offspring did not experience obvious birth defects or altered susceptibility to malaria infection. Alternatively, heterologous infection (HI) initiated with *Pcc*AS infection followed by *Pcc*CB infection during midgestation produces a robust pro-inflammatory response and severe pregnancy outcomes, including impaired pup post-natal growth and altered susceptibility to malaria. For these HI studies, the authors reported that mice infected intravenously with 2000 *Pcc*AS sporozoites, mated 35 days post-infection, and then inoculated with 10^5 *Pcc*CB iRBCs on E10 could be categorized into two distinct groups based on parasite density throughout the course of infection. Mice that experienced high parasite burdens (HI^{high}) had an average parasitemia of about 18% and experienced negative pregnancy outcomes, such as stillbirth and neonatal death. HI^{high} dams also

experienced elevated inflammatory cytokine levels of TNF, MCP-1, interleukin 12 (IL-12), and interleukin 10 (IL-10), characteristics not observed in mice that experienced low-density parasite burden after re-infection (HI^{low}). The majority of HI^{high} dams did not produce viable offspring, however of those that did successfully deliver, their offspring had persistently lower birth weights and increased susceptibility to malaria infection compared to offspring delivered by HI^{low} dams. Interestingly, the authors found that pups born to HI dams, regardless of parasite density, had significantly lower parasite burdens and did not experience spontaneous recrudescent infection 25-30 days post infection compared to pups born from malaria-naïve dams. Overall, the authors have characterized a rodent model of malaria infection that involves immune exposure to different parasite isolates and attempts to recapitulate the experience of women living in endemic regions, who have multiple malaria episodes in their lifetime and experience parasite recrudescence and reinfection during midgestation. One drawback of this model is that while it attempts to mimic natural infection by injecting sporozoites during the primary infection, the secondary infection must be done using iRBCs to induce the HI phenotype, which does not reflect how humans are naturally re-infected.

The abovementioned rodent models of malaria infection during pregnancy were conducted in mid-late gestation. To study the impact of malaria infection on pregnancy outcomes in early gestation, a novel mouse model was developed in the laboratory of Julie M. Moore [5,101,102]. In this model, C57BL/6J mice are intravenously injected with 10^3 *Pcc*AS-infected RBCs on E0.5, defined as the day a vaginal plug is observed following mating. To avoid stress-induced implantation failure, mice are rested until E6.5, when daily weight, hematocrit, and parasitemia measurements are obtained. Similar

to previously mentioned models, infected pregnant (IP) mice experienced higher parasitemia and anemia than infected non-pregnant (INP) controls and universally lost their pregnancies between E10.5-12.5. Mice sacrificed on E10.5 often have open cervices with active expulsion of embryos, and by E12.5, no viable embryos are found [101]. The course of infection in IP mice is characterized by peak peripheral parasitemia (approximately 22%) by E10.5-11.5 and low hematocrits indicative of maternal anemia at the same timepoint. INP mice experienced less accelerated disease kinetics, with a lower peak parasitemia (approximately 19%) observed at E11.5 and slower development of anemia. By E16.5, IP and INP mice resolved the infection with less than 2% parasitemia and no significant difference in survival between groups. Body weight measurements were used to determine the pregnancy progression and severity of morbidity in all groups of mice. The authors observed that both IP and UP mice gained weight steadily during the initial stages of pregnancy; however, only IP mice began to lose weight as parasitemia developed, indicative of malaria-induced morbidity and fetal resorption. When IP mice are compared to UP controls, pregnancy loss is significantly higher, with 100% dead embryos at E12.5 in IP dams compared to approximately 3% embryo loss in UP dams at the same timepoint. In mice undergoing abortion, placental parasitemia was more than 40% higher than in the peripheral parasitemia at E10.5 and E11.5 and significant accumulation of iRBCs in the maternal sinusoids was observed. Some drawbacks of this model are that it does not produce significant inflammatory cell infiltrate into the intervillous space of the placenta and it is not known if the iRBC accumulation observed is mediated by CSA binding. Moreover, infection is initiated in the blood stage, which bypasses the exoerythrocytic stage of the life cycle, which can

potentially impact host-parasite interactions. Finally, infection in this model is iniaited in virgin mice with no preexisting immunity to malaria infection during pregnancy. This characteristic of the model only simulates infection in a small subset of individuals (those who live in regions of low or unstable malaria transmission). However, this is the first model that allows for the study of malaria infection in early gestation and is not accompanied by maternal death as seen with *P. berghei* infection. Therefore, this model attempts to mimic human malaria infection during pregnancy, where immunologically naïve primigravid mothers experience malaria-induced adverse pregnancy outcomes early in gestation that are associated with severe maternal morbidity but not with maternal death.

Inflammation in PM pathogenesis

For decades, the exact mechanisms involved in PM pathogenesis have been intensely studied but remain incompletely understood. So far, scientists have learned that a balance is required between protective malaria-induced inflammation and an exaggerated inflammatory response associated with intervillositis, the birth of LBW infants, and preterm labor [37,103,104]. While healthy placentae display a bias towards type 2 cytokine expression [105], including IL-10, 4, 6, and 13, several type 1 proinflammatory cytokines such as TNF, IL-2, and interferon-gamma (IFNγ) are elevated systemically in mothers suffering from spontaneous pregnancy loss and pre-eclampsia [106,107]. In malaria-infected women who develop severe malaria, elevated type 1 proinflammatory cytokines such as TNF, IFNγ, and IL-1β in the peripheral blood are associated with placental pathology and poor birth outcomes [2,104]. At the placental

level in both mice and humans, upregulation of cytokines and chemokines secreted by infiltrating maternal immune cells include TNF, IFN-γ, MCP-1, MIP-1α, and soluble CD163, a marker for monocyte and macrophage activation [10,108–110]. This characteristic infiltration of mononuclear cells into the intervillous space of infected placentae is also associated with the secretion of soluble TNF receptors [111,112] and increased RNA expression of inflammation-associated genes. The most notable are chemokine genes for CCL-1, MCP-1, MIP-1α, and CXCL8 [108,113]. However, it is important to note that there is some disagreement about which cytokines and chemokines are significantly elevated in infected pregnant women in the field [4,108,114,115] and which can reliably predict poor pregnancy outcomes [2,4,109,116], which may be attributable to differences in data collection and analysis methods, sample sizes, and intrinsic differences between study populations (i.e., genetic background, malaria endemicity, etc.).

Additionally, infection with human immunodeficiency virus (HIV), a common virus in malaria-endemic regions, can impact the cytokine/chemokine responses during malaria infections. Intervillous blood mononuclear cells (IVBMC) from women with active PM and HIV infection demonstrated enhanced TNF and IFN-γ expression upon stimulation with hemozoin *in vitro* [117]. However, in the absence of HIV infection, IVBMCs secrete significantly less TNF and IFN-γ, even in the presence of substantial hemozoin, contributing to the body of evidence that co-infection with these two diseases increases the risk of severe malaria disease, which may be driven by exaggerated proinflammatory responses in pregnant women.

Serum levels of IL-10, a major anti-inflammatory type 2 cytokine, are reportedly elevated in many cases of malaria infection during pregnancy [10,109,114,116,118,119]. Low levels of IL-10 have been attributed to severe disease in humans [120,121], and in rodent models, IL-10 is sufficient to reduce clinical signs of severe malaria and maintain proper Th1/Th2 balance during infection [122,123]. Treatment of IL-10 deficient mice with antibodies to neutralize TNF function further confirmed the role of IL-10 in counteracting the negative impact of excessive proinflammatory cytokine levels in malaria-induced pathology [123]. However, in some rodent models, plasma levels of IL-10 do not seem to protect mice from malaria-induced pregnancy loss [102].

To better understand the role of inflammation in malaria pathogenesis, researchers have drawn parallels between malaria and other inflammatory diseases such as sepsis [124–126]. Sepsis, characterized as an excessive immune response to an infection, shares several systemic inflammatory mediators with malaria, including TNF, IL-1, INF-γ, IL-10, and others [126]. Additionally, there is evidence that thrombocytopenia, coagulopathy, and increased expression of endothelial adhesion molecules such as ICAM-1 (intracellular adhesion molecule 1) and VCAM-1 (vascular cell adhesion protein 1) are shared between malaria and sepsis [126], supporting the potential that both diseases develop through similar mechanisms. Research on sepsis in the late 1980s identified TNF as an essential mediator of severe disease [127,128], and anti-TNF antibody treatment in animal models of sepsis showed improved clinical outcomes [129,130]. Given those preclinical results, attempts were made to neutralize TNF activity in patients experiencing septic shock, and subsequently, anti-TNF treatment was also given to malaria patients. For septic shock patients, treatment exacerbated the disease

[131], suggesting TNF activity is required for proper immune control of these diseases and plays a multifaceted role in both protection and pathology. On the other hand, one study reported reduced fever after anti-TNF treatment in patients with cerebral malaria [132], perhaps supporting the therapeutic potential of TNF-directed therapy during severe malaria. TNF has also been shown to induce the activity of other inflammatory chemokines such as MIP-1α, the first chemokine associated with malaria infection and is elevated in malaria-infected placentas [126], and IFN-γ, which also plays a dual role in protection and pathology during malaria infection [133].

Further studies on TNF and its pathogenic role in the development of preeclampsia in pregnant women provides clues for its potential function in PM pathogenesis. Preeclampsia is a pregnancy complication characterized by high blood pressure and proteinuria and impacts approximately 8% of pregnancies worldwide [134]. Birth outcomes of preeclampsia are similar to PM and include preterm birth, placental insufficiency, and fetal growth restriction [135]. Levels of TNF have been reported to be elevated in preeclamptic compared to normative pregnancies and have been linked to perinatal morbidity and mortality [136]. Additionally, TNF has been named one of the major proinflammatory cytokines responsible for endothelial cell activation and dysfunction, a predominant characteristic of preeclampsia [137] and severe malaria pathogenesis [137,138]. Other aspects of preeclampsia, such as reduced placental perfusion and oxidative stress, are associated with PM [135].

Coagulation in PM pathogenesis

The role of coagulopathy in malaria pathogenesis is incompletely understood [9]. Some human studies seeking to understand the role of coagulation in disease outcomes report minimal evidence of disseminated intravascular coagulation (DIC), characterized as an inappropriate and hyper blood clotting response in most *P. falciparum*-infected patients [139,140]. Moreover, many studies in both malaria and sepsis argue that some level of activated coagulation plays a significant role in disease pathogenesis, even if DIC is not detected [141,142]. On the other hand, many studies have demonstrated that indeed activation of the coagulation cascade is implicated in severe malaria disease [10,143–145]. Tissue factor (TF), the potent mediator of the extrinsic coagulation pathway [146], has also been implicated in driving coagulopathy in malaria [147].

Coagulation, also known as blood clotting, is a biological process of repairing endothelial injury due to mechanical or inflammatory damage [148]. This process is divided into two pathways, the intrinsic and extrinsic pathways. The intrinsic pathway, also known as the "contact activation" pathway, is initiated through the interaction of a negatively charged surface, such as those found on collagen or activated platelets, with a clotting factor in the blood called Factor XII (FXII), leading to its activation. Upon activation, FXII catalyzes the sequential proteolytic cleavage of Factor XI (FXI), Factor IX (FXI), Factor XIII (FXIII), and Factor X (FX), which represents the point at which the intrinsic and extrinsic pathways converge. On the other hand, the extrinsic pathway is initiated upon endothelial injury when subendothelial TF is exposed to the blood and its clotting factors. When TF comes into contact with the blood, it immediately forms a complex with Factor VII (FVII), converting it to its active form, FVIIa. Together, the

FVIIa-TF complex cleaves FX, generating its active form FXa, which then interacts with Factor V (FV) to convert it to its active form, FVa. FVa then catalyzes the conversion of prothrombin to thrombin, which catalyzes the conversion of fibrinogen to fibrin. Fibrin molecules are the building blocks of a blood clot, and they become stabilized and crosslinked through the activity of activated factor XIII (FXIIIa), whose activity is also catalyzed by thrombin [148].

Under normal hemostatic conditions, inactive forms of the abovementioned clotting factors are circulating in the blood, allowing the coagulation cascade to progress rapidly upon activation through positive feedback amplification. This rapid response prevents excessive bleeding and facilitates proper wound healing. This process is tightly regulated by several anti-coagulant mechanisms that provide negative feedback at various points in the coagulation cascade [149,150]. For instance, thrombin binds to a nearby cell surface receptor known as thrombomodulin upon activation. The thrombin-thrombomodulin complex inhibits thrombin's ability to interact with FV and then activates a potent anti-coagulant molecule known as protein C. Activated protein C (APC) then interacts with the endothelial protein C receptors (EPCRs), which are highly expressed on blood vessels and within the placenta [151]. APC is generated on the endothelial cell surface via the activation of protein C by the thrombin-thrombomodulin complex; APC bound to EPCR cleaves and inactivates coagulation factors Va and VIIa, diminishing thrombin generation. The EPCR has been implicated as a contributor to malaria disease severity by acting as a receptor for *Pf*EMP-mediated iRBC adhesion to the endothelium [152,153]. This receptor-mediated sequestration directly contributes to the development of severe malaria by disrupting proper anti-coagulant and cytoprotective

functions of APC and describes a link between dysregulated hemostasis and malaria pathogenesis [152].

Another naturally occurring class of anticoagulant molecules is known as heparins, which are produced by mast cells that have migrated to the injury site [154]. They are known to activate another anti-coagulant molecule known as antithrombin III, which is responsible for binding to thrombin and inhibiting its activity [154]. Heparins can be purified from various animals, including bovine and porcine sources, and used to treat thrombotic disorders and other diseases characterized by hypercoagulation. One such example is low molecular weight heparin (LMWH), which is used to inhibit FXa and thrombin activity. LMWH has a relatively long half-life, high bioavailability, and is safe to use in pregnancy, although its use can have side effects such as heparin-induced thrombocytopenia [155,156]. The tissue factor pathway inhibitor (TFPI) is another anti-coagulant molecule that acts on FVIIa to prevent the TF-FVIIa complex from catalyzing the cleavage of FX to FXa [157].

In malaria, fibrin accumulation in the placenta is a universal histopathological feature [27,38]. Work produced by Avery et al. further revealed evidence of active coagulation and impaired fibrinolysis in the placentas of women with PM through the assessment of other coagulation-related biomarkers, including fibrin [10]. For instance, PM-positive women showed signs of elevated D-dimers and fibrin, markers of active coagulation, and elevated plasminogen activator inhibitor 1 (PAI-1), an indicator of fibrinolysis suppression. They also observed that PM-positive women with microscopic and submicroscopic infections displayed high fibrin deposition within the placenta and high PAI-1 levels, providing evidence for dysregulated fibrinolysis. The authors also

evaluated the birth weights of babies from PM positive compared to PM negative mothers to assess the potential impact of malaria-induced impaired homeostasis on pregnancy outcomes. They found that women with both microscopic and submicroscopic infections and increased fibrin deposition in the placenta had children with significantly lower birth weight compared to PM-negative mothers. These results could suggest that dysregulated fibrinolysis and inappropriate coagulation activation could contribute to *P. falciparum*-induced poor pregnancy outcomes.

Further *in vivo* experiments in the *Pcc*AS mouse model of malaria infection in early gestation revealed markers of dysregulated fibrinolysis and hypercoagulation, through upregulation of TF and PAI-1 in infected pregnant mice [10]. To address the role of hypercoagulation on pregnancy loss within the *Pcc*AS model, mice were treated with either research grade LMWH or enoxaparin [10], which is a Food and Drug Administration (FDA) approved drug in the LMWH family, that is used to treat thrombotic disorders during pregnancy. In these experiments, infected pregnant (IP) mice were treated twice daily with anticoagulant treatment from gestational day E6.5 to E12.5, administered via neck scruff. Infection kinetics did not differ between IP-untreated and IP-treated mice, regardless of treatment. All three groups of IP mice had similar parasitemia and hematocrit values throughout the course of infection; however, only the IP-LMWH treated group continued to gain weight through peak parasitemia at E10.5-11.5, which was comparable to uninfected pregnant (UP) controls. Remarkably, embryo survival at midgestation (E12.5) in IP-LMWH treated mice was significantly higher (61% embryo survival) than survival in the IP-untreated group (3% embryo survival), with only 3 out of 11 LMWH treated mice showing signs of abortion. Enoxaparin-treated IP mice

experienced steady weight gain until E10.5; however, they experienced poor embryo viability at E12.5 (14% embryo survival), which was not significantly different from embryo survival in the IP-untreated group. Notably, despite improved midgestational pregnancy outcome in IP mice treated with LMWH, embryo survival still did not achieve the level of viability observed in UP mice (97% embryo survival). Overall, these results suggest that hypercoagulation plays a significant role in pregnancy loss at midgestation in the *Pcc*AS model of PM since anticoagulant treatment can dampen its contribution to pregnancy compromise, albeit not completely.

Due to the hematological nature of malaria infection, activation of the coagulation cascade is also associated with thrombocytopenia. Thrombocytopenia, described as an abnormally low platelet count, is a common occurrence in both *P. falciparum* and *P. vivax* infection [158]. Unlike severe anemia, thrombocytopenia has not been identified as a factor involved in malaria-associated mortality; however, it is commonly used to rapidly diagnose malaria infection in febrile patients living in endemic areas. Activated platelets play an important role in malaria pathogenesis through platelet-mediated clumping, endothelial cell activation, and inflammation, which are strongly associated with severe malaria outcomes [159–162]. In cases of cerebral malaria, the severity of thrombocytopenia corresponds with the degree of clumping observed *in vitro,* and clumping is mediated by the adhesive molecules found on the surface of platelets, CD36, and P-selectin [163].

The inflammation-coagulation cycle and PM pathogenesis

Studies in sepsis, malaria, and other inflammatory diseases have provided evidence for the intricate balance between inflammation and coagulation known as the

"inflammation-coagulation cycle" [8,9,14,164–166]. A family of seven-transmembrane G-protein coupled receptors called protease-activated receptors (PARs) has already been identified as a biological link between inflammation and coagulation [13,165–168]. There are four members of the PAR family (PAR1-4), and they are all activated through proteolytic cleavage of their extracellular N-terminal domain by coagulation serine proteases such as thrombin, trypsin, and the factor FXa/FVIIa/TF complex. This proteolytic cleavage reveals a tethered ligand that activates the extracellular receptor, triggering conformational changes and downstream signaling[167,169,170]. Activated PAR receptors signal through G proteins like G_i (cAMP inhibitory), $G_{12/13}$ (Rho and Ras signaling), and G_q (calcium signaling) [171] and play essential roles in regulating hemostasis, thrombosis, inflammation, and cancer progression [13,167,172]. PAR activation is an irreversible process that results in immediate internalization and degradation of the receptor to avoid an exaggerated response [168,171]. PARs are expressed on the surfaces of endothelial and immune cells, platelets, neurons, astrocytes, and epithelial cells, including the trophoblast, where they regulate hemostasis and thrombosis [172,173]. Of note, some significant differences exist between human and mouse PAR-1, PAR-3, and PAR-4 expression and function, especially on platelets, that must be considered during study design and experimentation of PAR signaling [170,174,175].

Differential downstream outcomes via activation of the same PAR by different agonists are termed "biased activation" [175]. PAR1, 3, and 4 are activated by thrombin, whereas PAR1 can also be activated by FXa, plasmin, APC, neutrophilic enzymes, and other molecules [167]. Trypsin is a potent activator of PAR2, but PAR2 can also be

activated by PAR1 after it is cleaved [174]. Similarly, PAR1 and 3 can co-activate PAR4 after their cleavage by thrombin [167]. A study shows that in human endothelial cells, PAR1 activation via thrombin favors induction of endothelial barrier permeability and pro-inflammatory responses [171]. In contrast, APC, an anticoagulant protease, promotes endothelial barrier stabilization and anti-inflammatory responses through PAR1 signaling [176]. Other ligands, such as matrix metalloproteinases, which play important roles in endothelial function [177] and neutrophil proteases released during inflammation [178], contribute to biased activation of PARs that leads to differential gene expression when compared to thrombin-activated signaling [176]. In pregnancy, PAR 1 and 2 mRNA levels are increased in the conceptuses of malaria-infected mice [7] and are implicated in the disease pathogenesis of preeclampsia [179,180]. Although PAR activation can drive the expression of proinflammatory cytokines by endothelial cells [166], it is still unclear how PAR signaling functions as a molecular link between malaria-induced inflammatory responses and coagulopathy in placental tissues.

Oxidative stress in PM pathogenesis

Recently, Sarr et al. published evidence for the contribution of oxidative stress to pregnancy compromise within the *Pcc*AS model of PM [18]. Oxidative stress is generally characterized as an overabundance of free radicals in an environment compared to the antioxidant defenses available to neutralize them [181,182]. While oxidative stress is known to be associated with the regular physiological changes related to pregnancy [183], it has also been implicated in contributing to poor pregnancy outcomes such as the initiation of preterm labor [184], early pregnancy loss, and pre-eclampsia [185–188].

Recent studies conducted in women living in Cameroon, demonstrated that the lipid peroxide product of oxidative stress responses called malondialdehyde (MDA) could be used as a biomarker for malaria severity during pregnancy [16]. Further studies confirm the potential for oxidative stress in PM by evaluating lipid peroxidation product 4-hydroxynonenal (HNE), in the placenta of *Pcc*AS-infected mice [17–19].

The production of free radicals associated with oxidative stress is a natural product of oxidative phosphorylation and energy generation by living cells. Without antioxidant defenses, free radicals can induce damage to cellular components such as proteins, lipids, and DNA and ultimately lead to cell death. Antioxidant defenses include free radical scavengers that are always present in low levels within a cell to donate electrons to free radicals and reduce their reactivity. There are three main classes of free radical species: reactive oxygen species (ROS), reactive nitrogen species (NOS), and reactive chlorine species [181]. My research seeks to interrogate the potential contribution of ROS to pregnancy compromise within the *Pcc*AS model of PM.

Several types of ROS are naturally produced as products of oxygen metabolism across mammalian cell types and cause cellular damage if produced in excess. The most commonly referred to ROS include free radicals such as superoxide radicals (O_2^-), hydroxyl radicals (OH^-), and non-radicals such as hydrogen peroxide (H_2O_2) [181]. The free radical scavengers important for controlling ROS activity include superoxide dismutase (SOD), catalase, and glutathione peroxidase. SODs are responsible for converting O_2^- radicals into H_2O_2, which catalase detoxifies into water and oxygen. Biologically, O_2^- is one of the most important free radicals because most other ROS can be generated from reactions between it and other molecules. For instance, O_2^- has a

relatively short half-life and is moderately reactive; however, its interaction with H_2O_2 produces OH^-, which is highly reactive. Several biological processes can produce O_2^- radicals, but many are generated from the electron transport chain within the mitochondria [189]. Other organelles, such as the endoplasmic reticulum and peroxisomes, can also produce ROS [182]. In addition, the Fenton reaction results in the synthesis of OH^- radicals in the presence of free iron or copper, which are important catalysts for generating ROS [190,191]. Oxidative damage within cells caused by an overabundance of ROS includes lipid peroxidation, DNA hydroxylation, and cell death [181].

Oxidative stress can also be intentionally produced by immune cells. After an inflammatory response has been triggered at the sight of injury, rapidly responding immune cells such as monocytes and macrophages will often release ROS into the extracellular environment upon arrival [192]. This ROS "burst", a common characteristic of neutrophils, is designed to inflict damage on the invading pathogens but can also harm the surrounding tissue [193]. In the case of inflammatory disease, where inflammation is uncontrolled or chronic, a constant stage of tissue deterioration can be attributed to oxidative stress [192]. It has been described that under inflammatory conditions, oxidative stress can stimulate the activity of pattern recognition receptors on the surface of the tissue, leading to the activation of multiple transcriptional regulators such as nuclear factor- κB (NF- κB) [194]. Since NF-κB is one of the transcription factors responsible for gene expression of proinflammatory cytokines, chemokines, receptors, etc., activation by H_2O_2 represents a potential link between oxidative stress and inflammatory responses. In diseases characterized by endothelial activation and

dysfunction, such as cardiovascular diseases, elevated ROS levels have been associated with the onset of symptoms and severity [195]. Additionally, inadequate placental perfusion driven by repeated hypoxia/reoxygenation in preeclamptic patients induces excessive O_2^- production in the syncytiotrophoblast and cytotrophoblast [196]. Unsurprisingly, this increase in ROS is associated with elevated markers of lipid peroxidation and protein damage in preeclamptic placentas [196]. In the context of malaria, severe anemia has been implicated in the development of ischemia and reperfusion syndrome, driven by changes in tissue oxygenation during severe infection that contributes to tissue ROS production [197]. To date, no studies have directly examined the potential relationships between inflammation, coagulation, and oxidative stress in PM pathogenesis as an approach to discovering novel therapeutics.

Hemozoin's immunomodulatory role in malaria

Nearly 95% of the protein found in red blood cells (RBCs) is hemoglobin [198]. Hemoglobin is an iron-containing molecule responsible for transporting oxygen throughout the body. After the invasion of red blood cells, the *Plasmodium* parasites consume hemoglobin as a required part of their development [198,199]. Hemoglobin degradation by the parasite supplies nutrients that it needs for growth; however, some studies suggest that hemoglobin degradation protects the RBC from lysis, allowing the parasite to strike a balance between its growing volume and the total volume of the RBC [200]. Either way, hemoglobin degradation results in the release of free heme, which is toxic to the parasite. As a result, the parasite has developed a heme detoxification strategy to transform free heme into an inert, insoluble, crystalline product known as hemozoin

(Hz). Hz is then released into the extracellular environment upon lysis of iRBCs, where it is rapidly phagocytosed by nearby immune cells [199,201].

Whether hemozoin itself is immunomodulatory has been studied extensively [202]. It has been shown that macrophages recognize and ingest both iRBCs and hemozoin; however, some studies suggest that phagocytosis of these substances hurts macrophage, monocyte, and dendritic cell functionality [203–207]. Macrophages and monocytes that have ingested hemozoin cannot completely destroy the malarial pigment [203], generate oxidative burst [208], or kill other digested pathogens [209]. However, macrophages, monocytes, and dendritic cells are still capable of generating a pro-inflammatory response after contact with iRBCs or hemozoin, by secreting cytokines like TNF and IL-6 [210,211], reactive oxygen species[212], nitric oxide [213,214], MIP-1α and MIP-1β [214]. It should be noted that there is some controversy about the ability of monocytes to produce nitic oxide upon hemozoin and cytokine stimulation [215], and the preparation of hemozoin itself can produce varying results in vitro [202,216].

It has also been demonstrated that natural hemozoin (nHz), which is thought to more closely resemble hemozoin that might be found *in vivo* upon schizont rupture, is typically bound to various host and parasite-derived substances such as proteins and lipids [216]. One such substance is fibrinogen, the glycoprotein that is important for the formation of stabilized fibrin clots, the final product of the coagulation cascade. A recent report suggests that hemozoin's ability to induce immune responses from phagocytes is at least partially due to the stable attachment of fibrinogen to nHz [217]. One potential mechanism for fibrinogen-bound hemozoin-mediated immune responses is through interactions with pattern recognition receptors on the surface of innate immune cells,

such as toll-like receptors (TLRs). Specifically, there have been reports of fibrinogen-bound hemozoin interacting with TLR-4 to induce TNF secretion in monocytes [217]. Some reports show that heme, the subunit component of Hz, can activate TLR4 production of TNF from macrophages [218]. Coban et al. further assessed the role of hemozoin-induced immune system activation through TLR9 signaling. They found that nHz could activate dendritic cells to produce several proinflammatory cytokines in a Myd88-dependent fashion [219].

During pregnancy, the trophoblast can participate in the innate immune response by phagocytosing microbes and producing cytokines such as TNF [220,221]. In the *Pcc*AS model of murine malaria infection during pregnancy, trophoblast giant cells can phagocytose iRBCs and hemozoin [102]. Thus, the interaction between parasite-derived products such as hemozoin and the placenta may influence malaria-induced outcomes during pregnancy. Through a *P. berghei* NK65 infection model in pregnant C57BL/6, Barboza et al. demonstrated that TLR 2, 4, and 9 are upregulated in the placenta after infection [222]. They showed that placental pathology, increased TNF expression, and reduced neonatal growth rate could be attributed to TLR4 expression and signaling [222]. Given that it is possible for Hz to be phagocytosed by the trophoblast and activate TLR signaling, it may also be possible to induce programmed cell death responses under particular circumstances.

In summary, malaria infection during pregnancy represents a significant global public health challenge for malaria eradication efforts and maternal-fetal health in endemic regions. Maternal responses to infection, such as inflammation, coagulation, and oxidative stress, are protective responses that ultimately contribute to PM pathogenesis

and pregnancy compromise by becoming exaggerated or uncontrolled. Thus, researchers must identify therapeutic strategies that balance the protective properties of the maternal physiological response to infection and their unwanted impact on pregnancy. Given what is known so far about PM pathogenesis and its complexity, it seems unlikely that one maternal response to infection – inflammation, coagulation, or oxidative stress – is solely responsible for the adverse pregnancy outcomes associated with the disease. The nature of the interplay between inflammation, coagulation, and oxidative stress responses has not been thoroughly characterized, and direct evidence describing a synergistic relationship between these processes in PM has not been reported. The work discussed in the following chapters employs host-directed drug and genetic approaches to improve pregnancy outcomes in murine models of PM, to elucidate the relationships between pathogenic host responses to infection, and identify novel therapeutic interventions to prevent malaria-induced pregnancy compromise.

CHAPTER 2

CROSSTALK BETWEEN INFLAMMATION AND COAGULATION IN MALARIA-INDUCED PREGNANCY LOSS[2]

[2] Andrew AK, Poovassery JS, Gonzalvo KT, Bracken TC, Moore JM. To be submitted to *Blood*.

Abstract

Plasmodium falciparum malaria in pregnancy contributes to poor birth outcomes associated with placental malaria (PM), a syndrome partly characterized by dysregulated inflammation and coagulation. This work tested the hypothesis that these pathogenic processes synergize to drive poor pregnancy outcomes. We utilized an established murine model of PM and a combination of both genetic and therapeutic manipulation of the model to test our hypothesis. *Plasmodium chabaudi* infection in tumor necrosis factor null ($TNF^{-/-}$) and anticoagulant-treated wildtype C57BL6/J (B6) mice improve pregnancy outcome relative to controls. Embryonic transcripts for a molecule essential for anticoagulant responses, endothelial protein C receptor (*Procr*/EPCR), were significantly upregulated in both $TNF^{-/-}$ and anticoagulant-treated mice. In contrast, transcripts for markers of inflammation (*Ifnγ*, *Tnf*, *Il10*, *Il1β*, and *Ccl2*) and the initiator molecule of coagulation, tissue factor (*F3*/TF), were significantly downregulated in anticoagulant- relative to sham-treated B6 mice. Moreover, transcripts for protease-activated receptors (PARs) were downregulated in both $TNF^{-/-}$ and anticoagulant-treated B6 mice, suggesting functional linkages between inflammation and coagulation (inflammation-coagulation cycle) in this model. Plasma cytokine analysis corroborates this connection, as protein levels for pro-inflammatory cytokines IFNγ and TNF are reduced, and anti-inflammatory cytokine IL-10 is increased in anticoagulant-treated mice relative to sham controls. In sum, this work identifies a bidirectional connection between inflammation and coagulation in PM, thereby contributing to our current understanding of how these pathogenic responses may synergize and galvanize pregnancy compromise.

Introduction

The bidirectional relationship between inflammation and coagulation (also known as the inflammation-coagulation cycle) has been well described across several diseases [8,14,164,165,223]. Tissue factor (TF) is central to the connection between inflammation and coagulation because its expression initiates the activation of coagulation factors, that promote inflammatory signaling through protease-activated receptors (PARs) [21,168,224]. As a result, TF must be downregulated, anticoagulant and fibrinolytic activity engaged, and PAR signaling diminished or altered to antagonize this effect. The natural anticoagulant pathway, known as the protein C pathway, is critical in controlling blood coagulation and inflammation. In particular, endothelial protein C receptor (EPCR) activates protein C to promote its anticoagulant activity [150].

In women experiencing placental malaria (PM), excess inflammation and dysregulated coagulation are associated with poor pregnancy outcomes [10,37,38,145], representing a possible route for therapeutic intervention. Thus far, limited studies have conducted randomized controlled trials to evaluate the effect of anti-inflammatory and anti-coagulant therapy on disease outcomes in patients with severe malaria [225]. Anti-tumor necrosis factor (TNF) antibody therapy given to patients with cerebral malaria yielded mixed results, with some studies showing significant improvements in survival and coma recovery time and decreased serum TNF levels [226,227]. In contrast, other studies reported no improvements [228,229] or worsened outcomes [230]. Studies have also been performed using anticoagulant treatment in patients with non-severe malaria. Clinical outcomes such as duration of parasitemia, fever clearance, and length of hospitalization did not improve; however, elevated levels of serum TNF and lactate

dehydrogenase decreased after heparin treatment [231]. Moreover, a related study showed that Sevuparin, a heparan sulfate mimetic, can cause the de-sequestration of parasitized red blood cells in patients with uncomplicated malaria [232].

In general, anti-inflammatory therapy is not recommended during pregnancy, except in low doses and under certain circumstances. In 2020, the federal drug administration (FDA) recommended that women avoid using nonsteroidal anti-inflammatory drugs after 20 weeks of pregnancy due to concerns that they could lead to reduced amniotic fluid [233]. In contrast, anticoagulant therapy has been safely used in pregnant women [234]. FXa inhibitors such as low molecular weight heparin (LMWH), Fondaparinux, and Dalteparin have been well-tolerated during pregnancy; however, careful attention must be paid to parameters such as dosing, history of recurrent pregnancy complications, autoimmunity, and thrombophilia to avoid adverse side effects [234–236]. On the other hand, the ability of anticoagulants to prevent poor pregnancy outcomes during malaria infection remains to be elucidated.

Our previously published work demonstrated an increase in TF expression in the placenta of *Plasmodium chabaudi chabaudi* AS (*Pcc*AS)-infected C57BL6/J (B6) mice on embryonic day (E) 9.5, one day before the onset of pregnancy loss [5]. Remarkably, TNF ablation through treatment with a neutralizing anti-TNF antibody reduced TF expression in the placenta to undetectable levels by E12.5, a time point corresponding to total pregnancy failure in IgG control-treated mice [5]. Additionally, anti-TNF-treated B6 mice had approximately 88 percent embryo viability at E12.5, significantly improving from the zero percent viability observed in IgG controls at the same time point [5]. Moreover, transcript expression for critical molecules in the coagulation pathway was

significantly upregulated in the conceptuses of untreated infected mice. Moreover, LMWH treatment dramatically improved pregnancy outcomes [10]. Given these findings, I hypothesized that genetic removal of TNF will have a synergistic effect on coagulation, and anticoagulant treatment will reduce inflammation, leading to improved pregnancy outcomes during malaria infection.

Materials and Methods

Mice

C57BL/6J (B6), AJ, and TNFα-knockout (B6;129S-Tnftm1Gkl/J) mice were purchased from the Jackson Laboratory (Bar Harbor, ME). Mice with floxed TF ($F3^{fl/fl}$) and expressing Cre recombinase in vascular endothelial cells, called TFΔEc (also known as Tie2Cre+) and $F3^{fl/fl}$ mice without Cre recombinase expression (also known as TF-intact, Tie2Cre-) mice, were acquired from Nigel Mackman (University of North Carolina, Chapel Hill, NC). NCI BALB/cAnNCr (BALB/c) were purchased from Charles River (Frederick, MD). All mice were maintained by brother-sister mating for a maximum of ten generations (with the exception of Tie2Cre mice), partly in the University of Georgia (UGA) Coverdell Vivarium and partly in the University of Florida (UF) Veterinary Metabolic Building. All experiments and mouse handling followed guidelines and regulations set forth by the University of Georgia and the University of Florida Animal Care and Use (IACUC) Committees. All animals were maintained as *Helicobacter*-free to avoid any impact of *Helicobacter* infection on pregnancy success [237] and were routinely screened to confirm the absence of murine norovirus infection. Animals were supplied food (PicoLab® Rodent Diet 20: 5030, when housed at UGA;

Teklad Global 18% Protein Extruded Rodent Diet, irradiated, #2918, when housed at UF) and water ad libitum. Mice were adjusted to a 12-hour light/12-hour dark cycle and housed in 65-75 ˚F and 40-60% humidity conditions. All animal procedures reported in this study were reviewed and approved by the IACUC at UGA, protocol number A2018 02-016-Y1-A0; IACUC at UF, protocol number 201810169. Mice were anesthetized with 2.5% Tribromoethanol or isoflurane inhalation before sacrifice, and all efforts were made to minimize suffering.

Parasites and infection monitoring

The following reagent was obtained through BEI Resource Repository, NIAID, NIH: *Plasmodium chabaudi chabaudi*, Strain AS, MR4-741, contributed by David Walliker. Parasites were maintained as frozen stock according to supplier guidelines and passaged in A/J or BALB/c mice for the purposes of infecting experimental B6 mice. Peripheral parasitemia was assessed by flow cytometry with a method adapted from work published by Jimenez-Diaz et al. [238]. A 2µl blood sample was collected by tail clip [239], diluted in 98µl 0.9% NaCl and stained with 0.25µl SYTO-16 Green Fluorescent Nucleic Acid Stain (ThermoFisher Scientific, catalog # S7578) within 4 hours of collection. Stained samples were diluted 1:9 in 0.9% NaCl and incubated in the dark for 20 minutes at room temperature, then analyzed using a CyAn ADP Flow Cytometer (Beckman Coulter; Brea, CA) or Attune NxT flow cytometer and Attune NxT software version v3.1.2. A total of 30,000 cells were assessed daily for each mouse; infected red blood cells were distinguished based on size and fluorescence intensity. An uninfected blood sample was used as an internal negative control. Parasitemia is reported as the

percentage of infected red blood cells (% IRBCs) to the total number of red blood cells (RBCs).

Experimental Design

Female B6 and TNF-null mutant ($TNF^{-/-}$) mice aged 8-10 weeks were paired with males nightly and examined each morning until a vaginal plug was observed, indicating successful mating. The morning a vaginal plug was observed was considered embryonic day 0.5 (E0.5). After baseline measurements of weight and hematocrit were recorded, females were left undisturbed until E6.5 to minimize stress and increase the chances of successful blastocyst implantation. Mice were infected intravenously with 1000 *P. chabaudi chabaudi* AS-iRBCs diluted in 200ul 1X phosphate-buffered saline (PBS) per 20 grams of body weight and are termed infected pregnant (IP). In another control group, uninfected pregnant (UP) mice were sham injected with 200ul PBS per 20 grams body weight on E0.5. Immediately prior to infection or sham infection, experimental animals were switched to a high-fat rodent chow (PicoLab Mouse Diet 20 5058, when housed at UGA or Tekland Global 19% Protein Extruded Rodent Diet, irradiated, #2919, when housed at UF) suited for pregnant animals. Weight measurements were recorded on E0.5, E6.5 through E10.5 or E12.5 for all groups to assess pregnancy progress and allow mice to proceed to malaria-induced pregnancy loss. Parasitemia and hematocrit (a measure of anemia) were monitored daily in the infected groups beginning on E6.5 to assess the development of infection. At sacrifice, embryo viability was assessed, as previously described [10]. Embryos exhibiting extensive hemorrhaging and/or necrosis or described

as unusually small and pale for gestational age compared to embryos from UP controls were scored as nonviable.

In one experiment, B6 mice received either 20mg/kg of anti-tissue factor (1H1, OR-214239) antibody or control IgG antibody once daily, through intraperitoneal injection (i.p.) on E6.5 through E9.5 (4 doses total). In work done previously in the lab, B6 mice were treated with 1000 IU/kg low molecular weight heparin (LMWH) subcutaneously twice daily from E6.5 through E10.5, 1000 IU/kg dalteparin sodium (Dalteparin) i.p once daily from E6.5 through E11.5, 10mg/kg Fondaparinux subcutaneously once daily from E6.5 to E11.5, or sham treatment (PBS). Samples preserved from those anticoagulant studies were subsequently used in my studies to assess gene transcript expression and plasma cytokine concentration. In a final experiment, 2.5mg/kg of the oral anticoagulant, Apixaban (Brand name Eliquis, Pfizer) or sham (PBS), was delivered twice daily through oral gavage in BALB/c mice between E15.5 and E17.5 (2 doses).

Gene expression by quantitative real-time PCR

Total RNA from $TNF^{-/-}$ and B6 embryos collected on E10.5 was isolated using Trizol Reagent (Ambion, Ref # 15596026). Genomic DNA, RNA, and protein were collected from E10.5 embryos from 1H1-treated animals and sham controls using Zymo Research Quick-DNA/RNA Miniprep Kit (Cat # D7003). Embryos were homogenized using a bead shaker (BeadBlaster 24, Benchmark Scientific, SKU: D2400) with a minimum of two embryos per dam. RNA (regardless of extraction reagent) was DNase-treated (Invitrogen, Ref # AM1906) and then reverse-transcribed with High-Capacity

cDNA Reverse Transcription Kit (Applied Biosystems, Ref # 4368814). Relative transcript abundance for the genes of interest was quantified using PowerSYBR Green PCR Master Mix (Applied Biosystems, Cat # 4367659) and the BioRad CFX92 Real-Time System. Cq values were obtained from the BioRad CFX Maestro software version 2.0. Each sample was assayed in duplicate for target and housekeeping genes. Average Ct values of target genes were normalized to average Ct values of *Ubc* as the reference gene and relative transcript abundance of genes of interest was determined using the ΔΔCt method. Transcript expression in individual mice is presented relative to the mean expression value in UP mice at E6.5. Details of primer sets are summarized in Table 2.3.

Gene expression by magnetic bead array

Peripheral plasma collected from anticoagulant treated and tissue factor-modified (Tie2Cre) mice were diluted 1:4 and a mouse multiplex assay was used to determine the concentration of TNFα, IFNγ, IL10, IL1β, IL6, and Th17 (Biorad, Bio-plex Pro Mouse Cytokine Th17 Panel A, cat # M6000007NY). Luminex MAGPIX multiplex instrument and XLAT software were used to acquire and analyze the data. Relative concentrations were extrapolated based on concentrations generated from a standard curve for each analyte.

Statistics

All statistical analyses were performed using GraphPad Prism version 9.2.0 (GraphPad Software; La Jolla, California). All raw clinical data are presented as mean ± SEM. Error bars are not visible if they are shorter than the symbol's height. As

appropriate, the area under the curve (AUC) of percent starting weight, hematocrit, and parasitemia was calculated for each mouse between E0.5 and E12.5. AUC for weight and hematocrit was compared between UP, B6 IP, and $TNF^{-/-}$ IP groups using one-way ANOVA with Dunnett's T3 multiple comparisons test between UP and IP groups and between B6 IP and $TNF^{-/-}$ IP groups. In another study, AUC for weight, hematocrit, and parasitemia was compared between B6 IP 1H1 treated and B6 IP sham treated groups using a two-tailed unpaired t-test with Welch's correction. Similarly, AUC for parasitemia between B6 IP and $TNF^{-/-}$ IP groups was compared using a two-tailed unpaired t-test with Welch's correction. RT-qPCR data were analyzed using an unpaired t-test with Welch's correction and presented as a scatterplot with a bar representing the median. P values less than or equal to 0.05 were considered statistically significant. Proportional analysis tested by Fisher exact probability test was used to compare embryo viability between IP and UP dams, B6 IP and $TNF^{-/-}$ IP, or IP treated and IP sham dams.

Results

TNF deletion significantly improves embryo viability during malaria infection at midgestation

TNF-null mutant mice ($TNF^{-/-}$) experience a similar course of infection when infected with blood-stage *Plasmodium chabaudi chabaudi* AS (*Pcc*AS) compared to wild-type B6 control mice (Figure 2.1). Weight change, which was monitored throughout the experiment as a proxy for pregnancy success, was surprisingly unaffected by infection status when infected pregnant (IP) mice were compared to uninfected pregnant (UP) controls using area under the curve (AUC) analysis (Figure 2.1A-B). However,

maternal weight at the end of the experiment, on embryonic (E) day 10.5, was significantly reduced in both B6 and $TNF^{-/-}$ dams compared to UP controls (Figure 2.2A). Interestingly, there was a slight tendency for lower overall parasite burden in $TNF^{-/-}$ IP compared to B6 IP mice (Figure 2.1C-D); however, this observation did not affect hematocrit overall (Figure 2.1E-F) or at E10.5 (Figure 2.2B). At the end of the experiment, pregnancy outcome was assessed by measuring uterus weight and embryo viability. Uterus weights were significantly reduced in both B6 and $TNF^{-/-}$ IP dams relative to UP controls, but were not different in B6 IP relative to $TNF^{-/-}$ IP dams (Figure 2.3). Despite this observation, embryo viability was significantly improved by TNF deletion in this model (Table 2.1). It is possible that more dramatic differences in pregnancy outcome, such as uterus weight, could emerge later in gestation, especially given that embryo viability was improved on E12.5 in anti-TNF antibody-treated B6 IP mice [5].

TNF deletion is associated with the upregulation of anticoagulant gene transcripts and the downregulation of protease-activated receptor 2 transcripts during malaria infection.

To assess how genetic deletion of TNF impacts the expression of various coagulation and anticoagulation genes, quantitative real-time PCR (qPCR) analysis was performed in conceptuses from $TNF^{-/-}$ and B6 IP mice at E10.5. The results demonstrate that transcripts for a receptor that promotes anticoagulant responses, endothelial protein C receptor (*Procr*/EPCR), are significantly elevated in conceptuses from $TNF^{-/-}$ IP relative to B6 IP dams (Figure 2.4A). Conversely, transcripts for protease-activated receptor 2 (*F2rl1*/PAR-2) were significantly downregulated in $TNF^{-/-}$ IP compared to B6 IP mice

(Figure 2.4A). Given the complex relationship between EPCR-mediated anti-inflammatory and cytoprotective activity and protease-activated receptor signaling [149,240,241], elevated *Procr* transcripts could indicate that $TNF^{-/-}$ IP mice are experiencing a more robust anticoagulant response in the face of malaria infection relative to B6 dams, which may preserve embryo viability (Table 2.1).

Malaria-infected TNF null mice do not experience changes in antioxidant gene transcript expression at midgestation

Previously published findings in this model of PM have underscored the inability of antioxidant defense responses to protect the placenta from lipid peroxidation, a consequence of ongoing oxidative stress, and avoid malaria-induced pregnancy loss [18]. Markedly, antioxidant treatment significantly restored embryo viability in the same study. To understand the impact of TNF deletion on antioxidant defenses and oxidative stress in this model, we compared antioxidant transcript expression in IP $TNF^{-/-}$ and B6 dams. The qPCR results revealed no statistically significant differences in transcript abundance among the targeted genes (Figure 2.4C). However, there was a weak tendency for *Hif1α*, a gene involved in controlling cellular responses to hypoxic conditions, to be elevated in $TNF^{-/-}$ embryos (Figure 2.4C).

Anticoagulant treatment in B6 IP mice reduces inflammatory gene transcript and cytokine expression

To investigate the bidirectional relationship between inflammation and coagulation in the *Pcc*AS murine model of PM, qPCR analysis was performed on

conceptuses collected from low molecular weight heparin (LMWH) treated and sham treated B6 mice at E11.5. LMWH is an anticoagulant drug that has been safely used to treat thrombotic disorders in pregnant women [234] and improves pregnancy outcomes in the *Pcc*AS model of PM [10]. In mice that received LMWH treatment, pro-inflammatory transcripts *Ifnγ*, *Tnfα*, *Il10*, *Il1β*, and *Ccl2* were significantly decreased relative to B6 IP conceptuses, except for *Il10*, which remained unchanged (Figure 2.5A). Similar to the observations made in $TNF^{-/-}$ mice, transcripts for EPCR were significantly elevated in LMWH treated mice, while transcripts for PAR-2 were significantly suppressed (Figure 2.5B). Moreover, protease-activated receptor 1 (*F2r*/PAR-1) transcripts had a weak tendency ($P = 0.07$) to be downregulated in LMWH treated mice compared to sham (Figure 2.5B). Transcripts for tissue factor (*F3*/TF), the primary initiator of extrinsic coagulation, were also significantly downregulated (Figure 2.5B), providing strong evidence that anticoagulant treatment effectively reduced procoagulant responses in these mice. To evaluate oxidative stress, transcripts for antioxidant defense genes were assessed. Transcripts for superoxide dismutases (SOD) 1 and 3 and nuclear factor erythroid 2-related factor 2 (*NFE2L2/Nrf2*) were significantly downregulated in LMWH treated mice relative to sham treated controls (Figure 2.5C). Taken together, these data suggest that coagulation has a strong and direct influence on the expression of both inflammatory and antioxidant genes in this model of PM.

To assess functional cytokine levels, a multiplex array was performed on peripheral plasma collected from IP mice treated with anticoagulant drugs LMWH, Dalteparin, or Fondaparinux and their respective sham treated controls (Figure 2.6). IFNγ concentration was significantly lower in LMWH treated mice relative to sham controls,

corroborating the results of the qPCR analysis (Figure 2.6A). Additionally, Il10 concentration tended to decrease (P = 0.06) in LMWH treated mice compared to controls (Figure 2.6A). When mice were treated with Dalteparin, an FDA-approved formulation of LMWH similar to the biochemical grade used in previous studies [10], IL10 concentration was significantly decreased in treated mice, while TNF had a strong tendency (P = 0.06) to decrease (Figure 2.6B). Similar observations were made in mice treated with Fondaparinux, another FDA-approved drug used to bolster antithrombin's anticoagulant activity, where Il10 concentration was significantly reduced (Figure 2.6C).

In a related study, mice were given an anti-TF antibody (1H1) treatment from E6.5 to E9.5 to identify a potential mechanism for coagulation-driven pregnancy loss in this *Pcc*AS model. 1H1 treatment did not affect weight change in B6 IP dams (Figure 2.7A-B); however, treatment tended to reduce the overall parasite burden (Figure 2.7C-D) without impacting hematocrit (Figure 2.7E-F). When parasitemia was assessed on individual days, 1H1 treatment reduced peripheral parasite burden on E8.5 and tended to lower parasite burden on E9.5 (Figure 2.8A-B). Furthermore, no significant differences were revealed when maternal weight and hematocrit were evaluated on E10.5 (Figure 2.8C-D). Uterus weight at E10.5 was also not impacted by 1H1 treatment (Figure 2.9). To assess whether targeting TF impacts inflammatory transcript expression, qPCR analysis was performed in the 1H1 and sham treated mice. 1H1 treatment did not alter transcript expression of the pro-inflammatory genes measured (Figure 2.10). Likewise, peripheral plasma cytokine concentrations were unchanged between the treatment groups (Figure 2.6D), and no transcripts for the targets measured were significantly altered by 1H1 treatment (Figure 2.10). In an alternative approach to determining whether TF-

driven coagulation can explain the poor pregnancy outcomes shown in the *Pcc*AS model, plasma cytokines were measured in IP mice with endothelial-cell specific deletion of TF (TFΔEc) and TF-intact IP controls ($F3^{fl/fl}$) at E12.5. Peripheral plasma cytokine levels were not statistically different in IP TFΔEc relative to IP $F3^{fl/fl}$ mice (Figure 2.6E).

Discussion

To our knowledge, the inflammation-coagulation cycle has been described in many diseases but has not been directly addressed in PM. This work sought to investigate the bidirectional nature of the relationship between inflammation and coagulation in murine PM. Our first approach was to infect pregnant mice (infected pregnant, IP) deficient in tumor necrosis factor ($TNF^{-/-}$) with *Plasmodium chabaudi chabaudi* AS (*Pcc*AS) as a model for targeting malaria-induced inflammation during pregnancy. In our second approach, we evaluated the impact of anticoagulant treatment in pregnant mice on the expression of inflammatory markers. Additionally, we measured antioxidant gene expression as a marker of oxidative stress in the embryos of malaria-infected $TNF^{-/-}$ and anticoagulant-treated wild-type mice. In each case, one maternal response to malaria infection was targeted, and inflammation, coagulation, and oxidative stress markers were evaluated. Embryo viability or uterus weight determined pregnancy success in IP mice at midgestation (E10.5 or E12.5), and both TNF deletion and anticoagulant treatment demonstrated an improvement in pregnancy outcome.

This study expands on previous work showing that targeting inflammation through systemic treatment of neutralizing anti-TNF antibodies drastically improved pregnancy outcomes and reduced tissue factor (TF) expression in the placenta [5].

Importantly, this work is pivotal in bridging the findings made in the anti-TNF treatment study with the results from another earlier publication, demonstrating that anticoagulant treatment with low molecular weight heparin (LMWH) successfully rescues midgestational malaria-induced pregnancy loss [10]. Thus, this is the first study to bridge the findings of both key studies by investigating how targeting one pathogenic response to malaria infection during pregnancy – either inflammation or coagulation – impacts markers of the alternative response in the context of improved pregnancy outcome.

When pregnant $TNF^{-/-}$ mice were infected with *Pcc*AS, their weight change, an indicator of pregnancy progression, was not different relative to wildtype IP C57BL6/J (B6) mice (Figure 2.1). However, weight change on the final day of the experiment, E10.5, tended to be higher in IP $TNF^{-/-}$ compared to IP B6 (Figure 2.2). Uterus weight, a measure of pregnancy success, was also unaltered on E12.5 by TNF deletion (Figure 2.3). In unpublished work done in our lab, weight change in mice that progress to E12.5 is significantly increased in IP $TNF^{-/-}$ versus IP B6 at that later time point. Furthermore, E10.5 denotes the beginning of peak parasitemia, and E12.5 represents a time of descending parasitemia in this model [5]; thus, the E10.5 time point may be too early to observe overall changes in uterus weight. However, an alternative measure of pregnancy success, embryo viability, was remarkably increased at E10.5 in IP $TNF^{-/-}$ mice compared to IP B6 mice (90% versus 65% viability, respectively; Table 2.1), indicating that pregnancy is indeed affected by malaria infection on E10.5. Parasitemia tended to be lower in $TNF^{-/-}$ IP dams, supporting original observations that TNF activity contributes to malaria pathogenesis, while other inflammatory mediators such as IFNγ and IL-10 are crucial for immune protection [242,243]. Real-time quantitative PCR (qPCR) analysis

showed that TNF deletion did not impair the transcript expression for cytokines such as IFNγ, IL-10, IL-1β, and CCL2 (Figure 2.4B), corroborating other studies [244].

To establish a connection between inflammation and coagulation in PM, our next group of experiments measured mediators of inflammation in anticoagulant-treated mice relative to their controls and the expression of transcripts related to mediators of the coagulation in the embryos of malaria-infected $TNF^{-/-}$ dams (Figure 2.4; Figure 2.5; Figure 2.6). LMWH and Dalteparin treatment directly reduced pro-inflammatory and anti-inflammatory plasma cytokine concentration. On the other hand, TNF deletion led to the significant upregulation of transcripts belonging to the endothelial protein C receptor (*Procr/EPCR*) and downregulation of transcripts for protease-activated receptor-2 (*F2rl1*/PAR-2). Like TNF deletion, LMWH treatment resulted in *Procr* transcript upregulation and downregulation of both *F2r/*PAR-1 and *F2rl1*/PAR-2 transcripts.

EPCR is a receptor that regulates the anticoagulant and cytoprotective activity of activated protein C (APC). For instance, APC-EPCR binding augments APC's inactivation of coagulation factors, such as factors Va and VIIa, to interrupt ongoing coagulation and promote anticoagulant events [149,245,246]. Moreover, EPCR supports APC's stabilization of the thrombin-antithrombin complex, bolstering APC's anti-inflammatory and endothelial barrier protective signaling through PARs [149,241]. The literature on the relationships between the APC-EPCR complex PAR signaling is extensive; the consequences of these interactions are context-dependent [169]. However, a few observations are reported that contextualize the observations made in this study. EPCR-APC interactions can contribute to the anti-inflammatory and cytoprotective signaling through PAR-1 [169,247]. *Procr/*EPCR transcripts were upregulated with no

changes in *F2r* transcripts in IP TNF$^{-/-}$ mice relative to B6 controls. These data could suggest that without TNF, EPCR's cytoprotective and/or anti-inflammatory activity can be engaged without requiring the upregulation of *F2r* transcripts. At the same time, EPCR has been shown to bind directly to coagulation proteases such as factor Xa to cleave PAR-2, triggering inflammatory signaling [169]. Thus, decreased *F2rl1* transcripts may indicate reduced inflammatory signaling in the conceptuses of TNF$^{-/-}$ mice, further supporting the cytoprotective and anti-inflammatory properties of EPCR. Similar observations were made in LMWH-treated mice, where *Procr* transcripts were upregulated; however, both *F2r* and *F2rl1* transcripts were downregulated. This supports the notion that anticoagulant treatment, in addition to its direct effect on coagulation proteases, exerts a more substantial anticoagulant impact by simultaneously reducing the expression of both PAR-1 and PAR-2, while boosting possible EPCR-related and anticoagulant and cytoprotective potential. Indeed, inhibiting PAR signaling has anticoagulant and anti-inflammatory effects and anticoagulant treatment can inhibit PAR activation [149,248].

Under pathological conditions, including malaria infection, inflammation can play a role in ROS generation and contribute to oxidative stress and tissue damage [184,192,193]. Oxidative stress due to inflammation can be beneficial in supporting normal redox activities and eliminating pathogens; however, in some cases, oxidative stress responses can also be linked to disease development [249] and pregnancy complications [250,251]. Previous studies have shared compelling evidence for the pathogenic potential of oxidative stress in malaria-infected pregnant mice [17–19] and the therapeutic potential of antioxidant treatment in improving pregnancy outcomes [18].

In this study, antioxidant gene transcript expression was used as an indirect marker of oxidative stress. We found that TNF removal had no impact on antioxidant gene expression; however, there was a tendency for upregulation of *Hif1α* transcripts in embryos of IP $TNF^{-/-}$ dams. HIF1α, a transcription factor that controls the cellular expression of hypoxia response genes, can be activated by ROS and function to protect cells from oxidative stress [252,253]. Conversely, LMWH treatment reduced transcripts for antioxidant defense genes *Nrf2*, *Sod1*, and *Sod3*. *Nrf2* regulates both antioxidant and inflammatory responses [254]; thus, its downregulation in anticoagulant-treated IP mice supports that LMWH treatment may modulate both inflammatory and antioxidant responses while improving pregnancy outcomes during malaria infection.

In summary, excessive inflammation and coagulation contribute to PM pathogenesis, and the link between inflammation and coagulation through protease-activated receptor signaling has been well-described. Removal of TNF boosted the transcript expression for the anticoagulant gene, *Procr*, suggesting that $TNF^{-/-}$ mice may be better capable of promoting anticoagulant responses in the face of malaria infection, which could benefit pregnancy outcome. Moreover, *F2r* and *F2rl1* transcripts were significantly decreased in IP $TNF^{-/-}$ and LMWH-treated embryos, pointing to a potential molecular connection between inflammation and coagulation in this murine model of PM. Moreover, cytokine concentration and oxidative stress markers were significantly reduced by anticoagulant treatment, indicative of the strong impact of coagulation in promoting pathogenic responses in PM. Nevertheless, these data show a clear bidirectional relationship between inflammation and coagulation in *Pcc*AS-infected mice and lay the groundwork for future studies that delineate how the inflammation-

coagulation cycle can be therapeutically manipulated to improve pregnancy outcomes in human PM.

Figure 2.1. Weight change, parasitemia, and hematocrit in *P. chabaudi chabaudi* AS-infected TNF null mice and wildtype B6 controls.

A) Percent starting weight in uninfected pregnant (UP) and infected pregnant (IP) wildtype B6 and TNF null mice beginning on E0.5 and then from E6.5 to E10.5. Data represent mean ± SEM.
B) Area under the curve (AUC) analysis of starting weight measurements collected on E0.5 through E10.5. No statistical differences were found between groups (#P = 0.062; one-way ANOVA with Dunnett's T3 multiple comparisons test).
C) Percent peripheral parasitemia in B6 IP and TNF null IP mice from E6.5 to E10.5. Data represent mean ± SEM.
D) AUC analysis for percent peripheral parasitemia from E6.5 to E10.5. No statistically significant differences were found between groups (P = 0.059; unpaired t-test with Welch's correction).
E) Percent hematocrit in UP, B6 IP, and TNF IP mice was measured on E0.5 and then from E6.5 to E10.5.
F) AUC analysis for percent hematocrit from E0.5 to E10.5. No statistically significant differences were found between groups (P = 0.37; one-way ANOVA with Dunnett's T3 multiple comparisons test).

Sample sizes: UP group is both B6 and TNF combined, B6 UP, *n* =5; TNF UP, *n* = 3; B6 IP, *n* = 14; TNF IP, *n* = 15; *ns* = not significant, P > 0.05. Error bars are not depicted if the they are shorter than the height of the symbol.

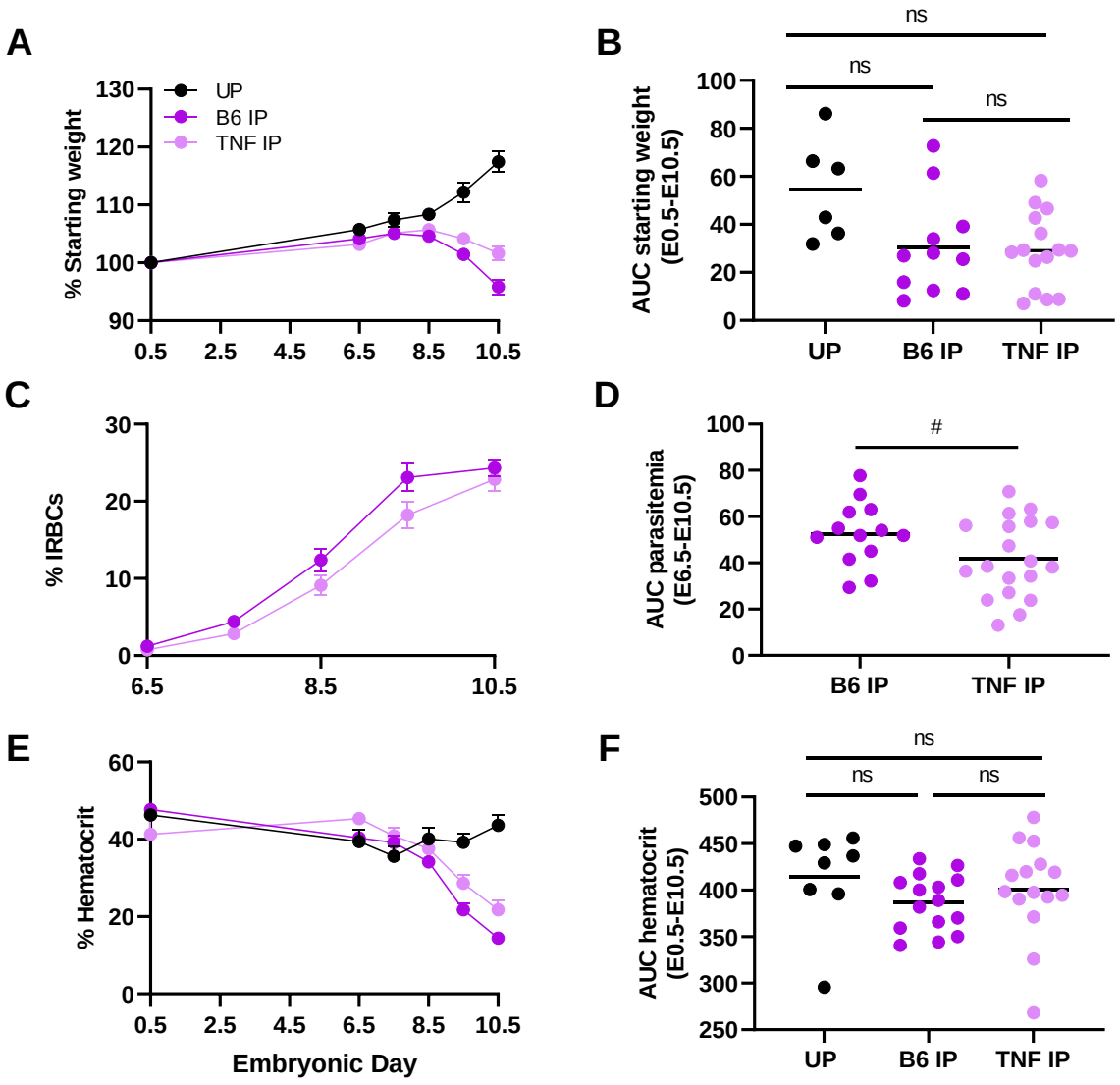
A
% Starting weight
130
120
110
100
90
UP
B6 IP
TNF IP
0.5
2.5
4.5
6.5
8.5
10.5
B
AUC starting weight (E0.5-E10.5)
ns
ns
ns
100
80
60
40
20
0
UP
B6 IP
TNF IP
C
% IRBCs
30
20
10
0
6.5
8.5
10.5
D
AUC parasitemia (E6.5-E10.5)
#
100
80
60
40
20
0
B6 IP
TNF IP
E
% Hematocrit
60
40
20
0
0.5
2.5
4.5
6.5
8.5
10.5
Embryonic Day
F
AUC hematocrit (E0.5-E10.5)
ns
ns
ns
500
450
400
350
300
250
UP
B6 IP
TNF IP

Figure 2.2. Weight change and hematocrit at E10.5 in malaria-infected TNF null mice relative to B6 controls.

A) Percent starting weight in uninfected pregnant (UP) and infected pregnant (IP) wildtype B6 and TNF null mice on the final day of the experiment, E10.5. Statistically significant differences are detected between UP mice and both IP groups (****P < 0.0001), while TNF IP weight tended to be higher than B6 IP dams (#P = 0.074; one-way ANOVA with Dunnett's T3 multiple comparisons test).

B) Percent hematocrit in UP and infected pregnant IP wildtype B6 and TNF null mice on the final day of the experiment, E10.5. Statistically significant differences are detected between UP mice and both IP groups (****P < 0.0001), while no significant differences were observed between B6 and TNF IP dams (P = 0.28); one-way ANOVA with Dunnett's T3 multiple comparisons test.

Sample sizes: UP group is both B6 and TNF combined, B6 UP, *n* =5; TNF UP, *n* = 7;

B6 IP, *n* = 8; TNF IP, *n* = 15; *ns* = not significant, P > 0.05.

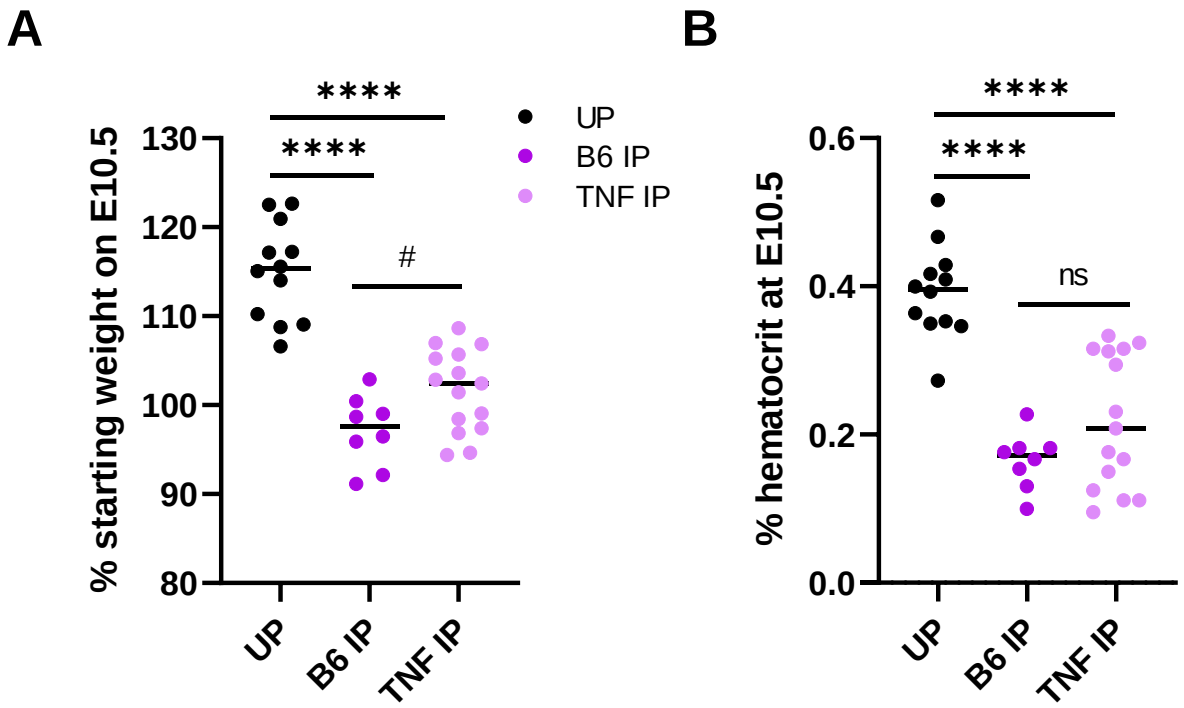

Figure 2.3. Uterus weight in malaria-infected TNF null and wildtype B6 mice at E10.5.

Uterus weight is presented for uninfected pregnant (UP) and infected pregnant (IP) B6 and IP TNF mice. UP dams had statistically greater uterus weights than both IP groups (**P ≤ 0.001; one-way ANOVA with Dunnett's T3 multiple comparisons test). Sample sizes: UP group is both B6 and TNF combined, B6 UP, *n* =6; TNF UP, *n* = 3; B6 IP, *n* = 8; TNF IP, *n* = 15; *ns* = not significant, P > 0.05.

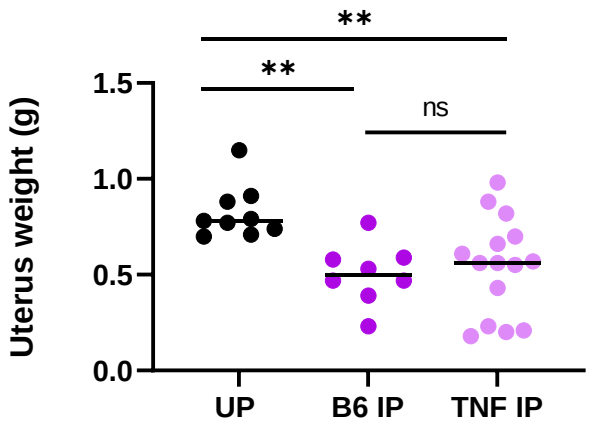

Table 2.1. Embryo viability in malaria-infected wildtype B6 compared to TNF null mutant mice.

Uninfected pregnant (UP) and infected pregnant (IP) B6 and TNF null ($TNF^{-/-}$) mice at mid-gestation. P values were obtained with a two-tailed Fisher exact probability test; percentages show percent viability within a group; bolded P values indicate statistical significance in embryo viability between groups.

Group	**Viable/total embryos (E10.5)**	**Viable/total embryos (E10.5)**	
	B6	$TNF^{-/-}$	P value
UP	74/75 (99%) n=10	26/27 (96%) n=3	**<0.0001[c]**
IP	48/74 (65%) n=10	125/130 (90%) n=18	**<0.0001[d]**
P value	**<0.001[a]**	0.73[b]	

[a]B6 UP versus B6 IP; [b]$TNF^{-/-}$ UP versus $TNF^{-/-}$ IP; [c]B6 UP versus $TNF^{-/-}$ UP; [d]B6 IP versus $TNF^{-/-}$ IP

Figure 2.4. *P. chabaudi* infection in TNF null mice modulates transcript expression of anticoagulant and protease-activated receptor genes.

A) Transcript abundance for coagulation/fibrinolysis-related mouse genes *F3*, *Tfpi*, *Serpine1*, *Thbd*, *Procr*, *F2r*, and *F2rl1* normalized to *Ubc* and quantified by qPCR in conceptuses taken from infected, pregnant (IP) TNF null and IP B6 mice. Group medians and transcript abundance in individual mice are depicted. *P < 0.05.
B) Transcript abundance for inflammation-associated mouse genes *Ifnγ*, *Tnf*, *Il10*, *Il1β*, *and Ccl2* normalized to *Ubc* and quantified by qPCR in conceptuses taken from IP TNF null and IP B6 mice. Group medians and transcript abundance in individual mice are depicted. #P = 0.071.
C) Transcript abundance for antioxidant mouse genes *NFE2l2*, *Sod1*, *Sod2*, *Sod3*, *Cat*, *Hmox1*, *and Hif1α* normalized to *Ubc* and quantified by qPCR in conceptuses taken from IP TNF null and IP B6 mice. Group medians and transcript abundance in individual mice are depicted. #P = 0.051.

Sample sizes: B6 IP, n = 4; TNF IP, n = 4; *ns* = not significant, P > 0.05.

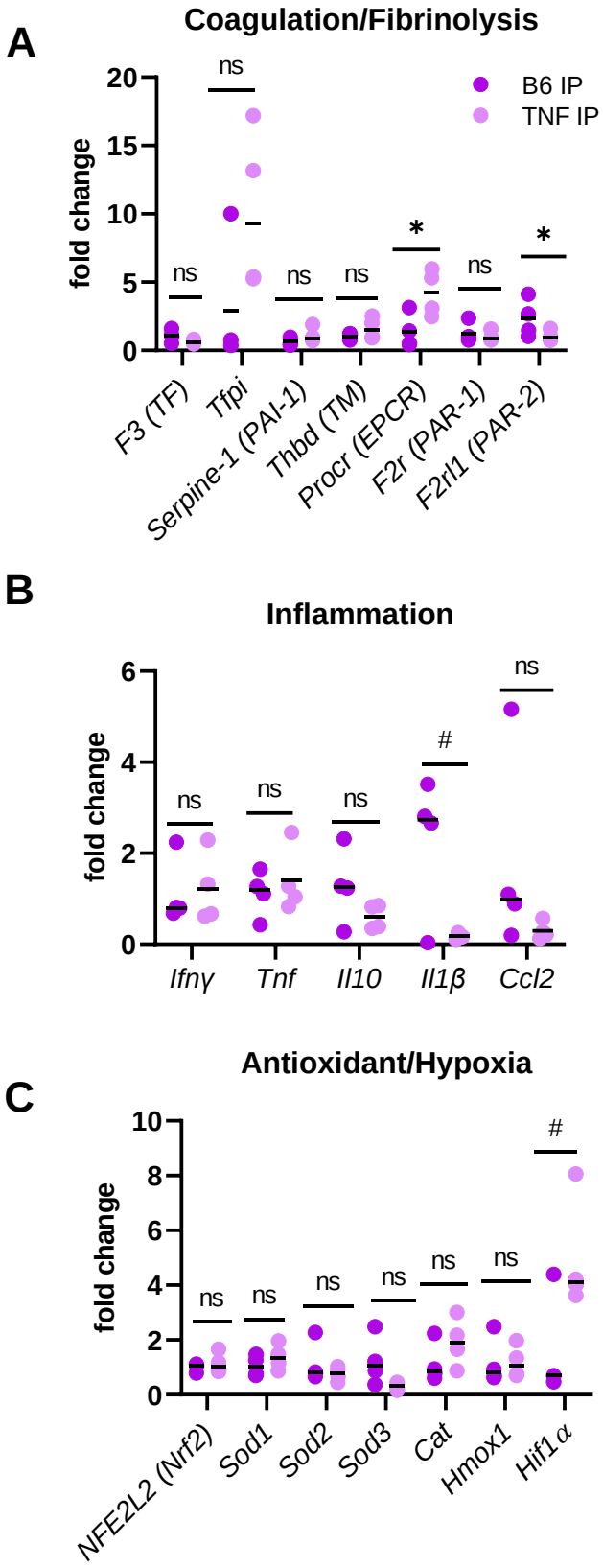
A
Coagulation/Fibrinolysis
B6 IP
TNF IP
fold change
20
15
10
5
0
ns
ns
ns
ns
*
ns
*
F3 (TF)
Tfpi
Serpine-1 (PAI-1)
Thbd (TM)
Procr (EPCR)
F2r (PAR-1)
F2rl1 (PAR-2)
B
Inflammation
fold change
6
4
2
0
ns
ns
ns
#
ns
Ifnγ
Tnf
Il10
Il1β
Ccl2
C
Antioxidant/Hypoxia
fold change
10
8
6
4
2
0
ns
ns
ns
ns
ns
ns
#
NFE2L2 (Nrf2)
Sod1
Sod2
Sod3
Cat
Hmox1
Hif1α

Figure 2.5. Low molecular weight heparin treatment in *P. chabaudi*-infected B6 mice modulates transcript expression of inflammatory and antioxidant genes.

A) Transcript abundance for inflammation-associated mouse genes *Ifnγ*, *Tnf*, *Il10*, *Il1β, and Ccl2* normalized to *Ubc* and quantified by qPCR in conceptuses taken from infected pregnant (IP) low molecular weight heparin (LMWH)-treated and sham-treated mice. Group medians and transcript abundance in individual mice are depicted. ***P < 0.0001, **P = 0.004, *P < 0.05.

B) Transcript abundance for coagulation/fibrinolysis-related mouse genes *F3*, *Tfpi*, *Serpine1*, *Thbd*, *Procr*, *F2r*, and *F2rl1* normalized to *Ubc* and quantified by qPCR in conceptuses from IP TNF null and IP B6 mice. Group medians and transcript abundance in individual mice are depicted. *P < 0.05, #P = 0.073.

C) Transcript abundance for antioxidant mouse gene transcripts *NFE2l2*, *Sod1*, *Sod2*, *Sod3*, *Cat*, *Hmox1*, *and Hif1α* normalized to *Ubc* and quantified by qPCR in conceptuses taken from IP TNF null and IP B6 mice. Group medians and transcript abundance in individual mice are depicted. *P < 0.05.

Sample sizes: Sham-IP, n = 5; LMWH-IP, n = 5; *ns* = not significant, P > 0.05.

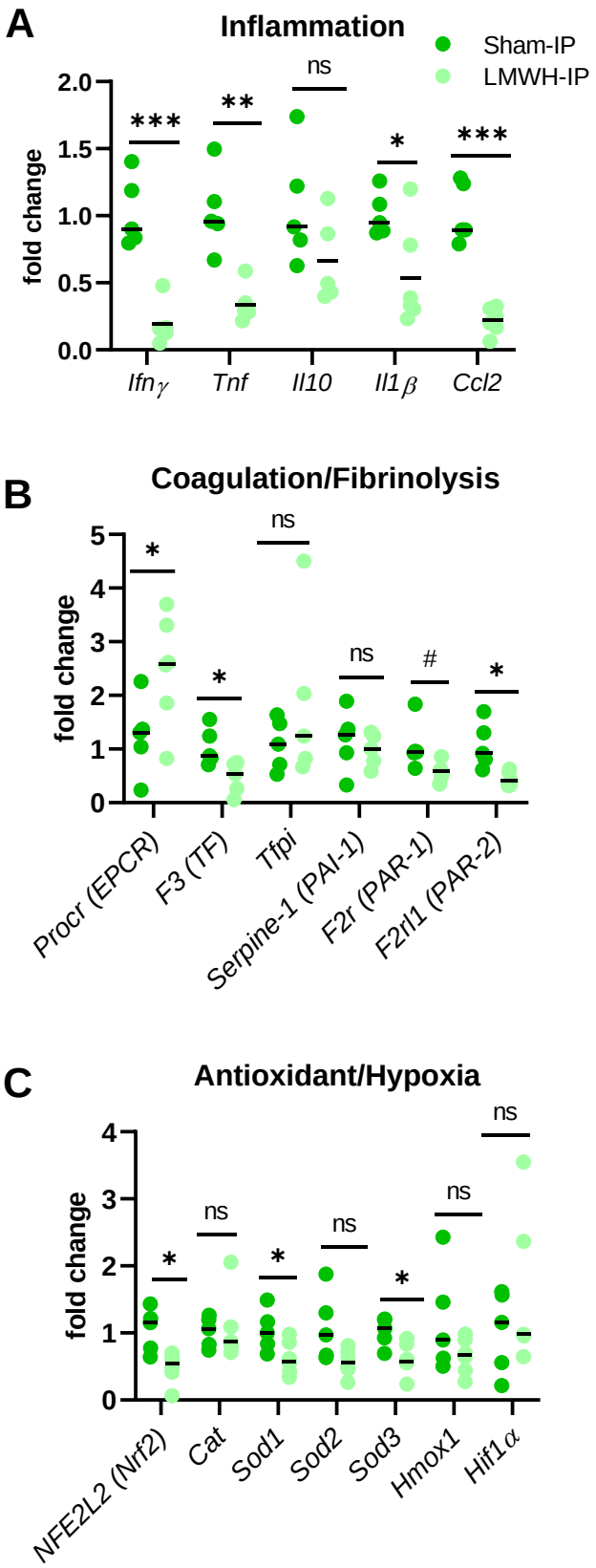
A
Inflammation
Sham-IP
LMWH-IP
fold change
2.0
1.5
1.0
0.5
0.0
***
**
ns
*
***
Ifnγ
Tnf
Il10
Il1β
Ccl2
B
Coagulation/Fibrinolysis
fold change
5
4
3
2
1
0
*
*
ns
ns
#
*
Procr (EPCR)
F3 (TF)
Tfpi
Serpine-1 (PAI-1)
F2r (PAR-1)
F2rl1 (PAR-2)
C
Antioxidant/Hypoxia
fold change
4
3
2
1
0
*
ns
*
ns
*
ns
ns
NFE2L2 (Nrf2)
Cat
Sod1
Sod2
Sod3
Hmox1
Hif1α

Table 2.2. Primer sequences for qPCR mouse targets.

Mouse-specific forward (FP) and reverse (RP) primers used in quantitative real-time PCR for the amplification of mRNA transcripts associated with inflammation, parturition, antioxidant activity, and reference (*Ubc*) genes.

Target	Forward and Reverse Primers (5' to 3')
Ubc	FP: CAGTGTTACCACCAAGAAGGT
	RP: GAAAACTAAGACACCTCCCCCA
Ifng	FP: AGCAAGGCGAAAAAGGATGC
	RP: CTTCCTGAGGCTGGATTCCG
Tnf	FP: ATCGGTCCCCAAAGGGATGA
	RP: GTCTTTGAGATCCATGCCGT
Il10	FP: CTGAAGACCCTCAGGATGCG
	RP: TGGCCTTGTAGACACCTTGG
Il1b	FP: TGAAGTTGACGGACCCCAAA
	RP: TGATACTGCCTGCCTGAAGC
Cox1	FP: GATTGTACTCGCACGGGCTAC
	RP: GGATAAGGTTGGACCGCACT
Cox2	FP: TGTGACTGTACCCGGACTGG
	RP: TGCACATTGTAAGTAGGTGGAC
Sod1	FP: GGAACCATCCACTTCGAGCA
	RP: CTGCACTGGTACAGCCTTGT
Sod2	FP: GGACCCATTGCAAGGAACAAC
	RP: TGAGTGAGGTTTCACTTCTTGC
Sod3	FP: GCAACTCAGAGGCTCTTCCTC
	RP: CCCCTGGATTTGACATGGTGA
Nrf2	FP: AGCCAGCTGACCTCCTTAGA
	RP: AGTGACTGACTGATGGCAGC
Cat	FP: CACTGACGAGATGGCACACT
	RP: TGTGGAGAATCGAACGGCAA
Hmox1	FP: CATAGCCCGGAGCCTGAATC
	RP: AGCATTCTCGGCTTGGATGT

Figure 2.6. Anticoagulant treatment reduces systemic plasma cytokine levels in *P. chabaudi*-infected B6 mice.

(A) Levels of plasma cytokines at E11.5 from B6 infected pregnant mice (IP) treated with low molecular weight (LMWH) from E6.5 to E11.5 and sham-treated controls. Datapoints shown are from individual mice with group medians. *P < 0.05, #P = 0.052; Sham-IP, *n* = 5; LMWH-IP, *n* = 5.

(B) Levels of plasma cytokines at E12.5 from B6 IP mice treated with anticoagulant, Dalteparin from E6.5 to E11.5 and sham-treated controls. Datapoints shown are from individual mice with group medians. **P = 0.004, #P = 0.06; Sham-IP, *n* = 3; Dalteparin-IP, *n* =3.

(C) Levels of plasma cytokines at E12.5 from B6 IP mice treated with an anticoagulant, Fondaparinux, from E6.5 to E11.5, and sham-treated controls. Datapoints shown are from individual mice with group medians. *P = 0.01; Sham-IP, *n* = 5; Fondaparinux-IP, *n* = 5.

(D) Levels of plasma cytokines at E10.5 in B6 IP mice treated with anti-tissue factor (1H1) antibody and sham-treated controls. Datapoints shown are from individual mice with group medians. No statistically significant differences were observed. *ns* = not significant, P > 0.05; Sham-IP, *n* = 3; 1H1-IP, *n* = 3.

(E) Levels of plasma cytokines at E12.5 in endothelial tissue factor-deficient (TFΔEc) and tissue factor-intact ($F3^{fl/fl}$) IP mice. Datapoints shown are from individual mice with group medians. No statistically significant differences were observed. *ns* = not significant, P > 0.05; TFΔEc, *n* = 5; $F3^{fl/fl}$, *n* = 5.

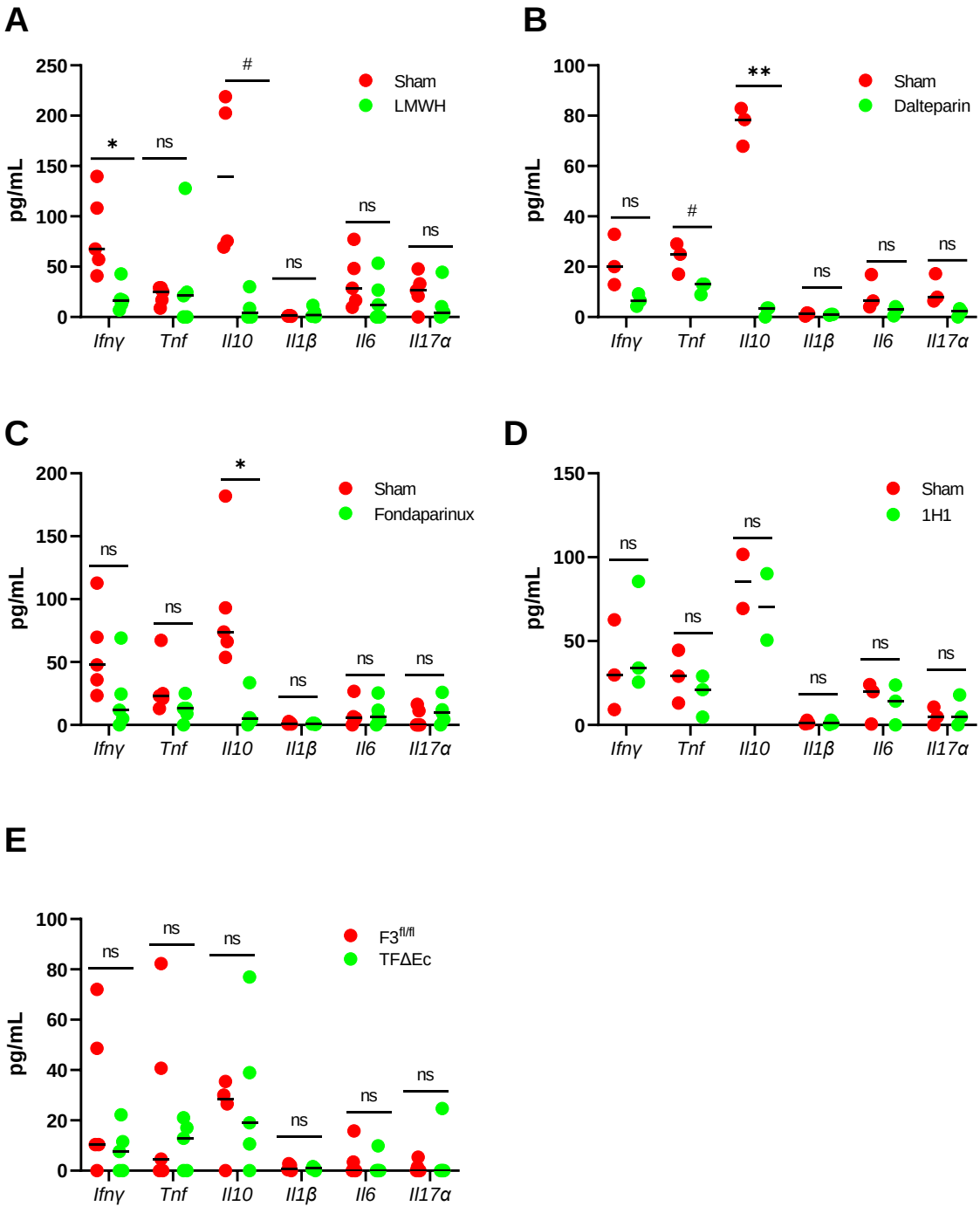
A
B
C
D
E
pg/mL
Sham
LMWH
Dalteparin
Fondaparinux
1H1
F3fl/fl
TFΔEc
Ifnγ
Tnf
Il10
Il1β
Il6
Il17α
ns
#
*
**

Figure 2.7. Weight change, parasitemia, and hematocrit in malaria-infected anti-tissue factor (1H1) treated B6 mice.

A) Percent starting weight in infected pregnant (IP) B6 sham treated and IP B6 1H1 treated mice beginning on E0.5 and then from E6.5 to E10.5. Data represent mean ± SEM.
B) Area under the curve (AUC) analysis of starting weight measurements collected on E0.5 through E10.5. No statistical differences were found between groups (P = 0.74; unpaired t-test with Welsh's correction).
C) Percent peripheral parasitemia (IRBCs) in IP B6 sham treated and IP B6 1H1 treated mice from E6.5 to E10.5. Data represent mean ± SEM.
D) AUC analysis for percent peripheral parasitemia from E6.5 to E10.5. No statistically significant differences were found between groups (#P = 0.08; unpaired t-test with Welch's correction).
E) Percent hematocrit in IP B6 sham treated and IP B6 1H1 treated mice measured on E0.5 and then from E6.5 to E10.5. Data represent mean ± SEM.
F) AUC analysis for percent hematocrit from E6.5 to E10.5. No statistically significant differences were found between groups (P = 0.51; unpaired t-test with Welch's correction).

Sample sizes: Sham-IP, *n* =7; 1H1-IP, *n* = 8; *ns* = not significant, P > 0.05. Error bars are not depicted if they are shorter than the height of the symbol.

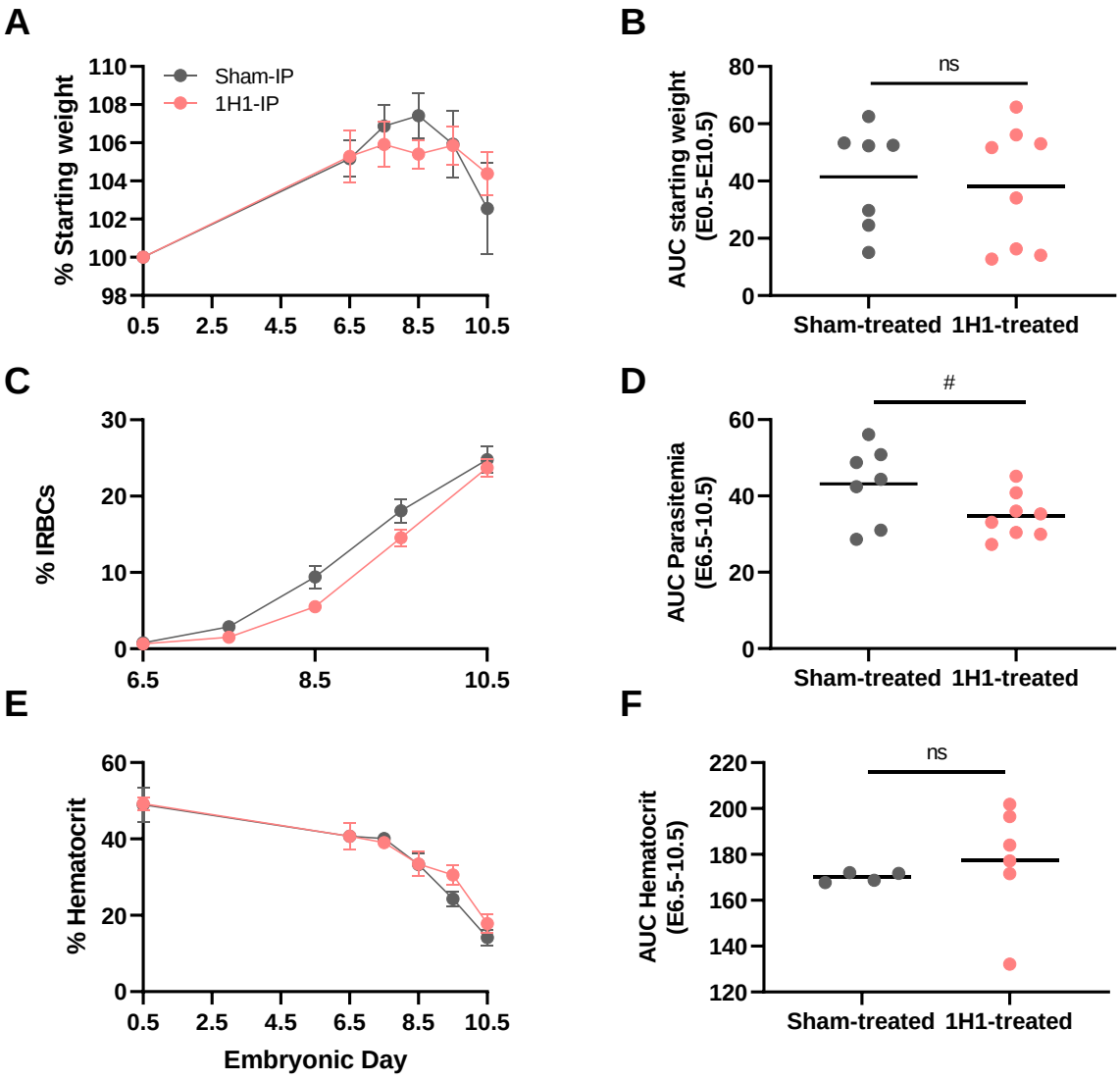
A
% Starting weight
Sham-IP
1H1-IP
110
108
106
104
102
100
98
0.5
2.5
4.5
6.5
8.5
10.5
B
AUC starting weight (E0.5-E10.5)
ns
80
60
40
20
0
Sham-treated
1H1-treated
C
% IRBCs
30
20
10
0
6.5
8.5
10.5
D
AUC Parasitemia (E6.5-10.5)
#
60
40
20
0
Sham-treated
1H1-treated
E
% Hematocrit
60
40
20
0
0.5
2.5
4.5
6.5
8.5
10.5
Embryonic Day
F
AUC Hematocrit (E6.5-10.5)
ns
220
200
180
160
140
120
Sham-treated
1H1-treated

Figure 2.8. Maternal weight and hematocrit at E10.5 in mice treated with 1H1.

A) Percent parasitemia in (IP) B6 sham treated and IP B6 1H1 treated mice on E8.5/8 days post-infection. Statistically significant differences are detected between the groups (*P = 0.04).
B) Percent parasitemia (IRBCs) B6 sham treated and IP B6 1H1 treated mice on E9.5/9 days post-infection. No statistically significant differences are detected between the groups (#P = 0.094).
C) Percent starting weight in infected pregnant IP B6 sham treated and IP B6 1H1 treated mice on the final day of the experiment, E10.5. No statistically significant differences are detected between the groups (P = 0.51).
D) Percent hematocrit in IP B6 sham treated and IP B6 1H1 treated mice on the final day of the experiment, E10.5. No statistically significant differences are detected between the groups (P = 0.38).

Sample sizes: Sham-IP, *n* =7; 1H1-IP, *n* = 8; *ns* = not significant, P > 0.05.

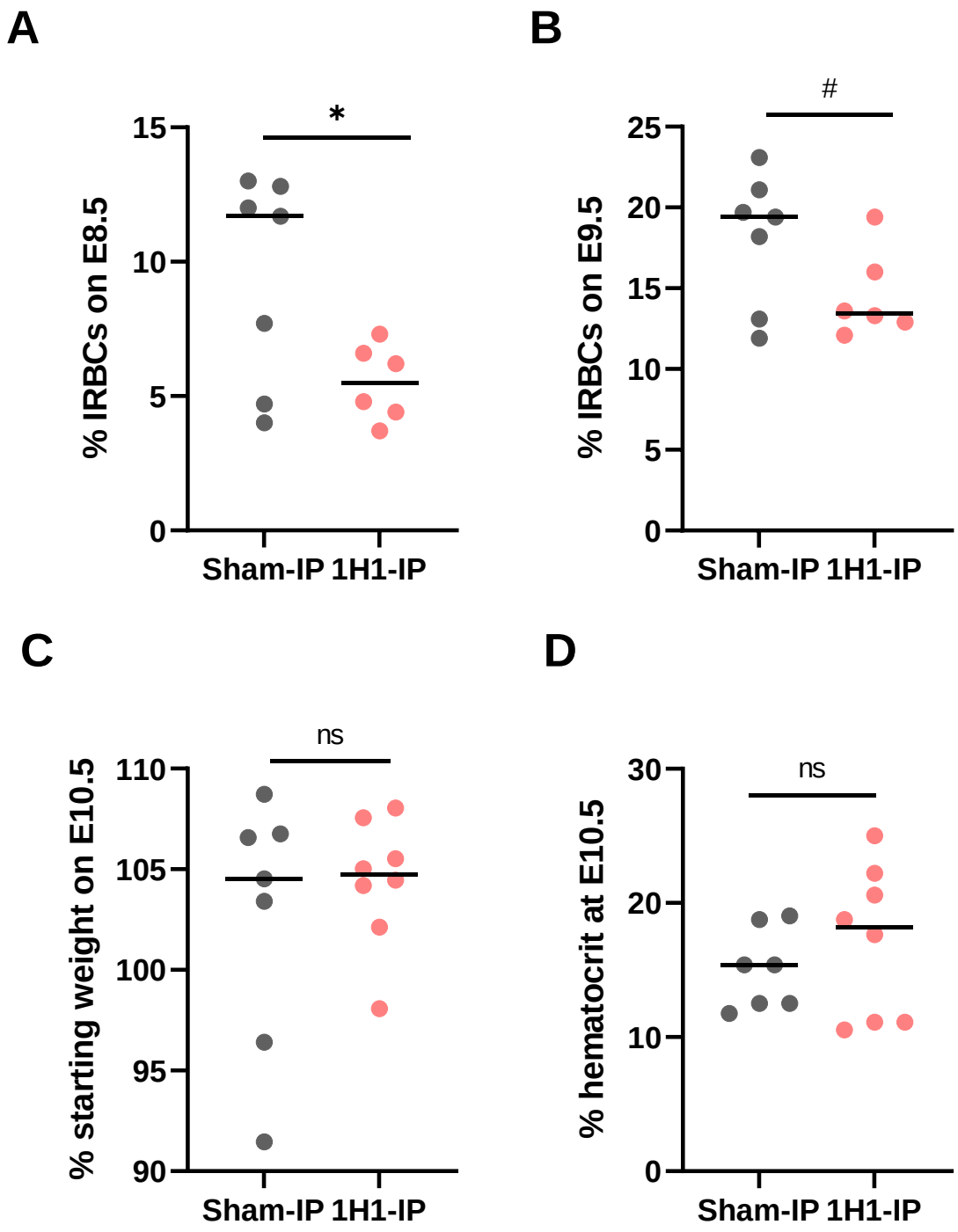
A
*
15
10
5
0
% IRBCs on E8.5
Sham-IP
1H1-IP
B
#
25
20
15
10
5
0
% IRBCs on E9.5
Sham-IP
1H1-IP
C
ns
110
105
100
95
90
% starting weight on E10.5
Sham-IP
1H1-IP
D
ns
30
20
10
0
% hematocrit at E10.5
Sham-IP
1H1-IP

Figure 2.9. Uterus weight in 1H1-treated malaria-infected mice at E10.5.

Uterus weight is presented for infected pregnant (IP) sham-treated B6 and IP 1H1 treated B6 mice. No statistical significance revealed between groups (P = 0.69; unpaired t test with Welsh's correction). Sample sizes: Sham-IP, *n* =7; 1H1-IP, *n* = 6; *ns* = not significant, P > 0.05.

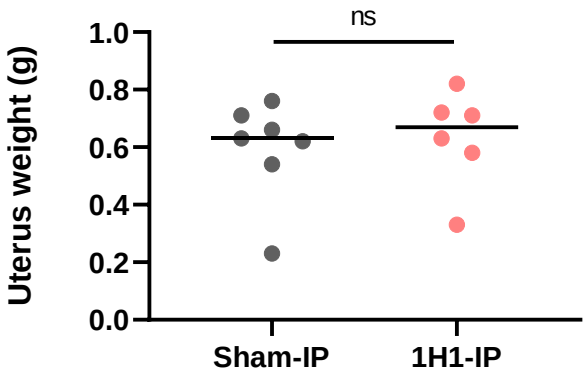

Table 2.3. Embryo viability in malaria-infected wildtype B6 mice treated with anti-tissue factor (1H1) antibody.

Embryo viability in uninfected pregnant (UP), infected pregnant (IP) B6 sham treated, and IP B6 anti-tissue factor antibody (1H1) treated mice at mid-gestation. Percentages show percent viability within a group. P value was obtained with a two-tailed Fisher exact probability test, comparing embryo viability in sham-treated versus 1H1 treated groups. $P < 0.05$ is statistically significant.

Group	**Viable/total embryos (10.5)**	**Viable/total embryos (E10.5)**	
	Sham-treated	1H1-treated	P value
UP	NA	16/16 (100%) n=2	NA
IP	47/69 (68.1%) n=10	49/53 (92%) n=7	**0.001**

Figure 2.10. 1H1 treatment does not alter transcript expression for select inflammation and coagulation-related genes.

Transcript abundance for inflammation-associated mouse genes *Ifnγ*, *Tnf*, *Il10*, *Il1β*, *Ccl2* and coagulation-related genes *F2r*, *F2rl1*, and *Procr* are normalized to *Ubc* and quantified by qPCR in conceptuses taken from infected pregnant (IP) 1H1-treated and sham-treated mice. Group means and transcript abundance in individual mice are depicted. No statistically significant changes were observed. *ns* = not significant, P > 0.05. Sample sizes: Sham-IP, *n* =4; 1H1-IP, *n* = 5.

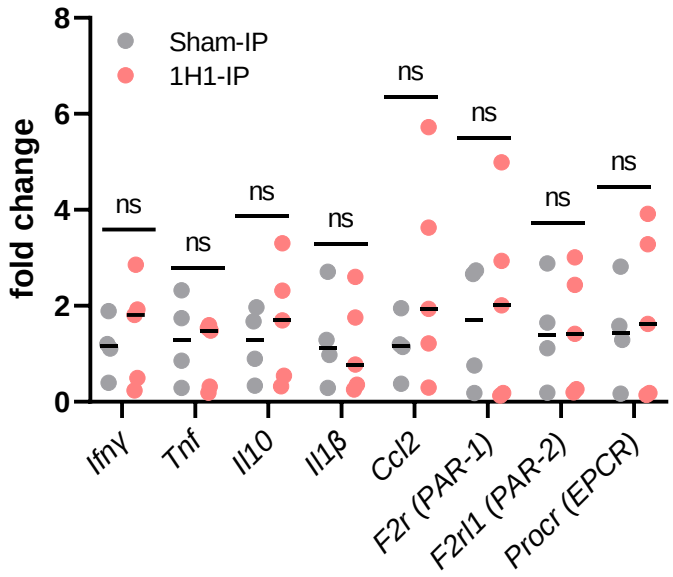

CHAPTER 3

A ROLE FOR OXIDATIVE STRESS IN PLACENTAL MALARIA[3]

[3] Andrew AK, Moore JM. To be submitted to *Malaria Journal*.

Abstract

Oxidative stress is a naturally occurring phenomenon that can have both positive and harmful biological effects. It can be broadly characterized as an imbalance between prooxidant and antioxidant mechanisms in a system, where the prooxidant input outweighs the antioxidant defenses of a host cell or pathogen. Recently, studies have interrogated oxidative stress in humans and murine models of PM and highlighted differential expression in oxidative stress markers, such as malondialdehyde (MDA) and 4-hydroxynonenal (HNE), in various tissue types in the presence of malaria infection. Moreover, activation of the inflammation and coagulation responses can induce oxidative stress, contributing to disease pathogenesis if left unchecked. This work aims to further characterize the presence of oxidative stress in murine models of PM and determine whether therapeutic interventions that limit oxidative stress can improve pregnancy outcomes. We hypothesized that antioxidant drug treatment that targets heme/iron toxicity, mitochondrial oxidative stress, or reactive oxygen species (ROS)-mediated oxidative damage will improve pregnancy outcomes during malaria infection. Our secondary hypothesis is that ferroptosis, the iron and ROS-dependent form of cell death, occurs in the placenta during PM and is associated with poor birth outcomes. We found that systemic administration of drugs against various contributors to oxidative stress may have off-target effects and be inefficient at improving pregnancy outcomes during malaria. Future studies should incorporate drugs that act specifically on the placenta and investigate redox systems that were not targeted in this work for their potential as therapeutic targets for PM.

Introduction

Reactive oxygen, nitrogen, sulfur, and carbonyl species are among the tightly regulated molecules that mediate a cell's essential metabolic, homeostatic, and protective functions [181]. These molecules are produced by organelles such as the mitochondria and the endoplasmic reticulum and, when left unchecked, can induce oxidative damage to cellular components such as DNA, RNA, protein, and lipids [255]. Due to the biological nature of these molecules, cells engage enzymatic and nonenzymatic defense mechanisms that control these reactive species and prevent excessive oxidative damage. However, when these defense systems fail or their activity is insufficient to protect against oxidative damage, a phenomenon known as oxidative stress occurs, which is described as an imbalance between oxidants and antioxidant defenses in favor of the oxidants. Biological markers of oxidative stress can be identified based on the cellular component being oxidized. For instance, the oxidation of lipids yields products such as malondialdehyde (MDA) and 4-hydroxynonenal (HNE), which can be quantified to estimate the level of oxidative stress occurring in the tissue [181].

Reactive oxygen species (ROS) are involved in signal transduction, redox homeostasis, energy production and utilization, and cellular defense against foreign agents. At the same time, ROS can induce oxidative stress under pathological conditions, which in turn may cause damage to cellular components and ultimately lead to cell death. For example, the reduction of molecular oxygen can produce highly reactive forms of ROS, including superoxide ion (O_2^-), hydroxide ion (OH^-), hydrogen peroxide (H_2O_2), peroxyl radicals (ROO^-), and lipid peroxides (ROOH). These ROS can then directly engage in signaling cascades required for cell death via apoptosis, necroptosis,

pyroptosis, and ferroptosis [192,256–258]. The effects of these ROS are controlled by cellular buffering systems such as glutathione-glutathione disulfide (GSH/GSSH), enzymatic antioxidants such as superoxide dismutases (SODs), catalase (CAT), and glutathione peroxidases (GPXs) and nonenzymatic antioxidants such as α-tocopherol (vitamin E), ascorbate (vitamin C), and others [259,260]. In particular, glutathione peroxidase 4 (GPX4) has been described as a master inhibitor of the iron-, lipid peroxidation-, and ROS-dependent form of programmed cell death called ferroptosis.

Ferroptosis was first described in 2012 and has attracted interest in determining its involvement in many pathological conditions and diseases, including cancer, ischemia-reperfusion injury, and neurodegenerative disease [261]. This form of programmed cell death is genetically, biochemically, and morphologically distinct from other forms of cell death and specifically requires intracellular iron overload, ROS accumulation, and lipid peroxidation. Intracellular iron overload can occur due to mechanisms that alter the appropriate absorption, utilization, storage, or release of iron and its derivatives, such as heme or iron-sulfur clusters [256]. Iron stored in labile pools in the cytosol and lysosomes and catabolism of ferritin, an iron storage molecule, can participate in the Fenton reaction and contribute to ROS production [190,256]. Other sources of ROS include the mitochondria due to superoxide ion leakage from the electron transport chain [262]. Mitochondrial superoxide dismutase, also known as SOD2, is responsible for scavenging these superoxide ions and protecting the organelle from oxidative damage [263], while cytoplasmic SOD1 and extracellular SOD3 provide similar protection in other cellular compartments [189]. Potentially harmful ROS is generated through the enzymatic activity of redox systems such as nicotinamide adenine dinucleotide phosphate

(NADPH) oxidases (NOXs) and xanthine oxidase [192,264]. Lipoxygenase, cyclooxygenase, and epoxygenase enzymes contribute to ROS production by generating lipid peroxide byproducts during fatty acid synthesis [265]. These lipid peroxides can initiate ferroptosis under pathological conditions [264,266–269].

Ferroptosis has been described in an immortalized placental cell line called BeWo cells [270], rodent models of pregnancy and hemostatic complications [271,272], and primary human trophoblasts [270,273]. Ferroptosis has also been implicated in the pathogenesis of preeclampsia [274,275]. Preeclampsia and placental malaria (PM) share many similarities [135], including disruptions in iron homeostasis [276–279]. Moreover, heme, an iron-containing molecule, is elevated in malaria-positive pregnant women [278], and excessive heme can mediate damage to trophoblast cells and provide a source of iron to drive ROS production and ferroptosis [280–282]. Since heme is a component of hemozoin [199], which is deposited in the placenta during malaria infection [283–285], we surmised that iron overload due to hemozoin deposition might be capable of triggering ferroptosis in our murine models of PM. Moreover, we investigated the expression of various markers of ferroptosis in samples obtained from endemically-exposed malaria-positive and malaria-negative women.

C57BL6/J (B6) mice infected with *Plasmodium chabaudi chabaudi* AS (*Pcc*AS) experience placental lipid peroxidation and elevated antioxidant transcript expression in their embryos compared to uninfected pregnant (UP) mice [18]. Additionally, pregnancy loss in this model was partially but significantly rescued by antioxidant treatment [18]. Hemozoin was highly deposited in the placenta and accompanied by elevated expression of heme oxygenase (*Hmox1*), the enzyme that detoxifies free heme [18]. In another

mouse model, outbred *Pcc*AS-infected Swiss Webster (SW) mice demonstrated an ability to carry their pregnancies to term despite significant parasite burden, inflammatory cell infiltrate, and hemozoin deposition in the placenta [286]. Although placental and fetal weights were indistinguishable between infected pregnant (IP) dams and UP controls at term, uterus weight at peak parasitemia, E10.5, was significantly reduced in IP mice, suggesting that malaria infection does impact pregnancy success in this model. This impact on uterus weight is accompanied by increased *Hmox1* transcript expression, which positively correlates with the percent of hemozoin deposited in the placenta at the same time point. Using the SW model, the following experiments seek to test the hypothesis that drug interventions that target various sources of oxidative stress as a means of directly or indirectly inhibiting ferroptosis will lead to improved pregnancy outcomes during malaria infection.

Materials and Methods

Mice

NCI BALB/cAnNCr (BALB/c) and Swiss Webster (Cw:SW) were purchased from Charles River (Frederick, MD) and the National Cancer Institute Mouse Repository (Frederick, MD), respectively. Mice were housed in the University of Florida's Veterinary Metabolic Building under specific pathogen-free conditions and free of mouse norovirus and *Helicobacter* species, which has been shown to affect pregnancy success [237]. All husbandry and experiments were performed following guidelines and regulations set forth by the University of Florida (UF) Animal Care and Use Committee (IACUC). All animals were supplied food (Takland, Global 18% protein Extruded

Rodent Diet, irradiated, #2918) and water ad libitum. Mice were adjusted to a 12-hour light/12-hour dark cycle and housed in 65-75 ˚F and 40-60% humidity conditions. All animal procedures reported in this study were reviewed and approved by the UF IACUC, protocol number 201810169. Mice were anesthetized with 2.5% Tribromoethanol or isoflurane inhalation before sacrifice, and all efforts were made to minimize suffering.

Parasites and infection monitoring

The following reagent was obtained through BEI Resource Repository, NIAID, NIH: *Plasmodium chabaudi chabaudi*, Strain AS, MR4-741, contributed by David Walliker. Parasites were maintained as frozen stock according to supplier guidelines and passaged in BALB/c mice for the purposes of infecting experimental Swiss Webster (SW) mice. Peripheral parasitemia was assessed by flow cytometry with a method adapted from work published by Jimenez-Diaz et al. [238]. A 2µl blood sample was collected by tail clip [239], diluted in 98µl 0.9% NaCl and stained with 0.25µl SYTO-16 Green Fluorescent Nucleic Acid Stain (ThermoFisher Scientific, catalog # S7578) within 4 hours of collection. Stained samples were incubated in the dark for 20 minutes at room temperature, further diluted 1:9 in 0.9% NaCl, then analyzed using an Attune NxT flow cytometer and Attune NxT software version v3.1.2. A total of 30,000 cells were assessed daily for each mouse; infected red blood cells were distinguished based on size and fluorescence intensity. An uninfected blood sample was used as an internal negative control. Parasitemia is reported as the percentage of infected red blood cells (IRBCs) to the total number of red blood cells (RBCs).

Experimental Design

Female SW mice aged 8-12 weeks were paired with males nightly and examined each morning until a vaginal plug was observed, indicating successful mating. The morning a vaginal plug was observed was considered embryonic day 0.5 (E0.5). After baseline measurements of weight and hematocrit were recorded, females were left undisturbed until E6.5 to minimize stress and increase the chances of successful blastocyst implantation. Mice were infected intravenously with 1000 *P. chabaudi chabaudi* AS-iRBCs diluted in 200ul 1X phosphate-buffered saline (PBS) per 20 grams of body weight and are termed infected pregnant (IP). As a control group, uninfected pregnant (UP) mice were sham injected with 200ul PBS per 20 grams body weight on E0.5. Immediately prior to infection or sham infection, experimental animals were switched to a high-fat rodent chow (Teklad Global 19% Protein Extruded Rodent Diet, irradiated, #2919) suited for pregnant animals. Weight measurements were recorded on E0.5 and E6.5 through E10.5 or E12.5 to assess uterus weight as a proxy for pregnancy outcome, as in previous studies [286]. Parasitemia and hematocrit (a measure of anemia) were monitored daily in the infected groups beginning on E6.5 to assess the development of infection. At sacrifice, embryo viability was assessed, as previously described [10]. Embryos exhibiting extensive hemorrhaging and/or necrosis or described as unusually small and pale for gestational age compared to embryos from UP controls were scored as nonviable.

In one experiment, mice received 5mg/kg of ferroptosis inhibitor, SRS16-86 (Cayman Chemical, item no. 26752), or sham treatment (1% DMSO) via intraperitoneal injection (i.p.) twice daily (2.5mg/kg per dose) on E6.5 through E11.5 (5 total doses) and

mice were euthanized on E12.5. In another experiment, mice received 70mg/kg of Deferoxamine mesylate salt (DFO, Millipore sigma, SKU D9533) or sham treatment (1X PBS) via i.p injection once daily between E6.5 through E9.5 (4 doses) and mice were euthanized on E10.5. In a final experiment, mice received 1mg/kg of the mitochondria-specific antioxidant, MitoTempo (Millipore sigma, SKU SML0737), or sham treatment (2.5% DMSO) once daily via i.p injection between E6.5 and E9.5 (4 doses) and mice were euthanized on E10.5. Since *Plasmodium chabaudi* is synchronous and the mammalian host's circadian rhythm dictates its erythrocytic cell cycle, both DFO and MitoTempo were delivered between 12-2 AM to ensure that the drug delivery coincides with peak heme/hemozoin expulsion into the bloodstream and to account for the unknown half-life of MitoTempol [287,288].

Real-time quantitative PCR

Total RNA was isolated from placental tissues collected from PM-positive (PM+) and PM-negative (PM-) women at the time of delivery and stored in liquid nitrogen. Tissues were rinsed with PBS to remove intervillous blood and assess a transcript pool mainly derived from the placental cells with limited maternal cell contribution. A detailed description of the study that generated these samples is described in [10]. RNA was isolated using (Qiagen RNeasy Mini Kit, Cat # 74104) DNase-treated (Invitrogen, Ref # AM1906) and reverse-transcribed with High-Capacity cDNA Reverse Transcription Kit (Applied Biosystems, Ref # 4368814). Relative transcript abundance for the genes of interest was quantified using PowerSYBR Green PCR Master Mix (Applied Biosystems, Cat # 4367659) and the BioRad CFx92 Real-Time system, and Cq values were obtained

from the CFX Maestro software version 2.0. Housekeeping genes recommended for more reliable human placental transcript expression were selected [289,290], and each sample was assayed in duplicate for the target and the housekeeping genes. Average Ct values of target genes were normalized to geometric mean Ct values of *Ck19* and *Top1* as the reference genes, and the relative transcript abundance of genes of interest was determined using the ΔΔCt method. Details of primer sets are summarized in Table 3.4

Western blot analysis

Placental villous tissue was homogenized in RIPA buffer, and proteins were extracted and quantified as described [291]. Proteins (2ug/ul) were separated by SDS-PAGE, blotted onto nitrocellulose membranes, and probed with recombinant anti-glutathione peroxidase 4 (Abcam, ab125066) or anti-beta actin antibody. Overnight incubation with primary antibody was followed by one-hour incubation with anti-rabbit horseradish peroxidase secondary antibody conjugates. Proteins were detected using a chemiluminescence reagent (details in notebook) and the ChemiDoc Touch Imaging System with Image Lab Touch Software (Biorad). Densitometry data are presented as a ratio of GPX4 protein to beta-actin.

Statistics

All statistical analyses were performed using GraphPad Prism version 9.2.0 (GraphPad Software; La Jolla, California). All raw clinical data are presented as mean ± SEM. Error bars are not visible if they are shorter than the symbol's height. The area under the curve (AUC) of percent starting weight, hematocrit, and parasitemia was

calculated for each mouse between E0.5 and E10.5 or E12.5, as appropriate, and sometimes percent starting weight at either E10.5 or E12.5 alone was compared between groups, using two-tailed unpaired t-test, with Welch's correction. AUC for weight, hematocrit, and parasitemia was compared between IP treated and IP sham mice using a two-tailed unpaired t-test with Welch's correction. Percent starting hematocrit on E12.5 and parasitemia on E8.5, E9.5, and E12.5 were compared between groups for the 16-86 treatment study, using a two-tailed unpaired t-test with Welch's correction. Proportional analysis tested by Fisher exact probability test was used to compare embryo viability between IP treated and IP sham dams. P values less than or equal to 0.05 were considered statistically significant.

Results

Iron chelation with deferoxamine treatment in Swiss Webster mice significantly reduces parasite burden and improves pregnancy outcome

Deferoxamine (DFO) is an iron chelator drug that has been approved by the Federal Drug Administration (FDA) and has been used to treat iron overload in adults and children for many years [292]. DFO binds to iron in a 1 to 1 ratio and can bind free plasma iron and intracellular labile iron pools without interfering with iron that is already bound to iron regulatory molecules such as transferrin and ferritin [293]. This characteristic makes DFO an efficient iron chelator that is well-tolerated and readily excreted in the urine or bile. To determine whether iron chelation could improve pregnancy outcomes in *Plasmodium chabaudi chabaudi* AS (*Pcc*AS)-infected, pregnant (IP) Swiss Webster (SW) mice at E10.5, dams received 70mg/kg DFO once a day

between E6.5 and E9.5 (Figure 3.1). DFO administration was timed with predicted parasite egress from the erythrocyte [287], to ensure that chelation would occur at peak heme/iron release into the bloodstream in light of DFO's short half-life [294]. DFO- and sham-treated mice experienced comparable weight changes throughout the experiment (Figure 3.1A-B); however, parasitemia was significantly lower in DFO-treated mice by area under the curve (AUC) analysis (Figure 3.1C-D). Hematocrit, a measure of anemia, had a weak tendency to be higher in DFO-treated dams compared to sham controls, (Figure 3.1E-F) as expected for animals with lower parasite burdens and, as a result, less parasite-driven hemolysis [295]. Likewise, uterus weight was improved in DFO-treated dams compared to controls (Figure 3.2); however, no significant changes in embryo viability were observed in either group (Table 3.1).

16-86 treatment in Swiss Webster mice worsened clinical measurements and did not improve pregnancy outcome

An alternative and more direct approach was taken to address the impact of ROS on pregnancy outcomes in IP SW mice. SRS16-86 (16-86) is a specific ferroptosis-inhibiting drug targeting ROS generated from lipids [296]. It is more stable and potent than its predecessor drug, Ferrostatin-1, and successfully decreases lipid peroxidation in models of ferroptosis-induced cell death [296,297]. In this experiment, SW IP mice were treated twice daily with 2.5mg/kg 16-86 from E6.5 through E11.5 or E12.5 (Figure 3.3). Although IP dams that received 16-86 displayed more visible signs of drug-induced morbidity than sham treated controls, defined as increased sensitivity at the injection site and labored breathing, the treatment did not result in statistically significant weight

changes, as demonstrated by AUC analysis (Figure 3.3A-B). Additionally, neither parasite burden nor hematocrit differed between the groups (Figure 3.3C-F), and uterus weights were not statistically different (Figure 3.4). Even though no differences were detected statistically in these clinical parameters over the course of the experiment, 16-86-treated dams weighed significantly less at the end of the experiment (E12.5) than their sham-treated counterparts (Figure 3.5A) and experienced a marked reduction in embryo viability (Table 3.2), suggesting that the drug had embryotoxic effects. The parasitemia at sacrifice was significantly decreased in the 16-86 treated group at E12.5 (Figure 3.5B), perhaps due to drug-induced increased parasitemia at earlier timepoints, as demonstrated by parasite burdens at E8.5 and E9.5 (Figure 3.5C-D).

MitoTempol treatment in Swiss Webster mice had no impact on pregnancy outcome

Mitochondria are a major source of intracellular ROS production. The role of mitochondria-derived oxidative stress in promoting cell death [298], including ferroptosis [299–301], and poor pregnancy outcomes [302,303], has widely been studied. To evaluate the therapeutic potential of mitochondria ROS-targeting drug intervention in *Pcc*AS-infected SW mice, a mitochondrial antioxidant drug called Mitotempo was administered once daily from E6.5 to E9.5. Mitotempo is a superoxide scavenger that readily enters the cell and accumulates in the mitochondria to modulate oxidative stress [304]. We hypothesized that if mitochondrial ROS contributes to oxidative stress and is involved in PM pathogenesis in our model, mice treated with Mitotempo will enjoy improved pregnancy outcomes at midgestation. Mitotempo treatment did not impact weight change, parasitemia, or hematocrit in IP mice compared to sham treated controls

(Figure 3.6). Additionally, treatment did not improve uterus weight or embryo viability (Figure 3.7; Table 3.3) at E10.5.

Discussion

Oxidative stress has been associated with malaria severity [197] and with malaria infection during pregnancy [16]. Recent studies conducted using C56BL6/J mice and *Plasmodium chabaudi chabaudi* AS (*Pcc*AS) infection early during pregnancy revealed a therapeutic potential for antioxidant drug treatment to improve pregnancy outcomes in a murine PM [18]. Since then, Swiss Webster mice infected with *Pcc*AS have provided an alternative model for PM, with remarkable inflammatory cell infiltration and hemozoin deposition in the placenta at midgestation (E10.5) and a significant reduction in uterus weight at the same time point [286]. Additionally, transcript expression for the heme scavenger, *Hmox1*, was significantly elevated in the placenta of infected SW mice, suggesting that heme or iron overload may be occurring in this model and possibly influencing pregnancy success.

To address these suspicions, we first tried to chelate excess iron in infected pregnant (IP) SW mice using the commonly used drug, Deferoxamine (DFO). DFO treatment improved uterus weight, our proxy for pregnancy success at midgestation; however, it did so in association with significantly reduced parasite burden. This outcome supports previously published work that reports the dual-activity of DFO as both an iron chelator and an antimalarial, independently of host iron status [305–307]. DFO has also been proposed to have antioxidant capabilities by inhibiting heme production and quenching ROS [308,309]. As a result, DFO may be best used in addition to antimalarial

drugs, especially in the face of growing parasite resistance to antimalarials. This possibility, however, will require meticulous examination, as one study has already found that simultaneous DFO and chloroquine treatment produced an antagonistic effect and permitted increased rates of hemozoin generation *in vitro* [310]. In addition, future experiments should aim to determine the extent to which DFO can specifically inhibit iron or heme-driven ROS generation in the placenta during malaria infection and whether iron chelation can protect pregnancies from malaria-induced ROS and cell death.

In another set of experiments, we interrogated the possibility that ferroptotic cell death could be a pathogenic feature in the SW model of malaria infection. Since ferroptosis is explicitly driven by iron and ROS accumulation and lipid peroxidation, we investigated whether SRS16-86 (16-86), a specific ferroptosis inhibitor, can improve pregnancy outcomes at midgestation. Treatment with 16-86 in IP SW mice resulted in no improvements in uterus weight or alteration to overall maternal weight, parasitemia, or hematocrit. However, parasitemia in treated mice was increased on E8.5 and E9.5, and on the final day of the experiment, treated dams weighed significantly less than their sham treated counterparts. This observation was accompanied by a tremendous loss in embryo viability in treated mice compared to sham treated controls. Taken together, these data demonstrate that 16-86 treatment enhanced parasite burden and was embryotoxic. Nevertheless, it would be important to explore lower drug doses to discover whether 16-86 treatment can be beneficial in mitigating malaria-induced pregnancy compromise.

Finally, mitochondria-specific targeting of ROS was performed in IP SW mice using the mitochondria superoxide mimetic drug, Mitotempo. Mitotempo treatment did not improve uterus weight at midgestation and did not have an impact on parasite burden

or embryo viability. A prior study evaluating the antioxidant drug, Tempol, in *Pcc*AS-infected C57BL6/J mice demonstrated a modest but significant improvement in pregnancy outcomes due to drug treatment [18]. Moreover, Tempol treatment was variable in its ability to reduce placental oxidative stress successfully; however, when efficacious, Tempol treatment reduction in lipid peroxidation in the placental, which corresponded with improved embryo viability in infected dams [18]. Interestingly, Tempol treatment was consistently effective at reducing oxidative stress in the spleens of IP mice, highlighting the drug's organ-specific capability. Since Tempol and Mitotempo function similarly as intracellular superoxide dismutase mimetics, it is conceivable that Mitotempo's efficacy in the placenta is also limited. Thus, future studies that allow for tissue-specific delivery of Mitotempo and other antioxidant drugs will offer better insight into the impact of oxidative stress has on placental health, cell death, and, ultimately, pregnancy outcome.

Figure 3.1. Deferoxamine treatment in malaria-infected outbred Swiss Webster mice significantly reduces parasite burden.

A) Percent starting weight in infected pregnant (IP) Swiss Webster (SW) sham treated and IP SW Deferoxamine (DFO) treated mice beginning on E0.5 and then from E6.5 to E10.5. Data represent mean ± SEM.
B) Area under the curve (AUC) analysis of starting weight measurements collected on E6.5 to E10.5. No statistical differences were found between groups (P = 0.64; unpaired t-test with Welsh's correction).
C) Percent peripheral parasitemia (IRBCs) in IP SW sham treated and IP SW DFO treated mice from E6.5 to E10.5. Data represent mean ± SEM.
D) AUC analysis for percent peripheral parasitemia from E6.5 to E10.5. Parasitemia was significantly decreased in treated mice compared to sham treated controls (****P < 0.0001; unpaired t-test with Welch's correction).
E) Percent hematocrit in IP SW sham treated and IP SW DFO treated mice measured on E0.5 and then from E6.5 to E10.5. Data represent mean ± SEM.
F) AUC analysis for percent hematocrit from E6.5 to E10.5. No statistically significant differences were found between groups (#P = 0.070; unpaired t-test with Welch's correction).

Sample sizes: Sham-IP, *n* =7; DFO-IP, *n* = 8; *ns* = not significant, P > 0.05. Error bars are not depicted if they are shorter than the height of the symbol.

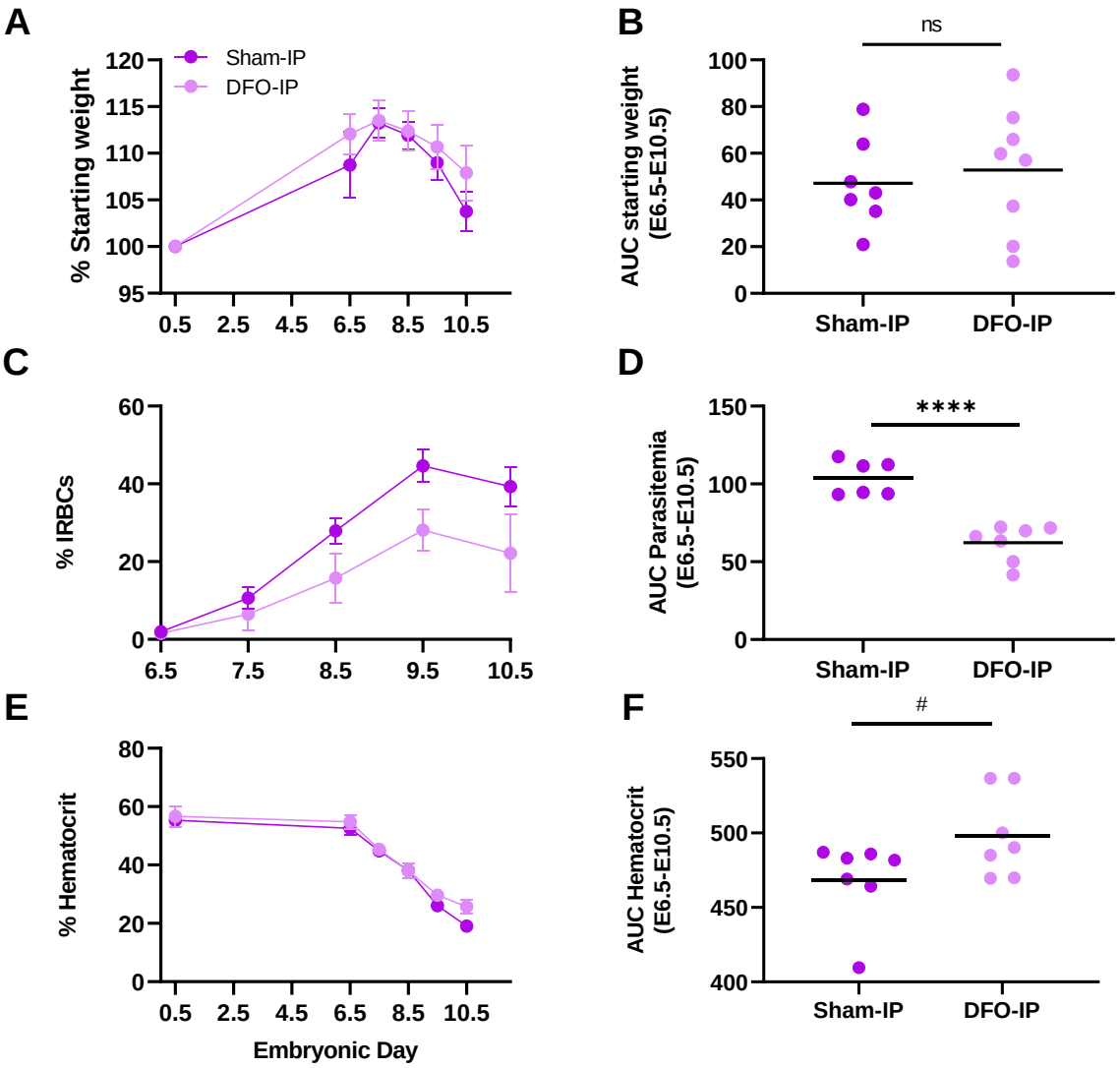
A
% Starting weight
Sham-IP
DFO-IP
120
115
110
105
100
95
0.5
2.5
4.5
6.5
8.5
10.5
B
AUC starting weight (E6.5-E10.5)
ns
100
80
60
40
20
0
Sham-IP
DFO-IP
C
% IRBCs
60
40
20
0
6.5
7.5
8.5
9.5
10.5
D
AUC Parasitemia (E6.5-E10.5)
****
150
100
50
0
Sham-IP
DFO-IP
E
% Hematocrit
80
60
40
20
0
0.5
2.5
4.5
6.5
8.5
10.5
Embryonic Day
F
AUC Hematocrit (E6.5-E10.5)
#
550
500
450
400
Sham-IP
DFO-IP

Figure 3.2. DFO treatment improves uterus weight in malaria-infected outbred Swiss Webster mice at midgestation.

Uterus weight is presented for infected pregnant (IP) sham-treated Swiss Webster (SW) and IP Deferoxamine (DFO) treated SW mice. A statistically significant improvement in uterus weights is revealed between groups (P = 0.012; unpaired t-test with Welsh's correction). Sample sizes: Sham-IP, *n* =6; DFO-IP, *n* = 8.

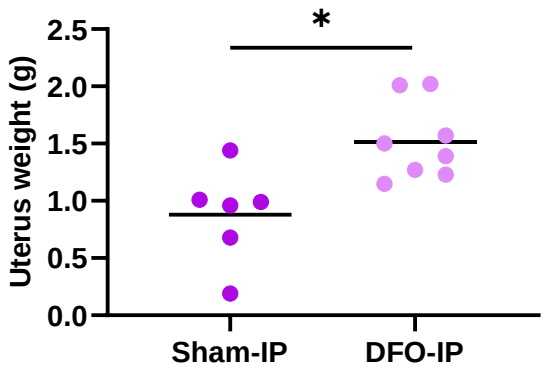

Table 3.1. Embryo viability in malaria-infected outbred Swiss Webster mice treated with iron chelator drug Deferoxamine.

Infected pregnant (IP) Swiss Webster (SW) sham treated and IP SW Deferoxamine (DFO) treated mice at mid-gestation. Percentages show percent viability within a group. P value was obtained with a two-tailed Fisher exact probability test, comparing embryo viability in sham treated versus DFO treated groups. *NS* = not significant.

Group	**Viable/total embryos (E10.5)**	**Viable/total embryos (E10.5)**	
	Sham treated	DFO treated	P value
IP	67/73 (91.7%) n=7	100/106 (94.3%) n=8	0.55 *NS*

Figure 3.3. Weight, parasitemia, and hematocrit in malaria-infected outbred Swiss Webster mice treated with ferroptosis inhibitor drug SRS16-86.

A) Percent starting weight in infected pregnant (IP) Swiss Webster (SW) sham treated and IP SW 1H1 treated mice beginning on E0.5 and then from E6.5 to E12.5. Data represent mean ± SEM.
B) Area under the curve (AUC) analysis of starting weight measurements collected on E7.5 through E12.5. No statistical differences were found between groups (P = 0.16; unpaired t-test with Welsh's correction).
C) Percent peripheral parasitemia (IRBCs) in IP SW sham treated and IP SW 16-86 treated mice from E6.5 to E12.5. Data represent mean ± SEM.
D) AUC analysis for percent peripheral parasitemia from E7.5 to E12.5. No statistically significant differences were found between groups (P = 0.33; unpaired t-test with Welch's correction).
E) Percent hematocrit in IP SW sham treated and IP SW16-86 treated mice measured on E0.5 and then from E7.5 to E12.5. Data represent mean ± SEM.
F) AUC analysis for percent hematocrit. No statistically significant differences were found between groups (P = 0.80; unpaired t-test with Welch's correction).

Sample sizes: Sham-IP, *n* =5; 16-86-IP, *n* = 10; *ns* = not significant, P > 0.05. Error bars are not depicted if they are shorter than the height of the symbol.

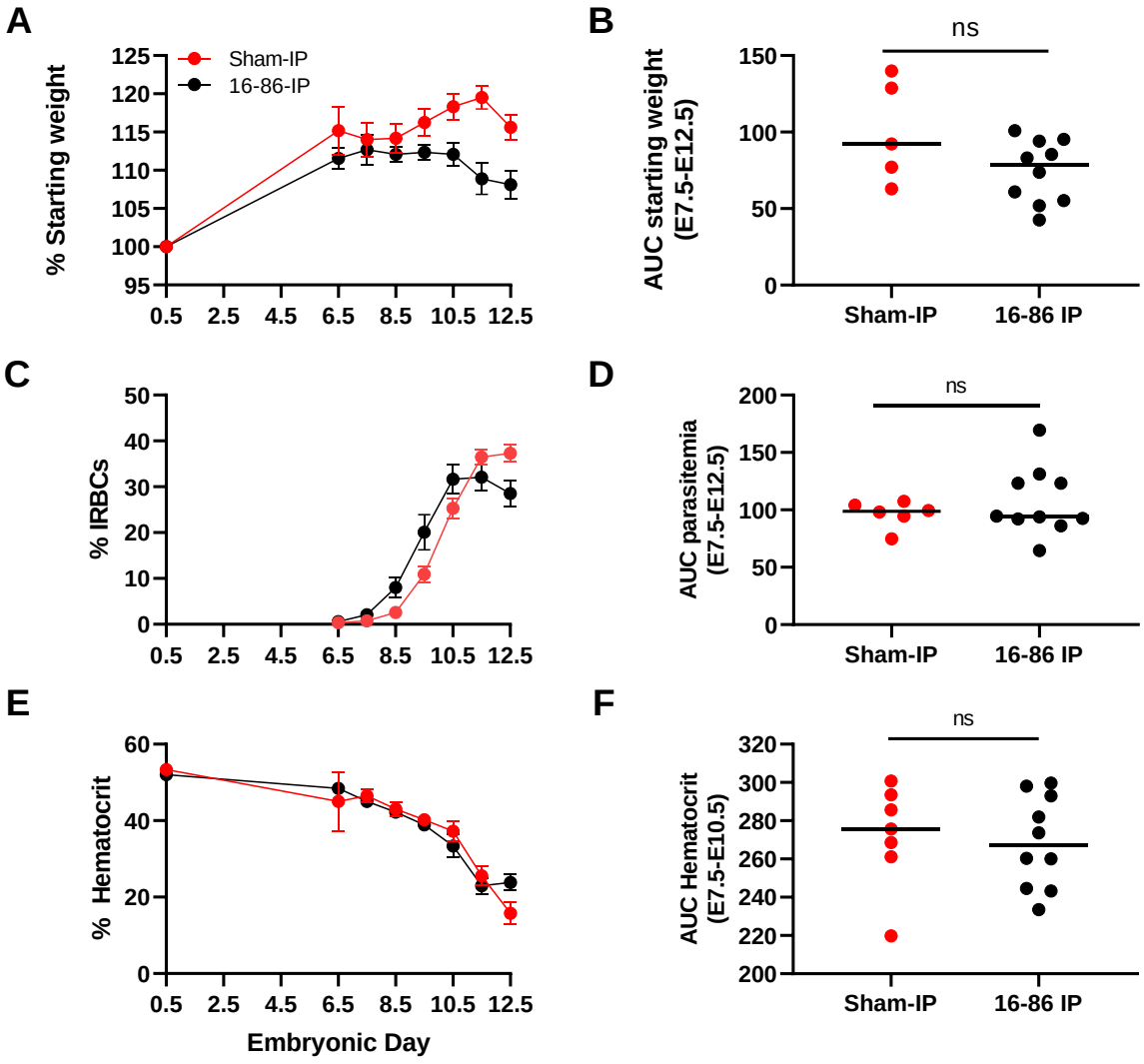
A
% Starting weight
Sham-IP
16-86-IP
125
120
115
110
105
100
95
0.5 2.5 4.5 6.5 8.5 10.5 12.5
B
AUC starting weight (E7.5-E12.5)
ns
150
100
50
0
Sham-IP
16-86 IP
C
% IRBCs
50
40
30
20
10
0
0.5 2.5 4.5 6.5 8.5 10.5 12.5
D
AUC parasitemia (E7.5-E12.5)
ns
200
150
100
50
0
Sham-IP
16-86 IP
E
% Hematocrit
60
40
20
0
0.5 2.5 4.5 6.5 8.5 10.5 12.5
Embryonic Day
F
AUC Hematocrit (E7.5-E10.5)
ns
320
300
280
260
240
220
200
Sham-IP
16-86 IP

Figure 3.4. Uterus weight in SRS16-68 treated malaria-infected mice at E12.5.

Uterus weight is presented for infected pregnant (IP) sham-treated Swiss Webster (SW) and IP 16-86 treated SW mice. No statistical significance revealed between groups (P = 0.55; unpaired t test with Welsh's correction). Sample sizes: Sham-IP, *n* =3; 16-86-IP, *n* = 8; *ns* = not significant, P > 0.05.

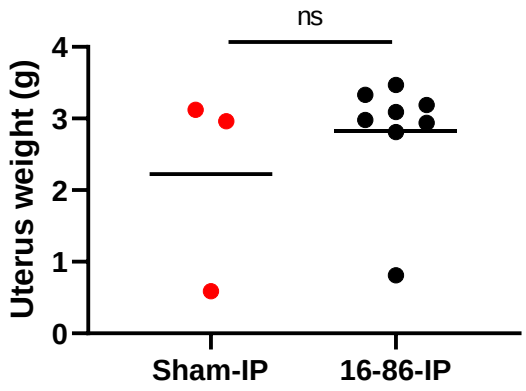

Figure 3.5. Maternal weight and parasitemia at E12.5 in malaria-infected outbred Swiss Webster mice treated with SRS16-86.

A) Percent starting weight in infected pregnant (IP) Swiss Webster (SW) sham treated and IP SW 16-86 treated mice on the final day of the experiment, E12.5. Statistically significant differences were detected between the groups (**P = 0.009).
B) Percent parasitemia (IRBC) in IP SW sham treated and IP SW 16-86 treated mice on the final day of the experiment, E12.5. Statistically significant differences were detected between the groups (*P = 0.04).
C) Percent parasitemia in IP SW sham treated and IP SW 16-86 treated mice on E8.5. Statistically significant differences were detected between the groups (*P = 0.02).
D) Percent parasitemia in IP SW sham treated and IP SW 16-86 treated mice on E9.5. Statistically significant differences were detected between the groups (*P = 0.05).

Sample sizes: Sham-IP, *n* =6; 16-86-IP, *n* = 10; *ns* = not significant, P > 0.05.

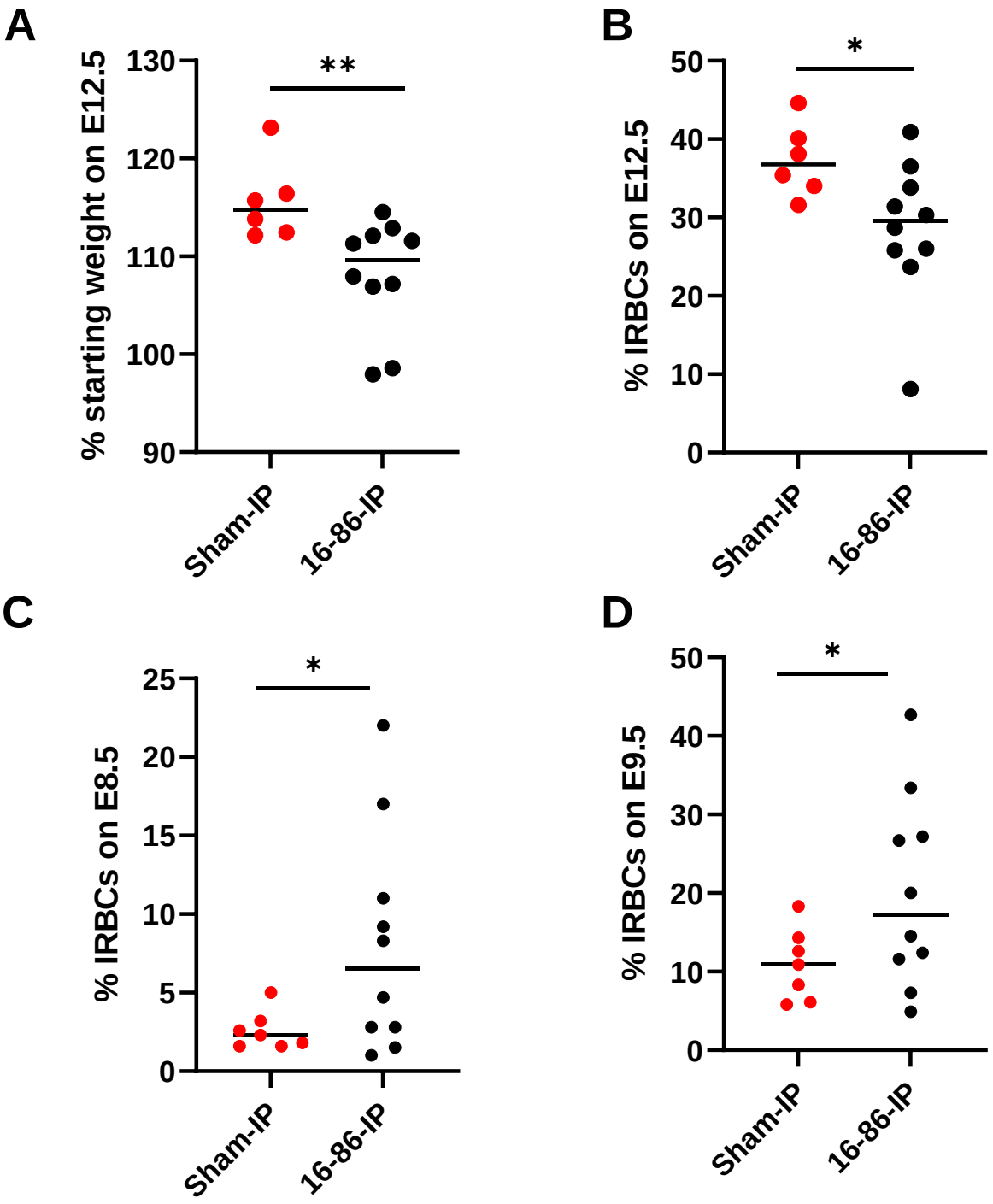
A
% starting weight on E12.5
130
120
110
100
90
**
Sham-IP
16-86-IP
B
% IRBCs on E12.5
50
40
30
20
10
0
*
Sham-IP
16-86-IP
C
% IRBCs on E8.5
25
20
15
10
5
0
*
Sham-IP
16-86-IP
D
% IRBCs on E9.5
50
40
30
20
10
0
*
Sham-IP
16-86-IP

Table 3.2. Embryo viability in malaria-infected outbred Swiss Webster mice treated with ferroptosis-inhibitor drug SRS 16-86.

Infected pregnant (IP) Swiss Webster sham treated and SRS16-86 treated mice at mid-gestation. Percentages show percent viability within a group. P value was obtained with a two-tailed Fisher exact probability test, comparing embryo viability in sham treated versus 16-86 treated groups. $P < 0.05$ is statistically significant.

Group	**Viable/total embryos (E12.5)**	**Viable/total embryos (E12.5)**	
	Sham treated	16-86 treated	P value
IP	34/38 (89.5%) n=6	24/58 (41.3%) n=6	**<0.0001**

Figure 3.6. Weight, parasitemia, and hematocrit in malaria-infected outbred Swiss Webster mice treated with Mitotempo.

A) Percent starting weight in infected pregnant (IP) Swiss Webster (SW) sham treated and IP SW Mitotempo treated mice beginning on E0.5 and then from E6.5 to E10.5. Data represent mean ± SEM.
B) Area under the curve (AUC) analysis of starting weight measurements collected on E6.5 through E10.5. No statistical differences were found between groups (P = 0.87; unpaired t-test with Welsh's correction).
C) Percent peripheral parasitemia (IRBCs) in IP SW sham treated and IP SW Mitotempo treated mice from E6.5 to E10.5. Data represent mean ± SEM.
D) AUC analysis for percent peripheral parasitemia from E6.5 to E10.5. No statistically significant differences were found between groups (P = 0.25; unpaired t-test with Welch's correction).
E) Percent hematocrit in IP SW sham treated and IP SW Mitotempo treated mice measured on E0.5 and then from E6.5 to E10.5. Data represent mean ± SEM.
F) AUC analysis for percent hematocrit from E0.5 to E10.5. No statistically significant differences were found between groups (P = 0.28; unpaired t-test with Welch's correction).

Sample sizes: Sham-IP, *n* =9; Mitotempo-IP, *n* = 10; *ns* = not significant, P > 0.05. Error bars are not depicted if they are shorter than the height of the symbol.

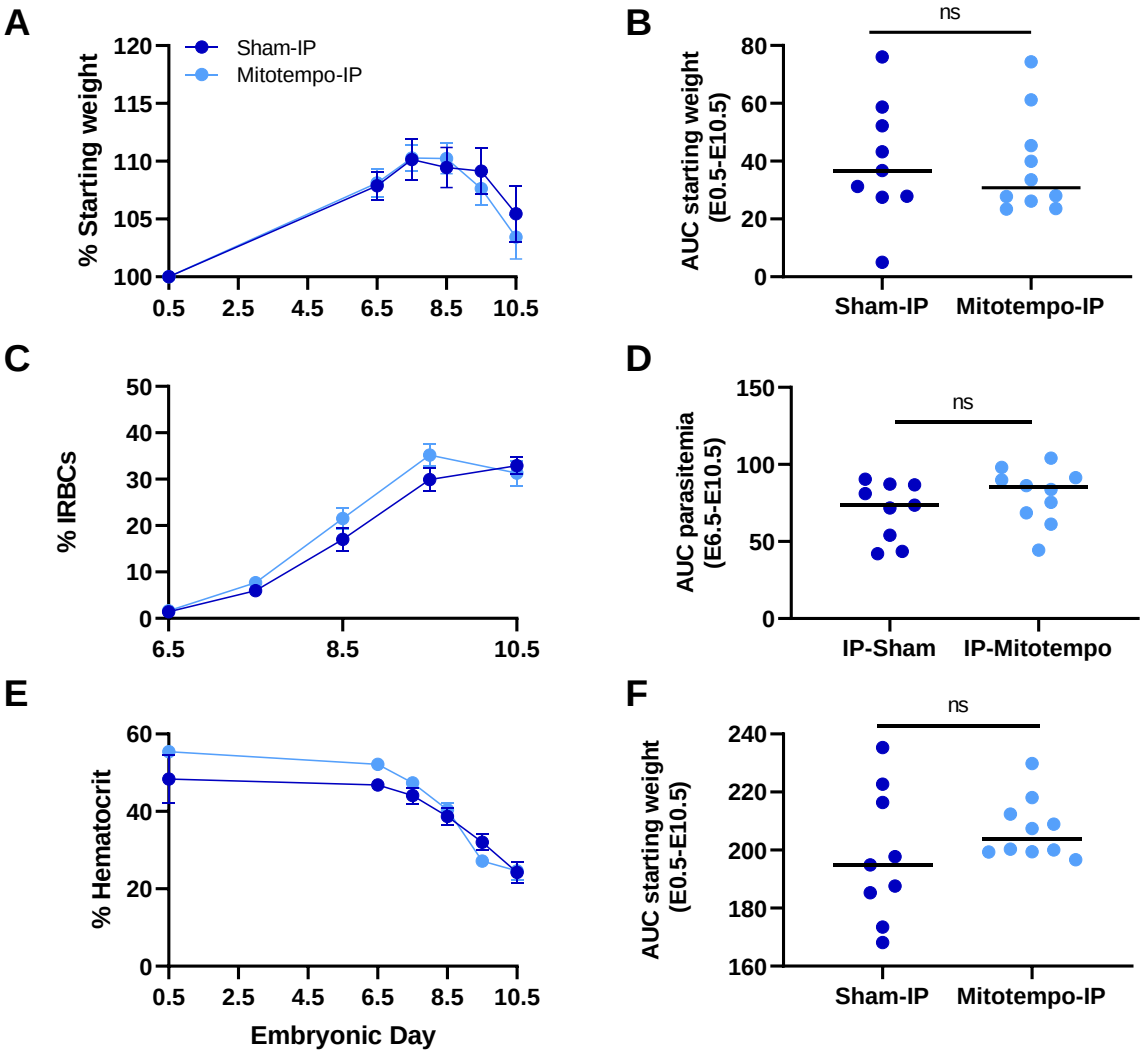
A
Sham-IP
Mitotempo-IP
% Starting weight
120
115
110
105
100
0.5
2.5
4.5
6.5
8.5
10.5
B
ns
AUC starting weight (E0.5-E10.5)
80
60
40
20
0
Sham-IP
Mitotempo-IP
C
% IRBCs
50
40
30
20
10
0
6.5
8.5
10.5
D
ns
AUC parasitemia (E6.5-E10.5)
150
100
50
0
IP-Sham
IP-Mitotempo
E
% Hematocrit
60
40
20
0
0.5
2.5
4.5
6.5
8.5
10.5
Embryonic Day
F
ns
AUC starting weight (E0.5-E10.5)
240
220
200
180
160
Sham-IP
Mitotempo-IP

Figure 3.7. Uterus weight in malaria-infected outbred Swiss Webster mice treated with Mitotempo.

Uterus weight is presented for infected pregnant (IP) sham-treated Swiss Webster (SW) and IP Mitotempo treated SW mice. No statistical significance revealed between groups (P = 0.33; unpaired t-test with Welsh's correction). Sample sizes: Sham-IP, *n* =8; Mitotempo-IP, *n* = 9; *ns* = not significant, P > 0.05.

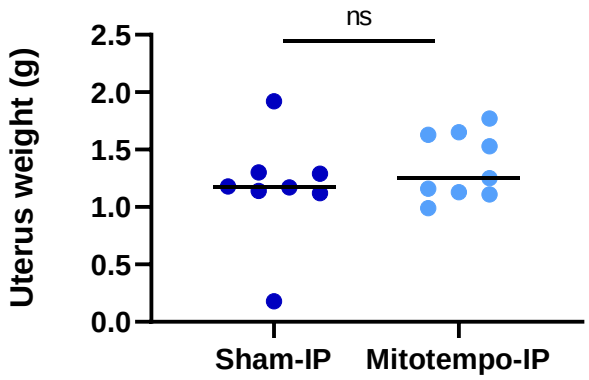

Table 3.3. Embryo viability in malaria-infected outbred Swiss Webster mice treated with mitochondria-specific antioxidant drug Mitotempo.

Infected pregnant (IP) Swiss Webster sham treated and Mitotempo treated mice at mid-gestation. Percentages show percent viability within a group. P value was obtained with a two-tailed Fisher exact probability test, comparing embryo viability in sham treated versus Mitotempo treated groups. *NS* = not significant.

Group	**Viable/total embryos (E10.5)**	**Viable/total embryos (E10.5)**	
	Sham treated	Mitotempo treated	P value
IP	88/97 (90.1%) n= 9	120/125 (96.0%) n=9	0.16 *NS*

Table 3.4. Primer sequences for qPCR human targets.

Human-specific forward (FP) and reverse (RP) primers used in quantitative real-time PCR for the amplification of mRNA transcripts associated with antioxidant activity, iron-regulation/ferroptosis, and reference (*Ck19 and Top1*) genes.

Target	Forward and Reverse Primers (5' to 3')
Ck19	FP: GAAATCAGTACGCTGAGGGG
	RP: CCGGCTGGTGAACCAGGCTT
Top1	FP: GATGAACCTGAAGATGATGGC
	RP: TCAGCATCATCCTCATCTCG
Nrf2	FP: GCGACGGAAAGAGTATGAG
	RP: GTTGGCAGATCCACTGGTTT
Sod1	FP: CAATGTGACTGCTGACAAAG
	RP: GTGCGGCCAATGATGCAAT
Sod2	FP: ACAGGCCTTATTCCACTGCT
	RP: CAGCATAACGATCGTGGTTT
Sod3	FP: CTTCGCCTTTGCTGAAGTCT
	RP: GGGTGTTTCGGTACAAATGG
Cat	FP: TAAGACTGACCAGGGCATC
	RP: CAAACCTTGGTGAGATCGAA
Hmox1	FP: ATGACACCAAGGACCAGAGC
	RP: GTGTAAGGACCCATCGGAGA
TfR1	FP: ACCATTGTCATATACCCGGTTCA
	RP: CAATAGCCCAAGTAGCCAATCAT
Ferritin	FP: GTCAACAGCCTGGTCAATTTGTAC
	RP: GGTCGAAATAGAAGCCCAGAGA
Slc7a11	FP: TCTCCAAAGGAGGTTACCTGC
	RP: AGACTCCCCTCAGTAAAGTGAC

CHAPTER 4

A NOVEL MURINE MODEL OF POST-IMPLANTATION MALARIA-INDUCED PRETERM BIRTH[4]

[4] Andrew AK, Cooper CA, Moore JM (2022). *PLoS ONE* 17(3):e0256060. Reprinted here with permission of publisher, July 7, 2022.

Abstract

Despite major advances in malaria treatment and control over recent decades, developing new models for studying disease pathogenesis remains a vital part of malaria research efforts. The study of malaria infection during pregnancy relies on mouse models to circumvent many challenges and costs associated with pregnancy studies in endemic human populations. Here, we introduce a novel murine model that will further our understanding of how malaria infection affects pregnancy outcomes. When C57BL/6J (B6) mice are infected with *Plasmodium chabaudi chabaudi* AS on either embryonic day (E) 6.5, 8.5, or 10.5, preterm birth occurs in all animals by E16.5, E17.5, or E18.5 respectively, with no evidence of intrauterine growth restriction. Despite having the same outcome, we found that the time to delivery, placental inflammatory and antioxidant transcript upregulation, and the relationships between parasitemia and transcript expression prior to preterm birth differed based on the embryonic day of infection. On the day before preterm delivery, E6.5 infected mice did not experience significant upregulation of the inflammatory or antioxidant gene transcripts examined; however, peripheral and placental parasitemia correlated positively with *Il1β*, *Cox1*, *Cat*, and *Hmox1* placental transcript abundance. E8.5 infected mice had elevated transcripts for *Ifnγ*, *Tnf*, *Il10*, *Cox1*, *Cox2*, *Sod1*, *Sod2*, *Cat*, and *Nrf2*, while *Sod3* was the only transcript that correlated with parasitemia. Finally, E10.5 infected mice had elevated transcripts for *Ifnγ* only, with a tendency for *Tnf* transcripts to correlate with peripheral parasitemia. Tumor necrosis factor deficient ($TNF^{-/-}$) and TNF receptor 1 deficient ($TNFR1^{-/-}$) mice infected on E8.5 experienced preterm birth at the same time as B6 controls. Further characterization of this model is necessary to discover the mechanism(s) and/or trigger(s)

responsible for malaria-driven preterm birth caused by maternal infection during early pregnancy.

Introduction

Despite unprecedented successes in vector control programs and antimalarial treatment, malaria remains a global public health issue. In 2020, the World Health Organization (WHO) reported that in regions with moderate to high *Plasmodium falciparum* transmission, roughly 11 million pregnancies were exposed to malaria infection [22]. Among those pregnancies, an estimated 819,000 infants were born with low birth weight, a well-documented risk factor for neonatal mortality [22]. Additional maternal-fetal health consequences of infection include maternal anemia and preterm delivery, especially in primigravid women [33]. Notably, malaria infection during pregnancy can manifest as an organ-specific syndrome known as placental malaria (PM), identified by the accumulation of *Plasmodium*-infected red blood cells (IRBCs), immune cell infiltration, and both malaria pigment (hemozoin) and fibrin deposition in the placenta [10,311,312]. To protect pregnant women from PM, WHO recommends the use of insecticide-treated mosquito nets (ITNs) and intermittent preventative treatment using antimalarial drugs such as sulfadoxine-pyrimathamine (IPTp-SP). However, in 2018 only 31% of women received the recommended dosages of IPTp-SP during their pregnancy and ITN coverage in sub-Saharan Africa has stalled since 2015 [313].

Despite decades of discovery and billions of dollars invested in malaria research, the underlying mechanisms involved in PM pathogenesis are still incompletely understood. One major reason is that access to the placenta is limited until after delivery, making it difficult to evaluate the impact of infection on the placenta during earlier stages

of pregnancy. As a result, most of what is known about human PM comes from studies focused on clinical outcomes throughout gestation, systemic evaluation for biomarkers of disease, and placental biopsies postpartum. Some studies provide evidence for the critical role of inflammation, specifically via the upregulation of tumor necrosis factor (TNF), interleukin-10 (IL-10), interleukin-1 beta (IL-1β), and interferon-gamma (IFN-γ), in driving poor pregnancy outcomes [2,4,108,114,116,314,315]. Other studies suggest that oxidative stress, resulting from a cell's inability to mount an effective antioxidant response to mitigate damage driven by reactive oxygen species (ROS), is a critical player in the placental pathology and poor fetal health outcomes associated with PM [16,316].

Mouse models have been central to furthering our understanding of PM pathogenesis by providing a more accessible and genetically tractable tool for recapitulating malaria infection during pregnancy. Infection with the murine-infective *Plasmodium chabaudi chabaudi* AS (*Pcc*AS) in C57BL/6J (B6) and Swiss Webster mice capture some of the important hallmarks of human PM, such as elevated proinflammatory cytokine production, accumulation of IRBCs in the placenta, increased fibrin deposition, and pregnancy loss [5,6,18,101,102]. In these models, mice infected with *Pcc*AS on the first day of gestation (embryonic day 0.5, E0.5) experience a non-lethal infection that is accompanied by severe maternal anemia, high parasite burden, elevated inflammatory responses, hemozoin accumulation, and lipid peroxidation in the placenta, a known sign of oxidative stress. Therapeutic interventions that target the pathogenic contributions of coagulation, TNF, and ROS in B6 mice protect against pregnancy loss at midgestation (E10.5-12.5) [5,10,18]. Alternatively, studies in later gestation commonly utilize *Plasmodium berghei* in either B6 or BALB/c mice; however, the infection must be

initiated between E10.5-13.5, due to the maternal lethality of the parasite. In these models, mice experience elevated placental inflammation and fibrin deposition, oxidative stress, IRBC adherence to the placenta, and preterm delivery [17,19,88,317]. Moreover, antimalarial and anti-inflammatory drug treatment restore maternal survival, reduce oxidative stress, and improve pregnancy outcomes [317,318].

While these well-established models are useful for studying PM pathogenesis, our understanding of how the timing of malaria infection determines maternal and fetal health outcomes remains unclear. Studies of women naturally exposed to malaria at various times during gestation report associations between peripheral and placental parasitemia and poor birth outcomes such as low birth weight, preterm delivery, and neonatal mortality [319–322], with some studies that focus on infection early in the first trimester [285,323–325]. However, due to a lack of histological and pathophysiological information related to PM pathogenesis during the first and second trimesters of pregnancy, it is challenging to envision host-directed therapeutic interventions that mitigate the impact of infection during these times in gestation. This represents a significant obstacle in PM prevention and treatment efforts, especially amidst emerging antimalarial drug and insecticide resistance [62,326].

Here, we describe a mouse model for studying malaria infection during early stages of pregnancy (early post-implantation) using *Pcc*AS in B6 mice. Given the developmental similarities between the first trimester human placenta and the last two-thirds of mouse gestation [85,327], this model offers an avenue for investigating the pathogenic mechanisms underlying malaria infection during early placentation, when *P. falciparum* prevalence in pregnant women is highest [33] and fetal health is significantly

impacted [320,323,325], but the placenta remains inaccessible to study. This work shows that malaria infection during the post-implantation period induces preterm birth and alters the expression of inflammatory and antioxidant-related gene transcripts in the placenta one day prior to preterm delivery.

Materials & Methods

Mice

C57BL/6J (B6), TNFα-deficient (B6;129S-Tnftm1Gkl/J), TNFRp55-deficient (Tnfrsf1atm1Mak/J), and A/J mice were purchased from the Jackson Laboratory (Bar Harbor, ME) and maintained by brother-sister mating for a maximum of ten generations in the University of Georgia Coverdell Vivarium, following guidelines and regulations set forth by the University of Georgia Animal Care and Use Committee. All animals were supplied food (PicoLab® Rodent Diet 20: 5030, St. Louis, MO) and water ad libitum. Mice were adjusted to a 14-hour light/10-hour dark cycle and housed in conditions of 65-75 ˚F and 40-60% humidity. All animal procedures reported in this study were reviewed and approved by the Institutional Animal Care Use Committee (IACUC) at the University of Georgia, protocol number A2018 02-016-Y1-A0. Mice were anesthetized with 2.5% Tribromoethanol before sacrifice and all efforts were made to minimize suffering.

Parasites and infection monitoring

The following reagent was obtained through BEI Resource Repository, NIAID, NIH: *Plasmodium chabaudi chabaudi*, Strain AS, MR4-741, contributed by David Walliker. Parasites were maintained as frozen stock in accordance with supplier guidelines and passaged in A/J mice for the purposes of infecting experimental B6 mice. Peripheral parasitemia was assessed by flow cytometry with a method adapted from work published by Jimenez-Diaz et al. [238]. A 2µl blood sample was collected by tail clip [239], diluted in 98µl 0.9% NaCl and stained with 0.25µl SYTO-16 Green Fluorescent Nucleic Acid Stain (ThermoFisher Scientific, catalog # S7578) within 4 hours of collection. Stained samples were diluted 1:9 in 0.9% NaCl and incubated in the dark for 20 minutes at room temperature, then analyzed using a CyAn ADP Flow Cytometer (Beckman Coulter; Brea, CA). 30,000 cells were assessed daily for each mouse; infected red blood cells were distinguished based on the size and fluorescence intensity. An uninfected blood sample was used as an internal negative control. Parasitemia is reported as the percentage of infected red blood cells (IRBCs) to the total number of red blood cells (RBCs).

Experimental design

Female B6, TNFα-deficient ($TNF^{-/-}$), and TNFRp55-deficient ($TNFRI^{-/-}$) mice aged 8-10 weeks were paired with age-matched males nightly and examined each morning until a vaginal plug was observed, indicating successful mating. The morning a vaginal plug was observed was considered embryonic day 0.5, E0.5. After baseline measurements of weight and hematocrit were recorded, females were left undisturbed

until E6.5 to minimize stress and increase the chances of successful blastocyst implantation. Mice were infected intravenously with 1000 *P. chabaudi chabaudi* AS-iRBCs diluted in 200ul 1X phosphate-buffered saline (PBS) per 20 grams of body weight on E6.5, E8.5, or E10.5 and are termed infected pregnant (IP). Age-matched non-pregnant mice were infected similarly as infection controls (infected non-pregnant, INP). In another control group, uninfected pregnant (UP) mice were sham injected with 200ul PBS per 20 grams body weight on the same gestation days. Immediately prior to infection or sham infection, experimental animals were switched to a high-fat rodent chow (PicoLab Mouse Diet 20 5058; St. Louis, MO) suited for pregnant animals. Weight measurements were recorded on E0.5, E6.5, E8.5, E10.5, and E12.5-E18.5 for all groups, depending on when the infection was initiated, to assess pregnancy progress and allow mice to proceed to spontaneous delivery. Parasitemia and hematocrit (a measure of anemia) were monitored daily in the infected groups beginning five days post-infection to assess the development of infection.

In a second series of experiments, mice infected on E6.5, E8.5, and E10.5, and along with their UP controls, were sacrificed on E15.5, E16.5, and E17.5, respectively. Weight, hematocrit, and parasitemia were recorded as described above until euthanasia. Mice were anesthetized before sacrifice and placentae were collected and preserved for histological and quantitative real-time PCR (RT-qPCR) analysis. Plump, pink, well-vascularized pups that reflexively responded to touch were considered viable and their weights and placenta weights were collected. Pup viability data are summarized in Table 4.1.

Histology

Placentae collected at the time of sacrifice were fixed for 24 hours in 10% buffered formalin, processed, and paraffin-embedded. Placental sections 5μm in thickness were mounted to microscope slides and stained with hematoxylin and eosin (H&E) for histological analysis. H&E images were obtained using a Keyence BZ-X710 with BZ Analyzer software and the 100X oil objective. Sections were Giemsa-stained and parasite burden in the placenta was determined by counting at least 1,000 erythrocytes in maternal blood sinusoids of at least two or more different placentae per dam, as previously described [5].

Gene expression by quantitative real-time PCR

Total RNA from mouse placentae collected on E15.5, E16.5, and E17.5 was isolated using Trizol Reagent (Ambion, Ref # 15596026) and a bead shaker (BeadBlaster 24, Benchmark Scientific, SKU: D2400) with a minimum of four placentae were pooled per dam. RNA was DNase-treated (Invitrogen, Ref # AM1906) and then reverse-transcribed with High-Capacity cDNA Reverse Transcription Kit (Applied Biosystems, Ref # 4368814). Relative transcript abundance for the genes of interest was quantified using PowerSYBR Green PCR Master Mix (Applied Biosystems, Cat # 4367659), the Roche LightCycler 96 Instrument (software version 1.01.01.0050), and the Mic qPCR cycler (Biomolecular systems, firmware version 2.25). Each sample was assayed in duplicate for target and housekeeping genes. Average Ct values of target genes were normalized to average Ct values of *Ubc* as the reference gene and relative transcript

abundance of genes of interest was determined using the ΔΔCt method. Transcript expression in individual mice is presented relative to the mean expression value in UP mice at E6.5. Details of primer sets are summarized in Table 2.3.

Statistics

All statistical analyses were performed using GraphPad Prism version 9.2.0 (GraphPad Software; La Jolla, California). All raw clinical data are presented as mean ± SEM. Error bars are not visible if they are shorter than the symbol's height. The area under the curve (AUC) of percent starting weight, hematocrit, and parasitemia was calculated for each mouse between E0.5 and E18.5, as appropriate. AUC for weight and hematocrit were compared between IP, INP, and UP mice infected on the same day and analyzed using a Kruskal-Wallis test between IP and INP groups and IP and UP groups. AUC for parasitemia between IP and INP groups was compared using a two-tailed unpaired t-test with Welch's correction. RT-qPCR data were analyzed using an unpaired t-test with Welch's correction and presented as a scatterplot with a bar representing the mean. Parasitemia and transcript data for correlation analyses were log-transformed. P values less than or equal to 0.05 were considered statistically significant. Mixed linear models analysis (SAS 9.4) was used to estimate differences in fetal and placental weights in dams sacrificed on E15.5, E16.5, and E17.5, and their controls. Proportional analysis tested by chi-square was used to compare pup viability between IP and UP dams. Univariate and multivariate regression analyses were done in SAS 9.4.

Results

P. chabaudi AS infection in the post-implantation period universally precipitates preterm delivery

In this observational study, *Pcc*AS blood-stage infection was initiated on E6.5, 8.5, or 10.5 in B6 mice. These time points coincide with a period of intense placental growth and vascularization in human pregnancy, representing the initial point at which placental sequestration of *P. falciparum* is proposed to occur [328,329]. Initial measurements of weight and hematocrit were taken on E0.5 and then mice were randomly assigned to one of six groups – E6.5 infected pregnant (IP), E8.5 IP, E10.5 IP, E6.5 uninfected pregnant (UP), E8.5 UP, and E10.5 UP, with the indicated embryonic day representing the day of infection for IP groups (Figure 4.1). After the infection was initiated, daily measurements of weight and parasitemia were collected beginning five days post-infection (Figure 4.1B-G). In each group, IP mice steadily gained weight alongside their UP controls until they experienced a sudden and precipitous decline in weight, suggestive of preterm pregnancy compromise (Figure 4.1B-D). Euthanasia of these dams at E19.5 revealed empty uteri, implicating preterm birth as the likely cause of the observed weight loss. The time to preterm birth was accelerated the later in gestation that infection occurred such that E6.5-, E8.5-, and E10.5-infected dams began losing weight nine, eight, and seven days post-infection, respectively (Figure 4.1B-D). UP mice continued gaining weight beyond E18.5, as expected during a normal pregnancy. Parasitemia was greater in IP dams compared to their infected non-pregnant (INP) counterparts (Figure 4.1E-G), which was confirmed statistically through area under the

curve (AUC) analysis in all groups except the E8.5 infection group (Figure 4.2D-F). Corresponding with higher parasite burdens, AUC for hematocrit was significantly lower in E6.5 infected dams compared to controls (Figure 4.2G), likely due to the prolonged destruction of red blood cells caused by the advanced stage of infection compared to the other infection groups [295]. AUC for hematocrit in the other infection groups, E8.5 and E10.5, was not statistically significantly different from UP controls (Figure 4.2H-I).

P. chabaudi AS-infected red blood cells accumulate prior to preterm delivery in the placentae of mice infected at E8.5 and E10.5 but do not significantly impact placenta or pup weight prior to preterm delivery.

To investigate the effect of maternal infection on placental and pup health in this model, dams infected on E6.5, E8.5, or E10.5 were euthanized one day prior to expected preterm parturition on E15.5, E16.5, and E17.5 respectively (Figure 4.1B-D, arrows indicate the day of euthanasia when placentae were collected for analysis). Daily weight, parasitemia, and hematocrit measurements were recorded, beginning five days post-infection. Placental parasitemia in dams of the E8.5 and E10.5 infection groups, but not in dams infected at E6.5, was significantly higher than their peripheral parasitemia at sacrifice (Fig 4.3). To further examine the impact of infection, pup and placental weights and pup viability were measured one day before expected preterm parturition. By mixed linear models analysis, neither pup nor placental weights were significantly impacted by maternal malaria across all infection groups; graphs are shown for visualization purposes only (Fig 4.4). Pup viability was also not different between IP versus UP dams, regardless of the infection group (Table 4.1). When holding infection constant, increased

pup viability in mice infected at E10.5 yielded a significant reduction in pup weight (by 0.7546 g, P = 0.0102), consistent with the well-documented observation that increased litter sizes result in reduced fetal weights [330]. Overall, these results indicate that despite having significant parasite burden, including in the placenta, malaria-induced preterm birth in this model occurs independently of changes in placental and fetal weight and viability.

Histology in PM-positive human placenta observed at term is generally characterized by immune cell infiltration, IRBC accumulation, and both fibrin and hemozoin deposition in placental tissues [10,311,312]. To assess the histological condition of the placenta prior to preterm delivery in our model, placentae collected from IP mice and their UP controls were stained with hematoxylin and eosin (H&E) (Figure 4.5). Representative images of placentae from each group depict IRBCs in the placentae of all infection groups (Figure 4.5B, D, F). Giemsa-stained tissue sections further demonstrate the presence of IRBCs in all infection groups (Figure 4.6). There was no evidence of immune cell accumulation or excessive fibrin deposition within the labyrinth in any of the placentae examined.

P. chabaudi infection induces upregulation of inflammatory and parturition-associated gene transcripts placenta prior to preterm delivery

The pathogenesis of preterm delivery has long been associated with excessive inflammation, induced by infection or other disorders [331]. Real-time quantitative PCR (RT-qPCR) analysis was performed using RNA isolated from the placental homogenates to probe the importance of inflammatory mediators in driving preterm delivery in this

model. The relative abundance of inflammatory gene transcripts, such as tumor necrosis factor (*Tnf*), interleukin-10 (*Il10*), interferon-gamma (*Ifnγ*), interleukin beta (*Il1β*), and genes essential in pregnancy maintenance and parturition, such as cyclooxygenases 1 and 2 (*Cox1* and *Cox2*) were measured (Figure 4.7). Transcript abundance in placentae collected on E15.5 from mice infected on E6.5 revealed no significant differences between IP and UP dams for all inflammatory targets measured (Figure 4.7A-F). However, *Il1β* transcripts were positively correlated with both peripheral parasitemia at euthanasia (E15.5) and peripheral parasitemia AUC for mice infected on E6.5 (Figure 4.8A-B). Additionally, there was a positive correlation between *Cox1* transcripts and peripheral parasitemia at sacrifice (Figure 4.8F) and a weak tendency toward a positive correlation between *Cox1* transcripts and parasitemia AUC for this same group (Appendix D). In the E8.5 infection group, transcript abundance of all the inflammatory genes targeted, except for *Il1β*, was significantly elevated in placentae collected on E16.5 (Figure 4.7A-F), but no correlative relationships with parasitemia at sacrifice or parasitemia AUC were found. In the E10.5 infection group, only transcripts for *Ifnγ* were elevated, while all other targets remained unchanged (Figure 4.7A-F). There was a tendency for *Tnf* transcripts to be positively correlated with both peripheral parasitemia at sacrifice and parasitemia AUC in mice infected on E10.5 (Appendix D).

To determine the parameters most critical in determining inflammatory gene expression, linear regression modeling was performed, considering infection status, day euthanasia was performed, and, as observed at euthanasia, uterus weight, number of embryos, and embryo viability. The latter three were considered together in multivariate analysis, and none were found to predict transcript abundance. Infection status

significantly influenced all targets (Table 4.2). Day of euthanasia also significantly influenced all targets except *Cox1;* relative to placentae from mice infected at E6.5 (i.e., E15.5), transcripts for *Ifnγ, Tnf, Il1β, Il10, and Cox2* in placentae from E8.5 infections (i.e., E16.5) were all elevated. In a multivariate model testing both status and day, membership in the E16.5 group was a significant predictor for *Ifnγ, Tnf, Il1β, Il10, and Cox2* abundance ($P \leq 0.0306$; Table 4.3), while holding infection status constant. Similarly, while holding day constant, infection status maintained a significant influence on *Ifnγ, Il1β, Il10, and Cox2* abundance ($P \leq 0.0273$), with tendencies for *Tnf* and *Cox1* ($p = 0.0569$ and $p = 0.0645$, respectively; Table 4.3).

Tumor necrosis factor and tumor necrosis factor receptor 1 deficient mice experience preterm delivery following *P. chabaudi* infection on E8.5.

TNF has long been implicated as one of the major contributors to poor pregnancy outcomes in malaria-positive primigravid women and in other infections [2,332,333]. Moreover, in a related mouse model, in which infection is initiated at E0.5, antibody-mediated ablation of TNF resulted in midgestational rescue from *Pcc*AS-induced abortion [5]. To directly evaluate a link between placental inflammation driven by TNF and subsequent precipitation of preterm delivery in the current mouse model, mice deficient in tumor necrosis factor ($TNF^{-/-}$) and tumor necrosis factor receptor 1 ($TNFRI^{-/-}$) were infected with 1000 *Pcc*-IRBCs on E8.5. This time point was chosen based on the multivariate modeling, which suggested that *Tnf* transcripts are elevated before preterm delivery (after E16.5) in B6 mice. Contrary to expectation, both $TNF^{-/-}$ and $TNFRI^{-/-}$ IP mice experienced preterm delivery after E16.5, similar to wild-type B6 mice (Figure 4.9).

Although parasitemia appears to be higher in $TNF^{-/-}$ IP compared to B6 mice, AUC analysis revealed no significant differences between the groups for either $TNF^{-/-}$ or $TNFRI^{-/-}$ IP dams (Figure 4.10). Taken together, these data demonstrate that TNF and TNF signaling through TNFRI are not required to drive preterm delivery in mice infected on E8.5.

P. chabaudi infection induces elevated antioxidant gene transcript expression in the placenta before preterm delivery

Oxidative stress, generally described as an imbalance between the formation of free radicals, such as reactive oxygen species (ROS), and antioxidant defense molecules within cells and tissues, leads to cellular damage to lipids, proteins, RNA, and DNA. Recently, oxidative stress has been documented to play a crucial role in pregnancy outcomes in some mouse models of PM [17–19] and is implicated in women experiencing malaria during pregnancy [16,316] as well as other types of pregnancy complications [185,186,331]. To interrogate the role of oxidative stress in this model, placentae were evaluated for alterations in antioxidant gene expression by RT-qPCR (Figure 4.11). In the placentae of B6 mice infected on E8.5, placental transcript abundance at E16.5 for superoxide dismutases 1 and 2 (*Sod1*, *Sod2*), catalase (*Cat*), and nuclear factor erythroid-2 related factor 2 (*Nrf2*) were significantly elevated compared to UP controls (Figure 4.11A-B, D-E). None of these targets were significantly elevated in IP mice infected and euthanized at the other time points (Figure 4.11). However, when the relationships between antioxidant transcript abundance and parasitemia were considered at E15.5 in the E6.5 infection group, *Hmox1* and *Cat* positively correlated

with placental parasitemia (Figure 4.8C, E). Additionally, *Hmox1* positively correlated with peripheral parasitemia AUC (Figure 4.8C-E). In the E8.5 infection group, E16.5 placental *Sod3* transcripts tended to correlate negatively with both peripheral parasitemia at sacrifice and parasitemia AUC (Figure 4.12). Significant correlations between antioxidant transcript expression and parasite burden were not found in the placenta at E17.5 in the E10.5 infection group.

Linear regression modeling was applied to assess factors important in driving differences in placental antioxidant gene expression. As with inflammatory markers, this analysis considered infection status, day euthanasia was performed, uterus weight, number of embryos, and embryo viability. The latter three were considered together and did not predict antioxidant transcript abundance. Infection status drove significant increases for genes except for *Sod3* ($p \leq 0.04$; Table 4.4). The day of euthanasia also significantly influenced all targets except *Sod 3* and *Hmox1.* Transcripts for *Nrf2, Sod1, Sod2,* and *Cat* in placentae from E8.5 infections (i.e., E16.5) were all significantly elevated relative to placentae from mice infected at E6.5 (i.e., E15.5; $p \leq 0.01$; Table 4.4). In a multivariate model testing influence of both status and day on these transcripts, holding day constant revealed a significant impact of infection was retained for *Nrf2, Sod1, Sod2, Cat,* and *Hmox1* ($p \leq 0.04$; Table 4.5). Membership in the E16.5 group independently predicted enhanced expression of *Nrf2, Sod1, Sod2, and Cat* ($p \leq 0.0254$; Table 4.5).

Discussion

Mouse models represent an affordable and genetically manipulable tool for investigating the pathogenesis of PM, a syndrome responsible for significant maternal morbidity and poor pregnancy outcomes globally. This study describes a novel murine model for malaria-induced preterm birth. This model requires a blood-stage infection in B6 mice using the murine infective parasite, *Plasmodium chabaudi chabaudi* AS (*Pcc*AS) at E6.5, E8.5, or E10.5. Although post-implantation *Pcc* infection in this model universally resulted in preterm birth, we observed that transcript abundance for certain genes in the placenta before delivery differed based on when the infection occurred in gestation. This model is the first to provide the flexibility to study malaria-induced pregnancy compromise driven by early post-implantation infection, without requiring acquired immunity or drug treatment for maternal survival. This is especially relevant to cases where immunity to PM is low or antimalarial treatment is not recommended, such as for primigravid women and those in their first trimester of pregnancy [315,334].

To varying extents, key features of human PM are recapitulated in this model, including maternal anemia, higher parasitemia in the placenta compared to the periphery, and preterm delivery [312,315]. Indeed, in the E8.5 and E10.5 infection groups, higher parasitemia in pregnant mice compared to non-pregnant controls corresponds with higher parasitemia in the placenta compared to peripheral parasitemia, corroborating previous studies in both mice and humans demonstrating that pregnancy itself can increase susceptibility to malaria [17,88,335] and lead to parasite accumulation in the placenta [311]. Thus, this novel model allows researchers to take a snapshot of the placenta at

various times during an acute malaria infection to investigate the relationships between parasite dynamics, placental development, and birth outcome.

Preterm delivery was a universal outcome of infection in the model reported here, with the time to delivery shortening the later in gestation the infection was introduced. When placental weight, pup weight, and pup viability were assessed one day before preterm delivery, the infection status of the dam had no impact. Thus, the physiological events that precipitate labor are acute. Analysis of the placenta preceding preterm delivery revealed differential expression of various inflammatory genes, highlighting the possibility that distinct mechanisms or triggers may be involved in driving preterm delivery in a gestational age-dependent manner in this model. Studies of cyclooxygenases, COX1 and COX2, have described their importance in the onset of labor in both mice and humans [336,337]; however, *Cox1* and *Cox2* transcripts were elevated only at E16.5 in mice infected at E8.5. Interestingly, whereas *Cox1* was positively correlated with parasitemia in the E6.5 infection group, no significant malaria-induced upregulation for either *Cox1* or *Cox2* relative to uninfected placenta was detected in the E10.5 infection group at E17.5 or in the E6.5 infection at E15.5, both sampled one day prior to expected preterm delivery. Consistent with this, multivariate modeling showed that *Cox2* expression was influenced by infection only at E8.5, with a weak tendency for *Cox1* to be affected by infection only.

IFNγ is elevated during acute malaria infection and required for parasite control [133]. *Ifnγ* transcripts were elevated only in the E8.5 and E10.5 infection groups even though all IP mice were experiencing ascending parasitemia at the time that placental analyses were conducted. Additionally, *Tnf* and *Il10* transcripts were increased in the

E8.5 infection group only, and multivariate modeling confirmed that only infection at this day significantly predicted these increases. This was unexpected given the association of these cytokines with human malaria-induced preterm delivery [2,109]. Likewise, $TNF^{-/-}$ and $TNFR1^{-/-}$ mice infected on E8.5 did not experience improved pregnancy outcomes or changes in the time to preterm delivery. This was contrary to expectation, given that ablation of TNF with antibody treatment successfully protected mice from *Pcc*AS-induced abortion following infection at E0.5 [5]. These data suggest that although TNF signaling may be an essential driver of poor pregnancy outcomes during human malaria infection [4,5,109] and early gestational malaria in the B6 mouse, its expression at the placental level is not required within the 24 hours preceding preterm delivery after infection at E8.5. *Il1β* transcript abundance positively correlated with parasitemia in the E6.5 infection group, and multivariate modeling showed that infection at E8.5 increased placental transcription of this factor. This observation is consistent with another model of malaria infection, in which reduced IL-1β signaling improved pregnancy outcomes [317]; thus, IL-1β appears to be a universal driver of poor birth outcomes in malaria, perhaps through inflammasome assembly and/or the initiation of pyroptosis [338].

Oxidative stress has been described in various models of preterm delivery [251] and implicated in both human and mouse PM [16–19,316]. To corroborate these observations, antioxidant gene transcripts were measured in placentae collected one day prior to expected preterm delivery. *Sod1*, *Sod2*, *Cat*, and *Nrf2* transcripts were elevated in the E8.5 infection group only, with *Hmox1* expression being predicted only by infection but not by infection day. Similar results were reported with induction of *Pcc*AS infection in B6 mice at E0.5, where *Sod1*, *Sod2*, *Cat*, and *Nrf2* transcripts were elevated in

conceptuses and antioxidant drug treatment mitigated pregnancy loss [18]. When the relationship between parasite burden and antioxidant gene transcript expression was considered, *Cat* and *Hmox1* transcripts were positively correlated with placental parasitemia at sacrifice and *Hmox1* shared this relationship with peripheral parasitemia AUC as well. These results are consistent with the observed strong association between *Hmox1* expression and hemozoin deposition in the placentae of *Pcc*AS-infected Swiss Webster dams at midgestation [286]. Since E6.5 IP mice exhibited significant anemia and the greatest interval between infection and preterm delivery, infection initiated at this time point may present another opportunity to study the impact of *Hmox1* regulation of heme in driving negative pregnancy outcomes. Elevated heme levels and altered *Hmox1* activity have been implicated in the pathogenesis of both human and murine PM [339–341] and other pregnancy complications [342]. For mice infected on E10.5, none of the antioxidant gene transcripts measured were differentially expressed or correlated with parasite burden. Since this group had an overall lower parasite burden relative to the other groups, these results may collectively indicate that a threshold of infectious burden is required to commensurate specific antioxidant transcript responses in this model.

Our analyses focused on placental inflammation and oxidative stress; however, this model did not assess other mechanisms of infection-induced preterm delivery. Some biological functions of clinical relevance in PM that could be explored in future studies include the coagulation pathway [8,10], the complement system [343], nutrient bioavailability [344] and transport across the placenta [345,346], angiogenic balance and vascularization [347], placental autophagy [348,349], and hormonal alterations [345].

Likewise, it is possible that pathological changes leading to preterm birth occurred in tissue types or sites not evaluated here, such as the uteroplacental interface.

Given the many remaining unresolved questions in PM pathogenesis, the model described here may be instrumental for future studies aimed at modeling maternal and/or fetal responses to malaria infection during pregnancy. Although *Pcc*AS infection was initiated on three distinct embryonic days in this study, the system might collectively be employed as a single model for malaria-induced pregnancy compromise because the time points assessed (infection and sacrifice days) have been reported to share functional and developmental similarities with 1st and early 2nd trimester human placental development [85,327]. Malaria infection in the 1st trimester is associated with detrimental effects on pregnancy [33,285,350] and represents a period in gestation where the placenta cannot be sampled, and preventative antimalarial treatment is not recommended [334]. Detailed reports on the histopathological impact of malaria infection during the 1st and early 2nd trimester of human pregnancy, which correspond to the time points modeled here, are currently unavailable. Thus, this model may provide a unique opportunity for researchers to gain insight into this underreported aspect of PM pathogenesis.

There are some limitations to this model and analysis, as reported here. First, mouse gestation remains an imperfect model of human gestation, with a shorter gestational period and the birth of altricial young [85,351–353]. However, the time points we evaluate in the mouse reportedly share similarities with the first trimester of human placentation [85,327]. Second, this model did not yield evidence of intervillositis, placental fibrin deposits, intrauterine restriction, or low birth weight, all well-documented features of PM described in postpartum gestational tissues [312,322,325,354], albeit at or

close to term. Of note, histological characterization of the early placenta during malaria infection has not yet been reported; thus, our model helps address this knowledge gap. Third, it is possible that the timing of our analyses may have contributed to a failure to detect critical physiological changes that occurred closer to the time of labor. Dams were euthanized at least 12 hours prior to expected preterm birth (which typically occurred overnight), and triggers for labor could have occurred inside this narrow window. Finally, the ability to successfully detect and characterize physiologically relevant changes by RT-qPCR alone may be limited. Thus, follow-up studies must consider expanding the timing of tissue collection and analyses, the types of tissues evaluated, and the breadth of techniques used to identify a more precise cause(s) of preterm birth in this model.

In conclusion, this model provides a new avenue for interrogating the pathological driver(s) of preterm birth following post-implantation malaria infection. This model adds a new dimension to our current arsenal for studying the mechanisms involved in PM pathogenesis and could help improve our understanding of how malaria during pregnancy may galvanize preterm delivery.

Figure 4.1. *P. chabaudi* AS infection in the post-implantation period universally precipitates preterm delivery.

(A) Schematic of experimental design.
(B-D) Percent starting weight presented for uninfected pregnant (UP), infected pregnant (IP), and infected non-pregnant (INP) groups. All IP mice experienced precipitous weight loss during ascending infection. Arrows indicate time points chosen for subsequent experiments
(E-G) Percent parasitemia are presented for infected pregnant IP and INP groups.

Sample sizes: E6.5 infection group (red solid circles): UP, *n* = 6; IP, *n* = 6; and INP, *n* = 4; E8.5 infection group (blue solid circles): UP, *n* = 6; IP, *n* = 8; INP, *n* = 4; E10.5 infection group (green solid circles): UP, *n* = 6; IP, *n* = 14; INP, *n* = 7.

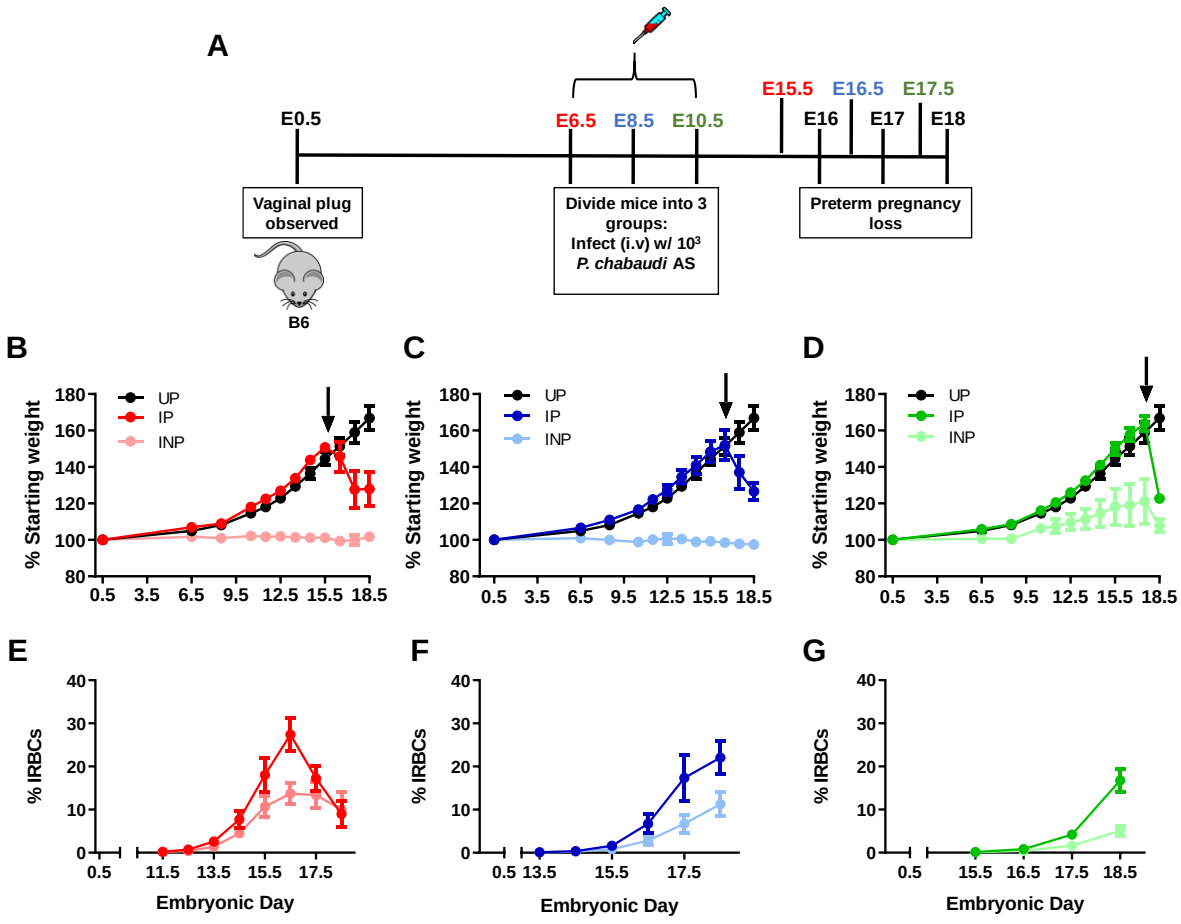

Figure 4.2. Area under the curve analysis for weight, parasitemia, and hematocrit in B6 mice infected with *P. chabaudi* AS on E6.5, E8.5, and E10.5.

(A-C) Area under the curve (AUC) was calculated for uninfected pregnant (UP), infected pregnant (IP), and infected non-pregnant (INP) mice belonging to the E6.5 infection group (A, D, G; red solid circles), E8.5 infection group (B, E, H; blue solid circles), or E10.5 infection group (C, F, I; green solid circles) in an observational study.
(D-F) Parasitemia AUC in IP mice and their INP counterparts. Statistically significant differences are revealed in the E8.5 and E10.5 infection groups but not in the E6.5 infection group.
(G-I) Hematocrit AUC in IP mice and their INP counterparts. Statistically significant differences were observed in the E8.5 infection group only.
Groups were compared either by using a Kruskal-Wallis test or unpaired t-test with Welch's correction (for parasitemia AUC). $^{**}P \leq 0.005$, $^{*}P < 0.05$; ns = not significant, $P > 0.05$.

Sample sizes: E6.5 infection group (red solid circles): UP, $n = 9$; IP, $n = 9$; and INP, $n = 5$; E8.5 infection group (blue solid circles): UP, $n = 12$; IP, $n = 15$; INP, $n = 7$; E10.5 infection group (green solid circles): UP, $n = 12$; IP, $n = 15$; INP, $n = 7$.

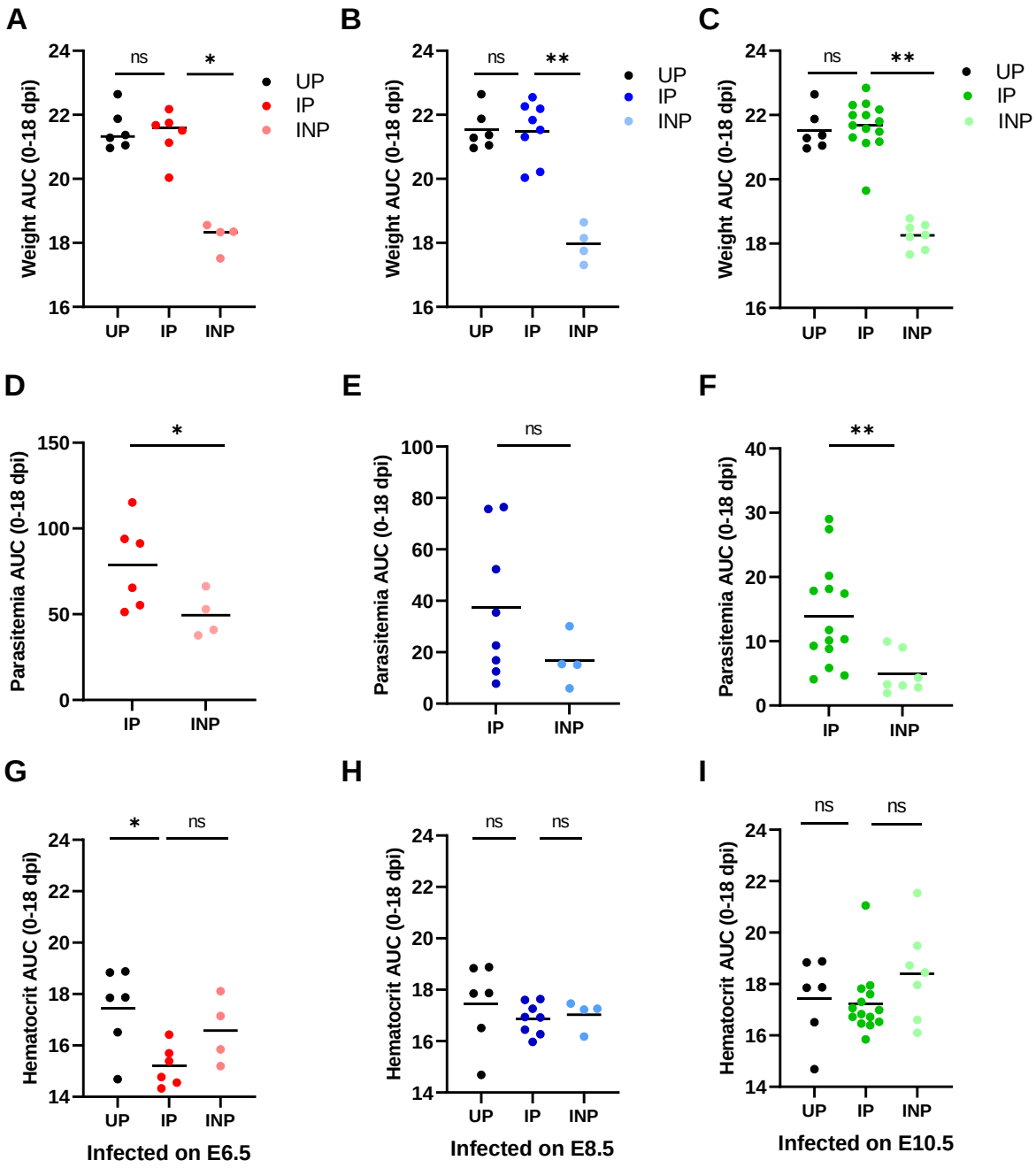
A
B
C
D
E
F
G
H
I
Weight AUC (0-18 dpi)
Parasitemia AUC (0-18 dpi)
Hematocrit AUC (0-18 dpi)
UP
IP
INP
ns
*
**
Infected on E6.5
Infected on E8.5
Infected on E10.5

Figure 4.3. *P. chabaudi* AS-infected red blood cells accumulate prior to preterm delivery in the placentae of mice infected at E8.5 and E10.5.

Peripheral and placental parasitemia from mice infected on E6.5 (red), E8.5 (blue) and E10.5 (green), sacrificed at E15.5, E16.5 and E17.5, respectively. **P < 0.002, unpaired t-test with Welch's correction; ns = not significant, P > 0.05.

Sample sizes: E15.5 (peripheral), *n* = 5; E15.5 (placental), *n* = 5; E16.5 (peripheral), *n* = 10; E16.5 (placental), *n* = 6; E17.5 (peripheral), *n* = 5; E17.5 (placental), *n* = 5.

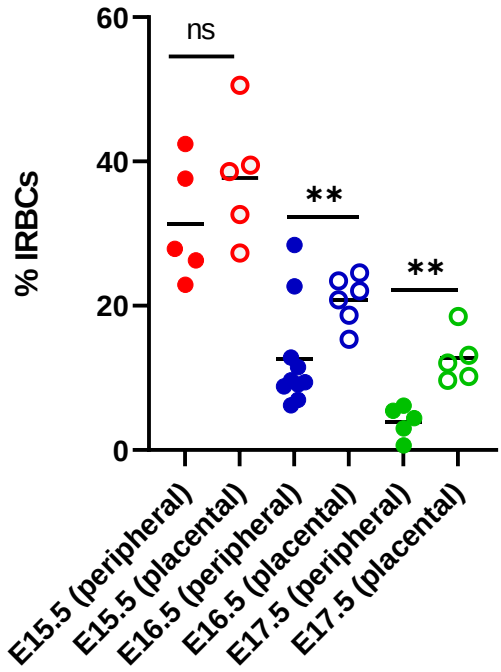

Figure 4.4. *P. chabaudi* AS infection does not significantly impact placenta or pup weight prior to preterm delivery.

(A) Placenta and (B) pup weights depicted for uninfected pregnant (UP) and infected pregnant (IP) mice sacrificed one day before preterm delivery. These data are shown for visualization only; statistical analysis is in the text. E15.5 group: 4 IP dams, 32 placentae; 4 UP dams, 30 placentae. E16.5 group: 4 IP dams, 31 placentae; 4 UP dams, 33 placentae. E17.5 group: 5 IP dams, 40 placentae; 5 UP dams, 41 placentae.

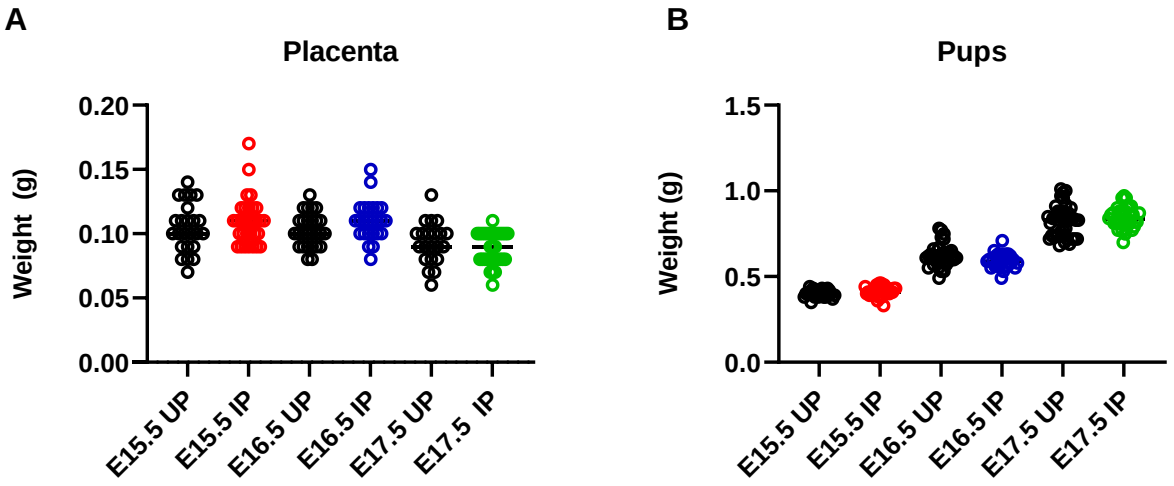

Table 4.1. Pup viability in mice infected on E6.5, E8.5, and E10.5 and euthanized on E15.5, E16.5, and E17.5, respectively.

Pup viability between infected pregnant (IP) and uninfected pregnant (UP) dams sacrificed one day prior to expected preterm delivery. Percentages show percent viability within a group. Statistical significance was determined via proportional analysis tested by chi-square. *NS* = not significant.

Infection group	Total # pups	# non-viable pups	% viable	P value
E6.5 IP	63	1	98.4%	*NS*
E6.5 UP	70	4	94.2%	
E8.5 IP	125	5	96.0%	
E8.5 UP	100	1	99.0%	
E10.5 IP	90	3	96.6%	
E10.5 UP	82	2	97.5%	

Figure 4.5. *P.chabaudi* AS-infected red blood cells in the placental labyrinth region one day prior to preterm delivery.

(A, C, E) Micrographs taken with 100x objective lens from uninfected pregnant (UP) controls at E15.5, E16.5, and E17.5. (B, D, F) micrographs from infected pregnant (IP) dams sacrificed one day prior to preterm delivery on E15.5, E16.5, and E17.5, respectively. Placental sections were stained with hematoxylin-eosin (H&E).

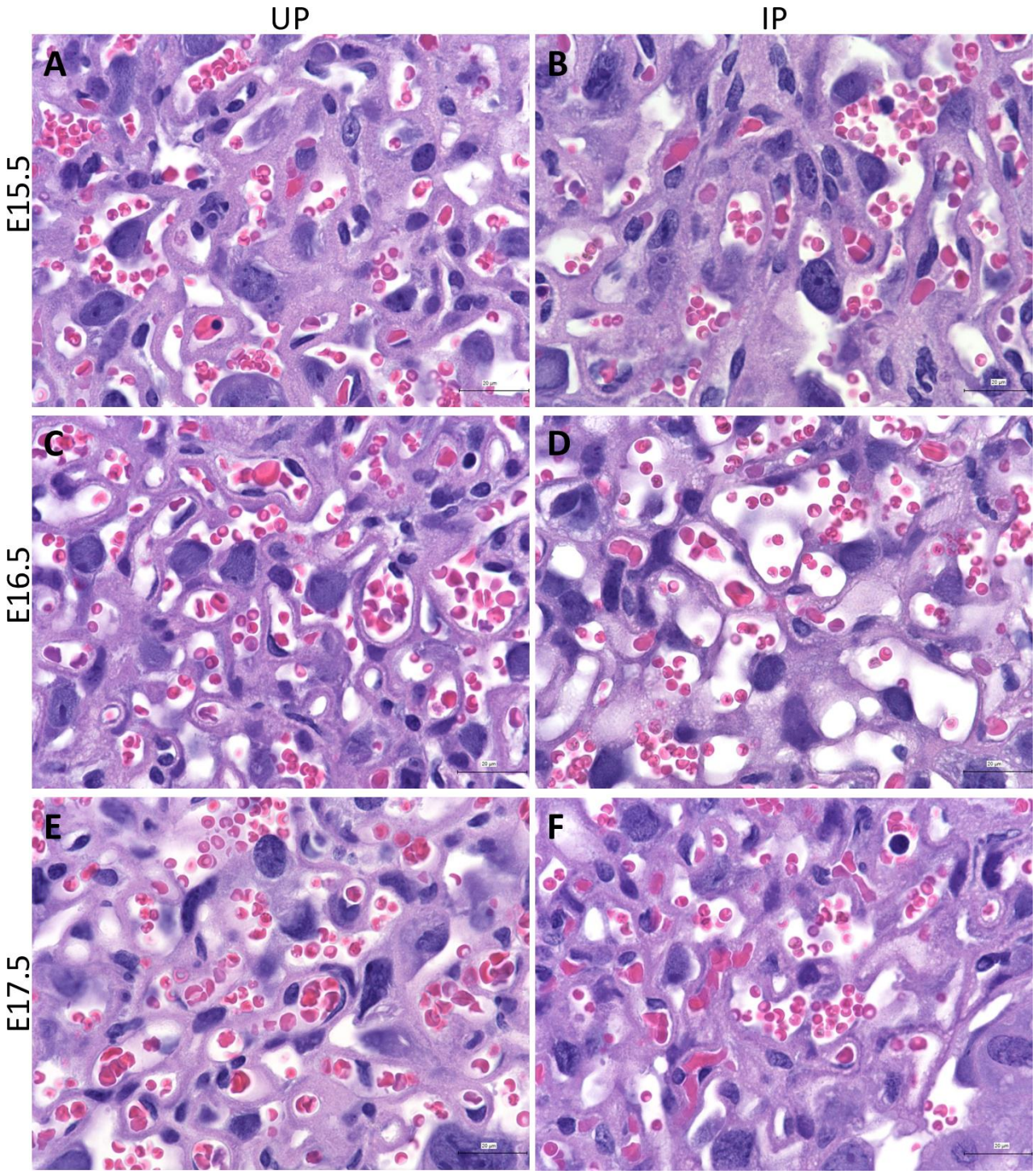
UP
IP
A
B
C
D
E
F
E15.5
E16.5
E17.5

Figure 4.6. *P.chabaudi* AS-infected red blood cells in the placental labyrinth region one day prior to preterm delivery.

(A-C) micrographs taken with 100x objective lens of Giemsa-stained placentae from infected pregnant (IP) dams sacrificed one day prior to preterm delivery on E15.5, E16.5, and E17.5, respectively.

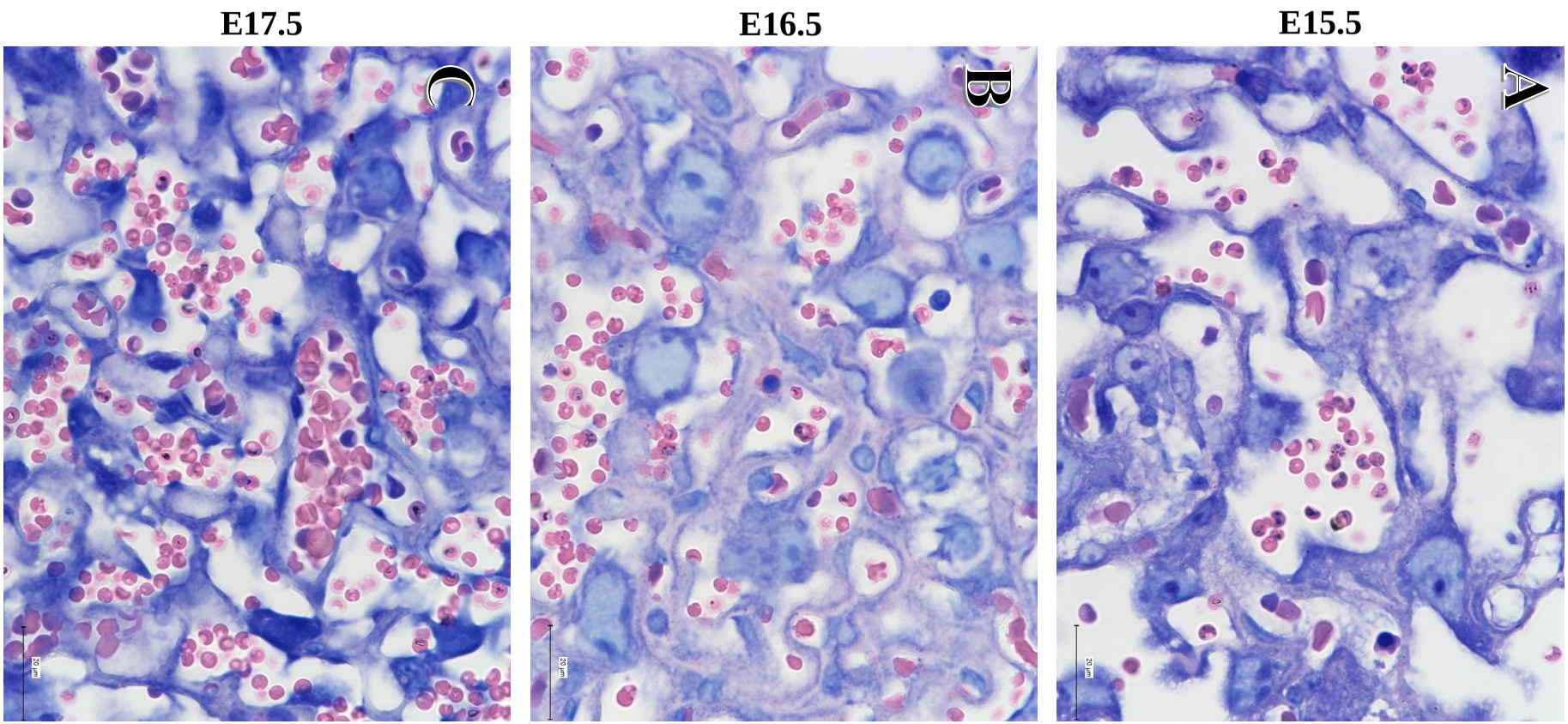
E17.5
E16.5
E15.5
C
B
A

Figure 4.7. *P. chabaudi* infection at E8.5 induces upregulation of inflammatory and parturition-associated gene transcripts at E16.5 prior to preterm delivery.

(A-F) Mouse *Ifnγ*, *Tnf*, *Il10*, *Il1β*, *Cox1*, and *Cox2* mRNA abundances normalized to *Ubc* and quantified by qPCR in placentae taken from infected pregnant (solid color circles) and uninfected pregnant (open black circles) dams. Solid color circles denote pooled placentae from individual infected dams sacrificed on E15.5 (red), E16.5 (blue), and E17.5 (green). Open black circles are pooled placentae from uninfected pregnant controls for each group. Group means and transcript abundance in individual mice are depicted. **P ≤ 0.005, *P < 0.05, unpaired t-test with Welch's correction; ns = not significant, P > 0.05; # denotes a trending result, P = 0.08.

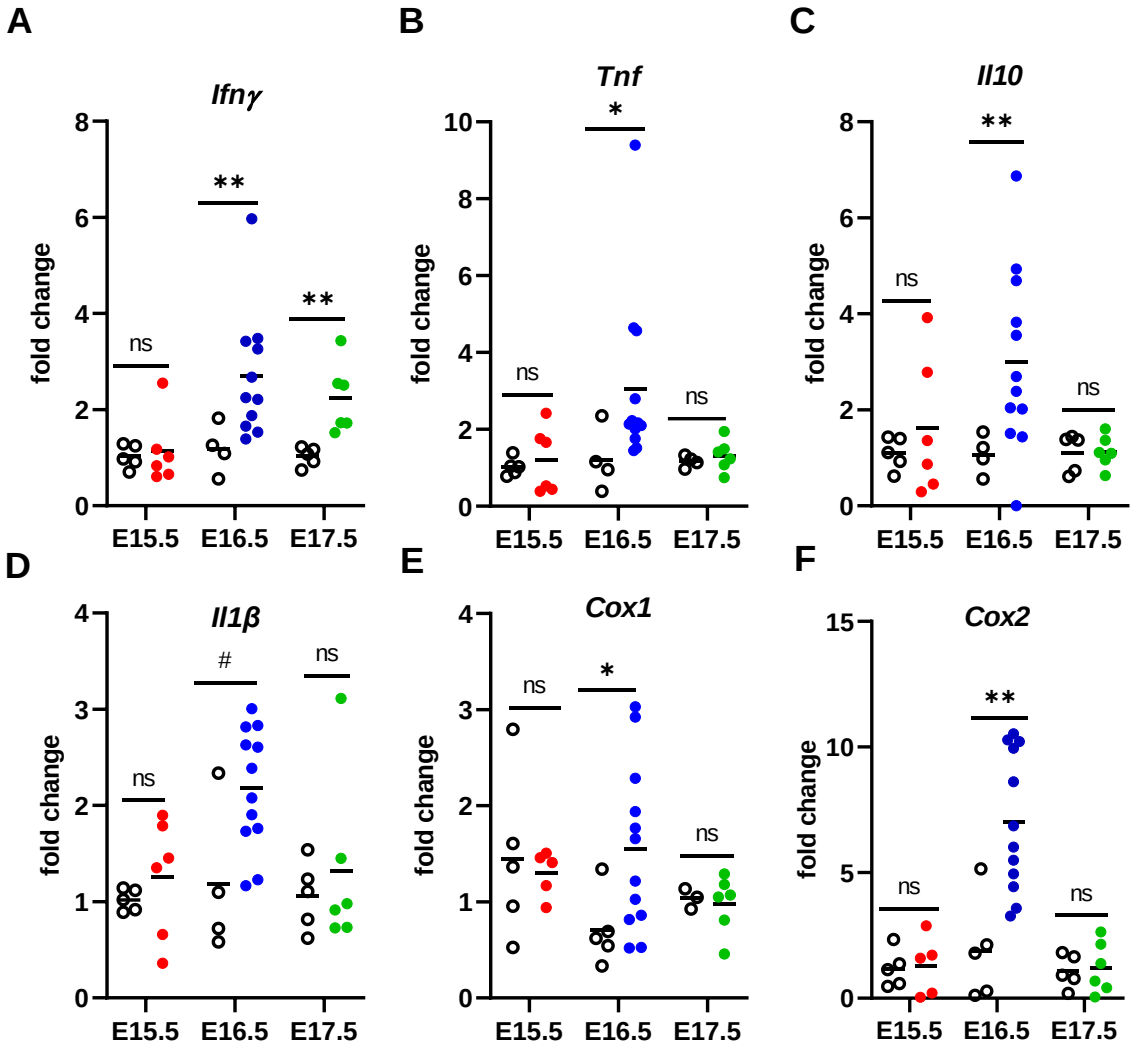

Figure 4.8. Inflammatory and antioxidant gene expression in the E15.5 placenta positively correlates with peripheral and placental parasitemia in mice infected on E6.5.

(A-F) Mouse mRNA transcript abundance relative to peripheral parasitemia at the time of sacrifice, peripheral parasitemia AUC, and placental parasitemia one day before expected preterm birth (E15.5).

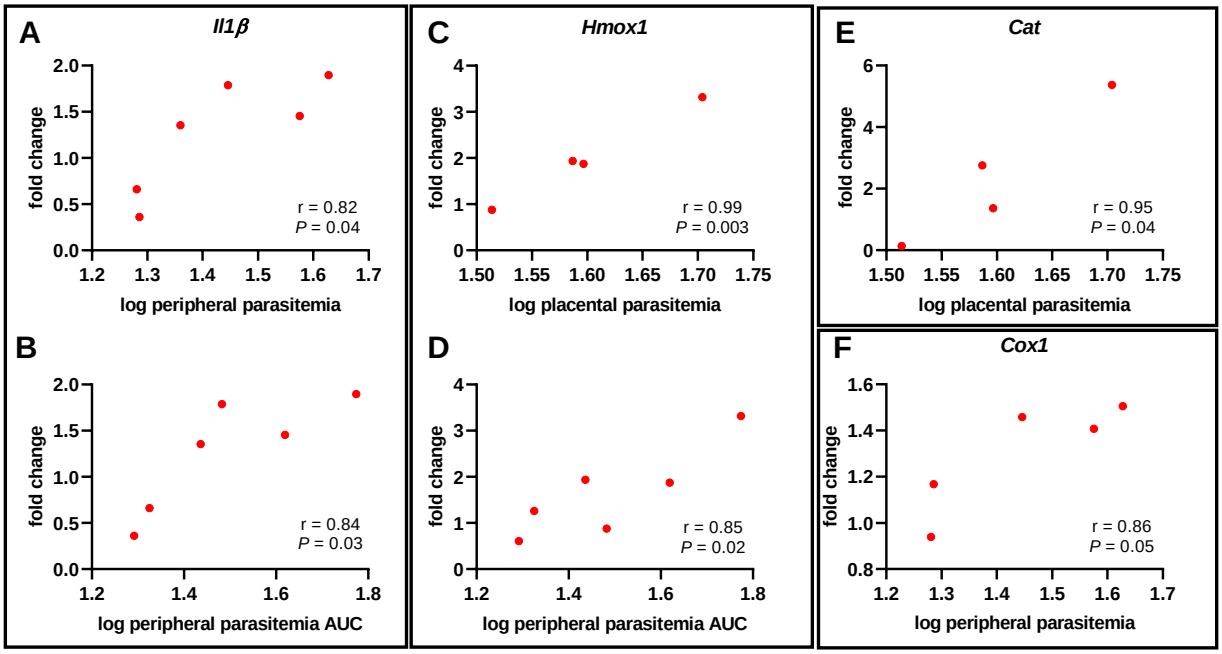

Table 4.2. Univariate logistic regression analysis of inflammatory and parturition-associated transcript expression and day of sacrifice.

Analysis performed with proc reg for dichotomous (status) and continuous (parasitemia) and variables and proc glm for categorical variables (sacrifice day). Parasitemia was log10-transformed for the analysis. Dashes indicate that E15.5 is the reference value. Sample sizes for the analysis are as follows: E15.5 IP, n = 4; E15.5 UP, n = 4; E16.5 IP, n = 11; E16.5 UP, n = 4; E17.5 IP, n = 6; E17.5 UP, n = 3.

	Ifnγ		***Tnf***		***Il1β***		***Il10***		***Cox1***		***Cox2***	
	Co-efficient; SEM	P	Co-efficient; SEM	P	Co-efficient; SEM	P	Co-efficient; SEM	P	Co-efficient; SEM	P	Co-efficient; SEM	P
Categorical variables												
Intercept	1.09; 0.30	0.001	1.12; 0.26	0.0001	1.15; 0.21	<.0001	1.38; 0.39	0.001	1.21; 0.21	<.0001	1.24; 0.77	0.12
E15.5 sacrifice	-	-	-	-	-	-	-	-	-	-	-	-
E16.5 sacrifice	2.29; 0.40	0.004	2.14; 0.33	0.004	1.92; 0.26	0.005	2.68; 0.51	0.01	1.29; 0.08	0.74	5.50; 0.97	<.0001
E17.5 sacrifice	1.69; 0.43	0.17	1.25; 0.37	0.71	1.20; 0.29	0.84	1.09; 0.57	0.61	0.997; 0.29	0.47	1.15; 1.06	0.93
Intercept	1.07; 0.26	0.0002	1.13; 0.25	<.0001	1.08; 0.19	<.0001	1.07; 0.38	0.007	0.925; 0.17	<.0001	1.38; 0.76	0.07
Status (IP)	2.17; 0.33	0.002	1.84; 0.31	0.02	1.73; 0.23	0.009	2.27; 0.47	0.01	1.34; 0.21	0.05	4.25; 0.97	0.005
Continuous variables												
Intercept	1.16; 0.27	0.0002	1.17; 0.20	<.0001	1.10; 0.16	<.0001	1.07; 0.25	0.0002	0.897; 0.16	<.0001	1.49; 0.65	0.03
Placental parasitemia	1.94; 0.28	0.009	1.74; 0.20	0.01	1.68; 0.16	0.001	1.88; 0.25	0.003	1.22; 0.16	0.05	3.69; 0.70	0.004
Intercept	1.38; 0.26	<.0001	1.30; 0.24	<.0001	1.20; 0.18	<.0001	1.32; 0.36	0.0008	0.940; 0.16	<.0001	1.84; 0.72	0.02
Peripheral parasitemia	1.98; 0.31	0.05	1.74; 0.28	0.12	1.65; 0.21	0.03	2.13; 0.41	0.06	1.34; 0.18	0.03	4.00; 0.89	0.02
Intercept	1.89; 0.17	<.0001	1.67; 0.16	<.0001	1.58; 0.12	<.0001	1.98; 0.24	<.0001	1.25; 0.10	<.0001	3.58; 0.51	<.0001
Peripheral parasitemia AUC	2.00; 0.037	0.007	1.74; 0.034	0.04	1.64; 0.026	0.01	2.11; 0.051	0.02	1.30; 0.023	0.04	3.88; 0.10	0.008

Table 4.3. Multivariate logistic regression analysis of inflammatory and parturition-associated transcript expression and day of sacrifice.

Analysis performed with proc glm. Dashes indicate that E15.5 is the reference value; dashes and NA indicate that these parameters were not considered in the analysis. Sample sizes for the analysis are as follows: E15.5 IP, n = 4; E16.5 IP, n = 11; E17.5 IP, n = 6.

	Ifnγ		*Tnf*		*Il1β*		*Il10*		*Cox1*		*Cox2*	
	Co-efficient; SEM	P	Co-efficient; SEM	P	Co-efficient; SEM	P	Co-efficient; SEM	P	Co-efficient; SEM	P	Co-efficient; SEM	P
Categorical variables												
Intercept	0.562; 0.32	0.09	0.809; 0.30	0.009	0.867; 0.23	0.0006	0.834; 0.44	0.07	0.982; 0.24	0.0002	0.165; 0.80	0.84
Status (IP)	1.53; 0.31	0.004	1.38; 0.30	0.06	1.89; 0.22	0.027	1.83; 0.43	0.03	1.40; 0.22	0.06	2.31; 0.75	0.007
E15.5 sacrifice	-	-	-	-	-	-	-	-	-	-	-	-
E16.5 sacrifice	1.59; 0.32	0.008	1.73; 0.33	0.009	1.37; 0.26	0.01	1.95; 0.57	0.03	1.00; 0.25	0.93	4.00; 0.90	0.0002
E17.5 sacrifice	1.16; 0.40	0.13	0.915; 0.36	0.77	0.924; 0.27	0.83	0.492; 0.54	0.53	0.717; 0.29	0.37	-0.0138; 0.972	0.85
Continuous variables												
Placental parasitemia	NA	-	NA	-	NA	-	NA	-	NA	-	NA	-
Peripheral parasitemia	NA	-	NA	-	NA	-	NA	-	NA	-	NA	-
Peripheral parasitemia AUC	NA	-	NA	-	NA	-	NA	-	NA	-	NA	-

Figure 4.9. Tumor necrosis factor ($TNF^{-/-}$) and tumor necrosis factor receptor 1 ($TNFRI^{-/-}$) deficient mice experience preterm delivery following malaria infection on E8.5.

(A) Percent starting weight for $TNF^{-/-}$ and (B) $TNFRI^{-/-}$ mice are depicted for infected pregnant (IP) and infected non-pregnant (INP) groups. $TNF^{-/-}$ IP: n = 3, INP n =3; $TNFRI^{-/-}$ IP: n = 7, INP n = 3; B6 IP: n = 5. All IP mice experience precipitous weight loss, indicating preterm pregnancy compromise.

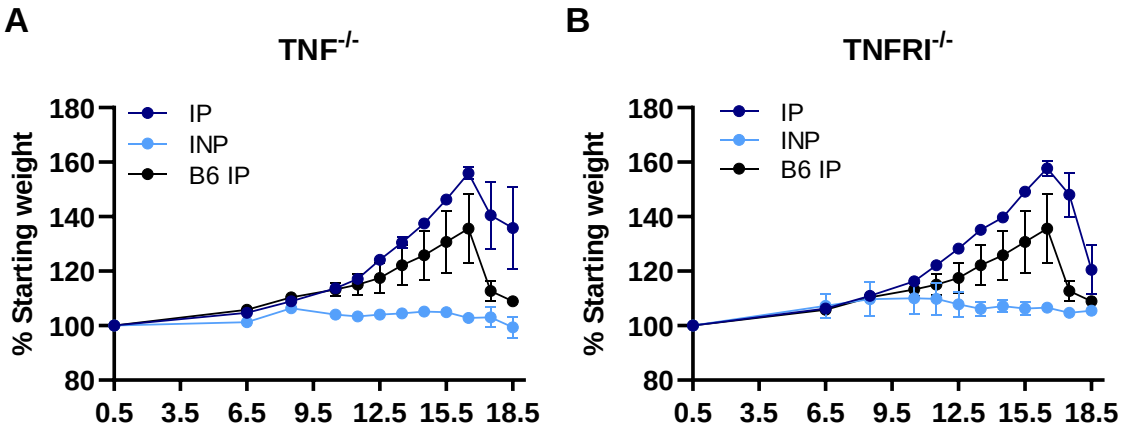

Figure 4.10. Parasitemia and area under the curve for parasitemia in TNF$^{-/-}$ and TNFR1$^{-/-}$ mice infected on E8.5.

(A) Parasitemia (% IRBCs) in TNF$^{-/-}$ and (B) TNFRI$^{-/-}$ mice. (C-D) Area under the curve (AUC) analysis do not show a statistically significant increase in parasitemia between IP versus INP groups for both strains. TNF$^{-/-}$ IP: n = 3, INP n = 3; TNFRI$^{-/-}$ IP: n = 7, INP n = 3; ns = not significant, P > 0.05.

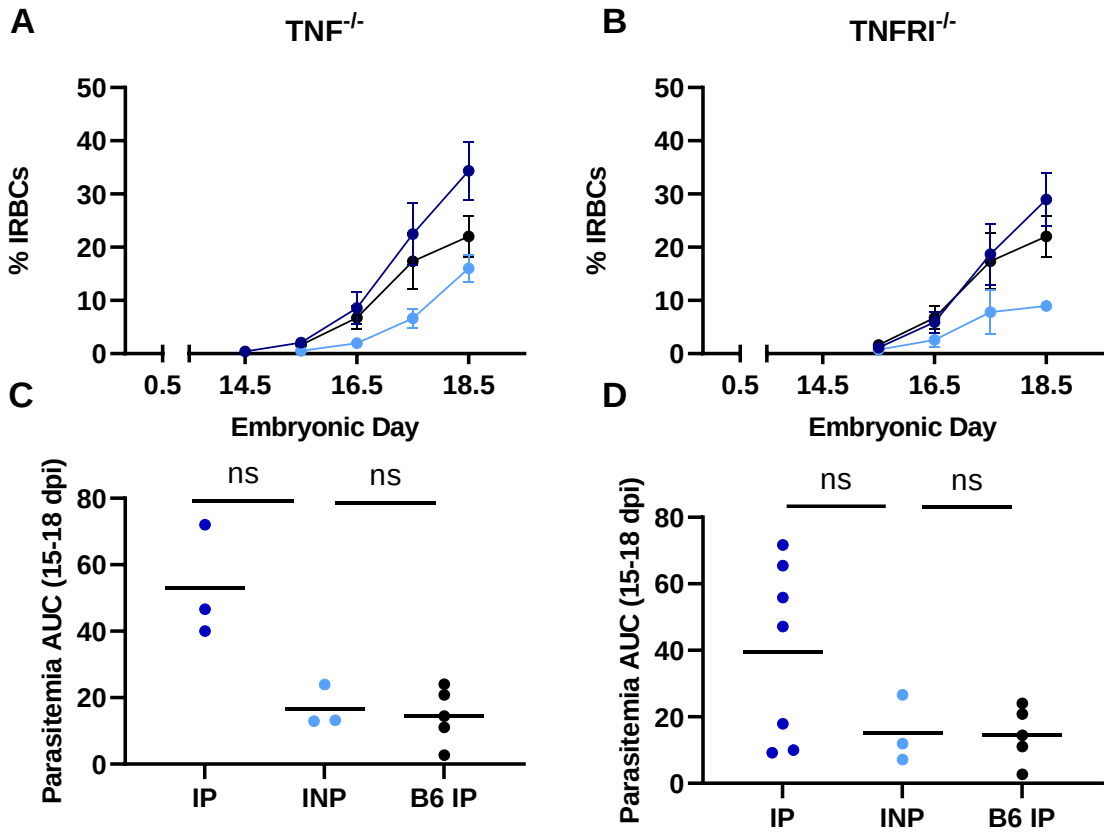

Figure 4.11. *P. chabaudi* infection at E8.5 induces elevated antioxidant gene transcript expression in the E16.5 placenta prior to preterm delivery.

(A-F) Mouse *Sod1*, *Sod2*, *Sod3*, *Cat*, *Nrf2*, and *Hmox1* mRNA abundance relative to *Ubc* and quantified by qPCR in placentae taken from infected pregnant (solid circles) and uninfected pregnant (open black circles) dams. Solid color circles denote pooled placentae from individual infected dams sacrificed on E15.5 (red), E16.5 (blue), and E17.5 (green). Open black circles are pooled placentae from uninfected pregnant controls for each group. Group means and transcript abundance in individual mice are depicted. ***P ≤ 0.005, **P = 0.02; ns = not significant, P > 0.05.

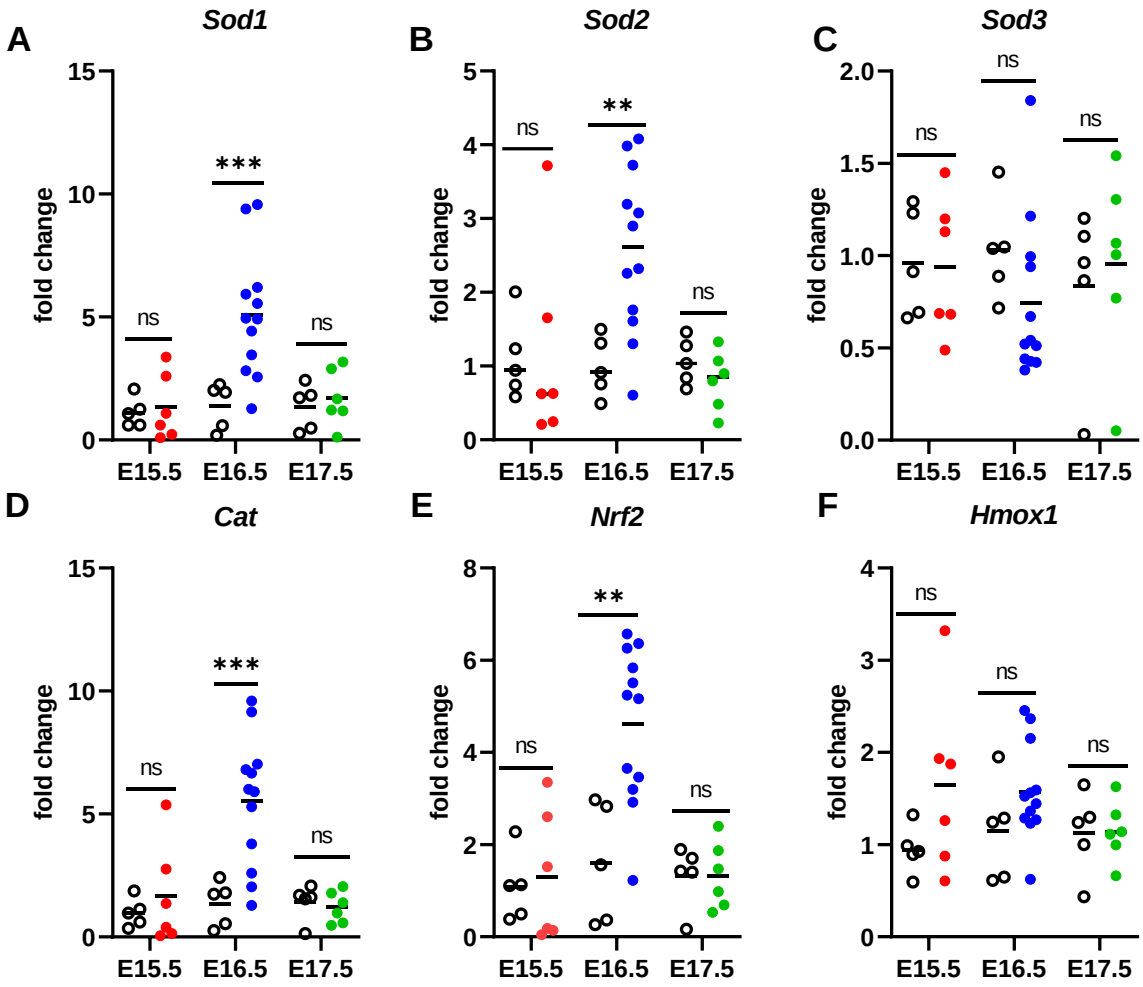

Figure 4.12. Placental *Sod3* gene expression negatively correlates with peripheral parasitemia at sacrifice on E16.5 in mice infected on E8.5.

Mouse *Sod3* mRNA transcript abundance measured in placentae collected one day before expected preterm birth (E16.5) relative to (A) peripheral parasitemia at the time of sacrifice and (B) peripheral parasitemia AUC.

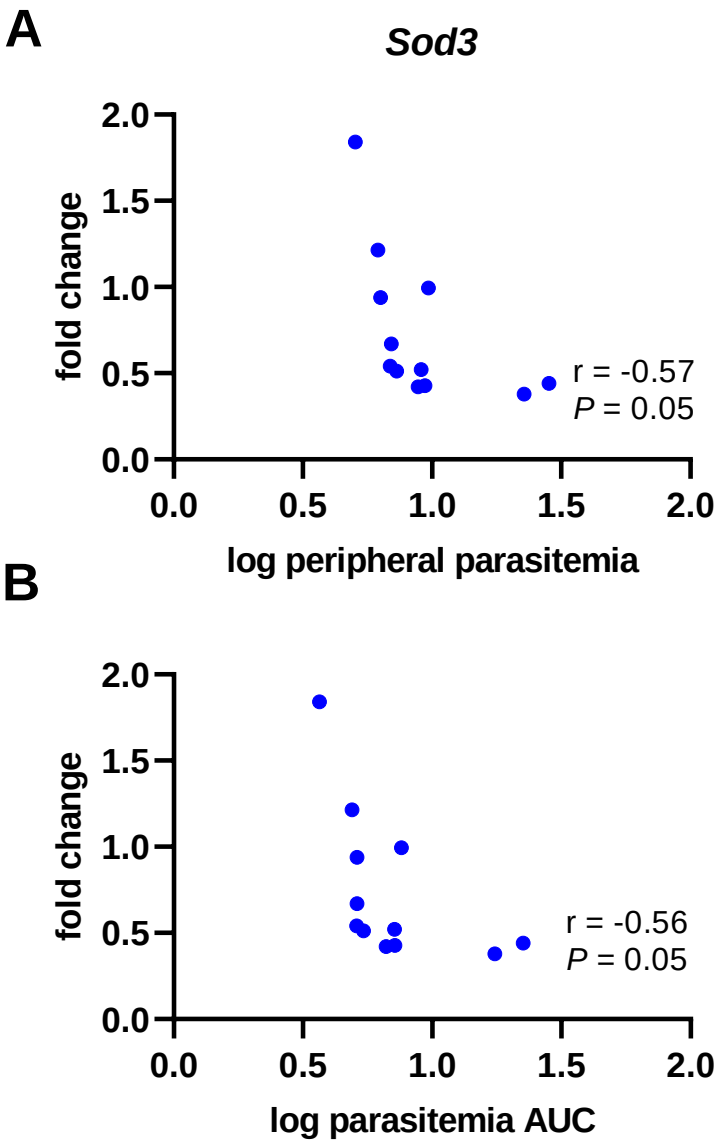

Table 4.4. Univariate logistic regression analysis of antioxidant transcript expression and day of sacrifice.

Analysis performed with proc reg for continuous (parasitemia) and dichotomous (status) variables and proc glm for categorical variables (sacrifice day). Parasitemia were log10-transformed for the analysis. Dashes indicate that E15.5 is the reference value. Sample sizes for the analysis are as follows: E15.5 IP, n = 4; E15.5 UP, n = 4; E16.5 IP, n = 11; E16.5 UP, n = 4; E17.5 IP, n = 6; E17.5 UP, n = 3.

	Nrf2		***Sod1***		***Sod2***		***Sod3***		***Cat***		***Hmox1***	
	Co-efficient; SEM	P	Co-efficient; SEM	P	Co-efficient; SEM	P	Co-efficient; SEM	P	Co-efficient; SEM	P	Co-efficient; SEM	P
Categorical variables												
Intercept	1.20; 0.46	0.01	1.23; 0.60	0.04	1.14; 0.29	0.004	0.94; 0.12	<.0001	1.36; 0.65	0.04	1.32; 0.17	<.0001
E15.5 sacrifice	-	-	-	-	-	-	-	-	-	-	-	-
E16.5 sacrifice	3.73; 0.60	0.0002	3.99; 0.77	0.001	2.10; 0.37	0.01	0.825; 0.15	0.44	4.28; 0.84	0.0013	1.44; 0.22	0.59
E17.5 sacrifice	1.32; 0.66	0.86	1.54; 0.84	0.71	0.915 ; 0.41	0.59	0.89; 0.17	0.75	1.29; 0.92	0.94	1.12; 0.25	0.44
Intercept	1.33; 0.47	0.007	1.29; 0.56	0.02	1.05; 0.27	0.0004	0.940; 0.10	<.0001	1.25; 0.61	0.05	1.07; 0.14	<.0001
Status (IP)	2.96; 0.59	0.009	3.29; 0.70	0.007	1.77; 0.72	0.04	0.84; 0.13	0.47	3.46; 0.78	0.007	1.48; 0.41	0.03
Continuous variables												
Intercept	1.26; 0.40	0.002	1.33; 0.39	0.002	1.05; 0.23	0.0001	0.927; 0.088	<.0001	1.24; 0.49	0.01	1.02; 0.14	<.0001
Placental parasitemia	2.65; 0.42	0.005	2.55; 0.40	0.005	1.59; 0.24	0.03	0.756; 0.09	0.07	2.88; 0.51	0.003	1.48; 0.15	0.004
Intercept	1.56; 0.44	0.001	1.63; 0.53	0.004	1.13; 0.25	<.0001	0.956; 0.095	<.0001	1.53; 0.58	0.01	1.02; 0.13	<.0001
Peripheral parasitemia	2.81; 0.53	0.02	3.08; 0.64	0.02	1.72; 0.30	0.05	0.834; 0.11	0.29	3.29; 0.69	0.01	1.50; 0.15	0.002
Intercept	2.57; 0.30	<.0001	2.81; 0.36	<.0001	1.61; 0.18	<.0001	0.865; 0.067	<.0001	2.95; 0.40	<.0001	1.40; 0.052	<.0001
Peripheral parasitemia AUC	2.74; 0.066	0.01	3.02; 0.078	0.013	1.68; 0.038	0.047	0.854; 0.015	0.42	3.19; 0.086	0.008	1.45; 0.019	0.012

Table 4.5. Multivariate logistic regression analysis of antioxidant transcript expression and day of sacrifice.

Analysis performed with proc glm. Dashes indicate that E15.5 is the reference value; dashes and NA indicate that these parameters were not considered in the analysis. Sample sizes for the analysis are as follows: E15.5 IP, n = 4; E16.5 IP, n = 11; E17.5 IP, n = 6.

	Nrf2		***Sod1***		***Sod2***		***Sod3***		***Cat***		***Hmox1***	
	Co-efficient; SEM	P	Co-efficient; SEM	P	Co-efficient; SEM	P	Co-efficient; SEM	P	Co-efficient; SEM	P	Co-efficient; SEM	P
Categorical variables												
Intercept	0.517; 0.50	0.31	0.347; 0.65	0.60	0.837; 0.34	0.01	0.992; 014	<.0001	0.392; 0.71	0.58	1.16; 0.20	<.0001
Status (IP)	1.77; 0.48	0.01	1.97; 0.61	0.01	1.40; 0.34	0.08	0.911; 0.14	0.56	2.17; 0.67	0.01	1.50; 0.19	0.05
E15.5 sacrifice	-	-	-	-	-	-	-	-	-	-	-	-
E16.5 sacrifice	2.84; 0.56	0.0002	2.86; 0.72	0.001	1.71; 0.27	0.02	0.883; 0.16	0.50	3.03; 0.79	0.002	1.18; 0.20	0.80
E17.5 sacrifice	0.635; 0.61	0.85	0.656; 0.78	0.70	0.612; 0.42	0.58	0.944; 0.18	0.79	0.328; 0.86	0.94	0.924; 0.24	0.43
Continuous variables												
Placental parasitemia	NA	-	NA	-	NA	-	NA	-	NA	-	NA	-
Peripheral parasitemia	NA	-	NA	-	NA	-	NA	-	NA	-	NA	-
Peripheral parasitemia AUC	NA	-	NA	-	NA	-	NA	-	NA	-	NA	-

CHAPTER 5

CONCLUSIONS AND FUTURE DIRECTIONS

The data presented in this dissertation focused on the genetic and therapeutic manipulation of pathogenic maternal responses to malaria infection during pregnancy. First, I outlined my approach for evaluating the synergistic relationship between maternal inflammation and coagulation in a murine model of placental malaria (PM). It is crucial to state that inflammation and coagulation are natural responses to infection critical for controlling the infection and ensuring maternal survival. However, the activation of these pathways often comes at a cost to the developing fetus. Moreover, the exaggeration/dysregulation of these malaria-induced responses contribute to PM pathogenesis. My goal was to mitigate the pathogenic aspect of these responses instead of eliminating them entirely. Second, I investigated the therapeutic potential of systemic antioxidant drug administration to improve pregnancy outcomes in malaria-infected dams. These studies add to the growing literature that seeks to pinpoint how systemic oxidative stress conditions contribute to pregnancy compromise.

The results of the studies outlined in Chapter 2 provide compelling evidence for the crosstalk between inflammation and coagulation in our murine model of PM. The precise mechanism(s) that mediates this connection remains unclear; however, differential protease-activated receptor (PAR) transcript abundance with both tumor necrosis factor (TNF) genetic deletion and anticoagulant therapy provides a clue for

where future studies should begin. Antagonizing PAR signaling in this murine model is a crucial next step to determining whether the connection between inflammation and coagulation is PAR-dependent. However, special attention must be given to the differences in human and mouse PAR expression and function to interpret the results appropriately. Moreover, *in vitro* studies using cells isolated from PAR-1 and PAR-2 knockout mice would provide an excellent opportunity to discover the mechanism of TNF-induced tissue factor expression in PM and would allow for more mechanistic studies to determine which coagulation factors and/or anticoagulant molecules, such as endothelial protein C receptor, are primarily responsible for mediating pathogenic or protective signaling. An exciting prospect of these studies will be determining the extent to which the maternal compartment (i.e., immune cells) or the fetal compartment (i.e., placental cells) is most responsible for driving poor pregnancy outcomes or if they both contribute equally. Another area of future work could involve using other mouse models of PM, which recapitulate different aspects of PM pathogenesis. One of these models uses *Plasmodium berghei* infection in BALB/c mice during midgestation (between E10.5-E13.5). A preliminary study in this model used the oral anticoagulant drug, Apixaban, to determine whether anticoagulant treatment would be effective across various PM models. The results of that preliminary work are shown in Appendix A of this dissertation. Malaria-infected dams were allowed to carry to term and time to delivery, and the ability to deliver live pups was observed. Future experiments would include a sacrifice study, where embryo viability on E18.5, one day prior to expected partition in healthy pregnant mice, would be assessed in treated animals relative to sham controls. Since this parasite and mouse combination is characterized by aberrant

antioxidant protein levels and placental oxidative stress, this model would be appropriate for interrogating the connection between coagulation and oxidative stress in PM. Additionally, a fostering experiment would help assess postnatal pup survival, which is already reduced in this model but could be a robust readout for determining the impact of anticoagulant treatment on offspring survival after maternal infection. It would also be exciting to assess offspring susceptibility to malaria infection and explore any differences in immune responses or function in the offspring attributed to maternal exposure to malaria.

In Chapter 3, the studies focused on oxidative stress and cell death, specifically the iron-, reactive oxygen species (ROS)-, and lipid peroxidation-dependent form of cell death known as ferroptosis. Prior research from Dr. Moore's laboratory and others has highlighted the inability of antioxidant defense systems to protect the dam or placenta from oxidative stress during malaria. The studies described in this chapter are the first steps to delineating the source ROS that could be mediating this damage and determining whether oxidative stress is a consequence of other pathogenic processes, such as inflammation and coagulation, or can mediate poor health outcomes independent of those. My data hint that oxidative stress may occur downstream of other pathogenic responses because targeting it directly did not improve pregnancy outcomes. Antioxidant transcript expression was reduced by anticoagulant treatment in the face of reduced inflammation, but no changes occurred when TNF-driven inflammation was targeted. This could suggest that another cytokine besides TNF may be more involved in modulating antioxidant transcript expression or that oxidative stress in this model results from a hypercoagulable state induced by infection. Thus, the need to upregulate

antioxidant transcripts is diminished when coagulation is under control. For a study to address this question, the most critical source of ROS needs to be determined.

Another future study should focus on distinguishing the proposed antimalarial activity of Deferoxamine (DFO) from its iron-chelation properties. One way to do so would be by removing the parasite from the equation and investigating whether DFO treatment improves pregnancy outcomes under heme/iron or hemozoin overload conditions. Furthermore, characterizing the iron status of malaria-infected mice in our models is a required step to be able to interpret any data related to possible DFO-mediated protection. Does malaria infection downregulate iron regulatory processes in our model, or are they overwhelmed by heme/iron or hemozoin insult?

Most of the data presented in this document have come from mouse studies; however, I have included some preliminary data that begins to probe the relevance of oxidative stress and even cell death through ferroptosis in the human placenta. Appendix B shows data from real-time quantitative analysis of transcripts related to antioxidant gene expression. Nuclear factor erythroid 2-related factor 2 (*NFE2L2/Nrf2*) and antioxidant genes superoxide dismutase 1 through 3 (*Sod1-3*) and catalase (Cat) were measured in placental tissues collected from women who were naturally exposed to malaria and controls. Due to small sample sizes and the inherent variability expected from human samples, I included these data for visualization purposes only (malaria-negative (PM-) group (n = 6) without statistical analyses). Transcripts for the heme detoxifying enzyme heme oxygenase 1 (*Hmox1*), iron absorption (Transferrin receptor 1, *TfR1*), and iron storage (ferritin) were also measured.

Moreover, transcripts for *Slc7a11*, a member of a cysteine-glutamate antiporter implicated in ferroptosis [355], were also measured (Appendix B). Additionally, transferrin receptor expression has been recently identified as a reliable marker of ferroptosis in placental cells; thus, preliminary immunofluorescence staining was performed in malaria-positive and malaria-negative samples. Representative images are presented in Appendix C, but no statistical analyses were performed due to sample size limitations. Finally, a preliminary investigation was conducted to quantify the protein expression of glutathione peroxidase 4 (GPX4), a key regulator of ferroptosis, in malaria-positive and malaria-negative human placenta (Appendix D). Together, these data demonstrate the need for future studies to add more samples to the experimental groups to determine if any markers of oxidative stress or regulators in ferroptosis are changing with infection status. Furthermore, a critical analysis would compare transcript and protein expression to birth outcome, inflammatory cytokine levels, and markers of dysregulated coagulation and fibrinolysis.

Overall, the data presented in this dissertation provide a solid foundation for future studies that can explore a mechanistic basis for malaria-induced pregnancy compromise. Future studies must take advantage of the various mouse strains and parasite combinations available and consider looking for universal mechanisms in PM models where the infection is initiated early and late in gestation. Future studies should also focus on validating findings made in the murine models *in vitro* and incorporate human samples to determine the translatability of the work. In the face of growing parasite resistance to antimalarials, research must explore possible avenues for adjunctive

treatment that is host-directed and helps preserve pregnancy even in the face of one of the most severe manifestations of malaria infection, placental malaria.

APPENDICES

Appendix A. Observational study using the oral anticoagulant Apixaban in BALB/c mice infected with *Plasmodium berghei* ANKA on E13.5.

A) Percent starting weight in infected pregnant (IP) BALB/c sham treated and IP BALB/c Apixaban treated mice beginning on E13.5 through E18.5. Data represent mean ± SEM.
B) Area under the curve (AUC) analysis of starting weight measurements collected on E13.5 through E18.5. Apixaban-treated dams tended to weigh more than sham-treated mice overall (#P = 0.085; unpaired t-test with Welch's correction).
C) Percent peripheral parasitemia in IP BALB/c sham treated and IP BALB/c Apixaban treated mice from E15.5 to E18.5. Data represent mean ± SEM.
D) AUC analysis for percent peripheral parasitemia. No statistically significant differences were found between groups (P = 0.39; unpaired t-test with Welch's correction).
E) Percent hematocrit in IP BALB/c sham treated and IP BALB/c Apixaban treated mice measured on E13.5 and then from E15.5 to E18.5. Data represent mean ± SEM.
F) AUC analysis for percent hematocrit. No statistically significant differences were found between groups (P = 0.49; unpaired t-test with Welch's correction).
G) Percent starting weight in IP BALB/c sham and IP BALB/c Apixaban treated mice on the final day of the experiment, E18.5. No statistically significant differences are detected between groups (#P = 0.084).

Sample sizes: Sham-IP, *n* =4; Apixaban-IP, *n* = 5; *ns* = not significant, P > 0.05.

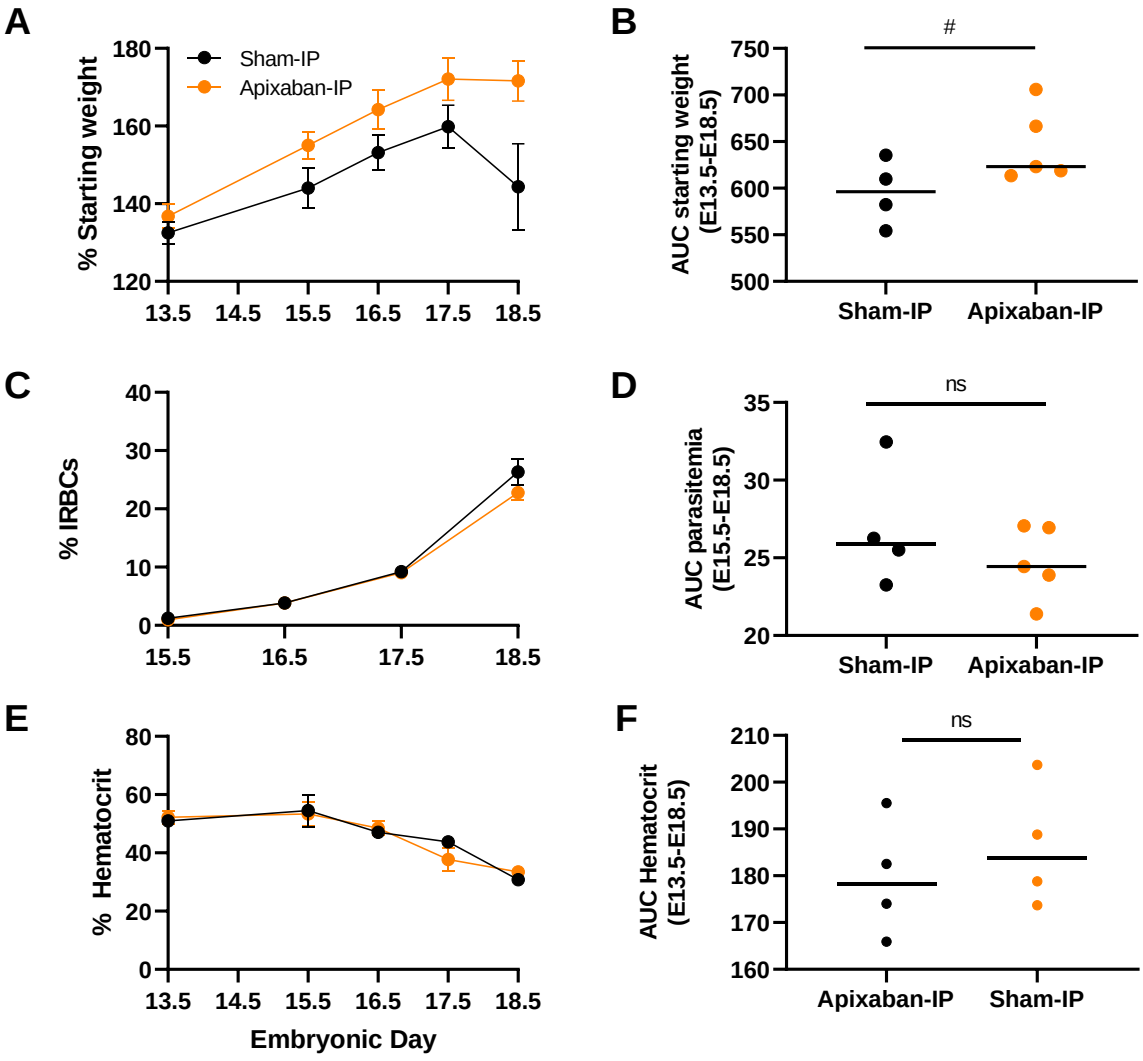
A
% Starting weight
Sham-IP
Apixaban-IP
180
160
140
120
13.5
14.5
15.5
16.5
17.5
18.5
B
AUC starting weight (E13.5-E18.5)
#
750
700
650
600
550
500
Sham-IP
Apixaban-IP
C
% IRBCs
40
30
20
10
0
15.5
16.5
17.5
18.5
D
AUC parasitemia (E15.5-E18.5)
ns
35
30
25
20
Sham-IP
Apixaban-IP
E
% Hematocrit
80
60
40
20
0
13.5
14.5
15.5
16.5
17.5
18.5
Embryonic Day
F
AUC Hematocrit (E13.5-E18.5)
ns
210
200
190
180
170
160
Apixaban-IP
Sham-IP

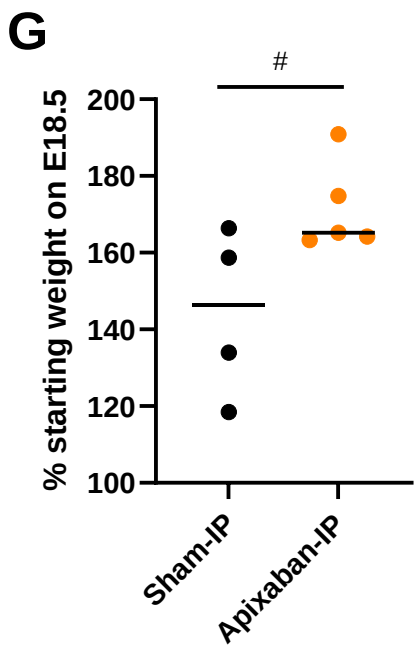
G
#
% starting weight on E18.5
200
180
160
140
120
100
Sham-IP
Apixaban-IP

Appendix B. Relative transcript abundance for antioxidant, iron regulatory, and ferroptosis-related genes in human placenta

A) Transcript for human antioxidant gene transcripts *NFE2l2 (Nrf2)*, *Sod1*, *Sod2*, *Sod3*, and *Cat*, normalized to *Ck19* and *Top1* and quantified by qPCR in rinsed placental tissue. Group means and transcript abundance in individual samples are depicted.

B) Transcript abundance for iron regulatory and ferroptosis-associated human genes *Hmox1*, *TfR1*, *Ferritin*, and *Slc7a11* normalized to *Ck19* and *Top1* and quantified by qPCR in rinsed placental tissue. Group means and transcript abundance in individual samples are depicted.

Sample sizes: PM+, *n* = 17; PM-, *n* = 6.

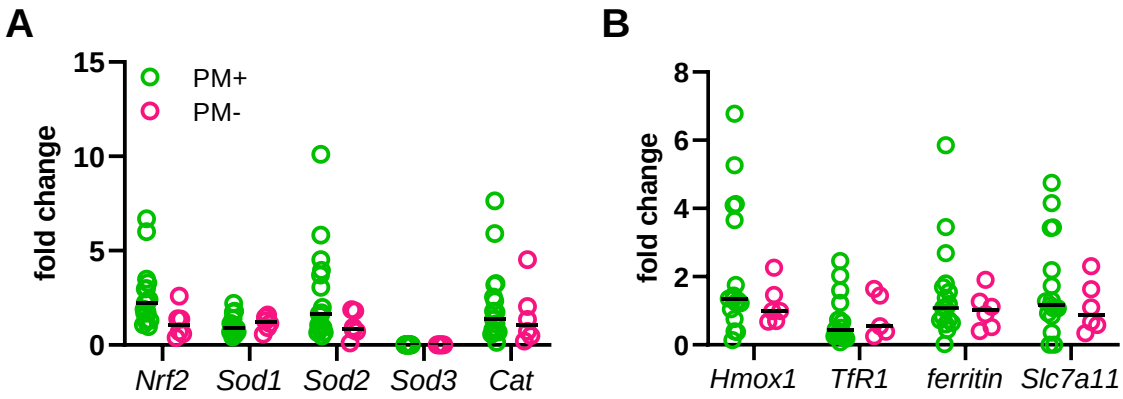

Appendix C. Immunofluorescence staining for transferrin receptor expression in placental sections of malaria-positive women.

Samples were collected from Kenyan women living in a malaria-endemic region; placental sections were stained in malaria-positive and malaria-negative groups using the ferroptosis-specific, anti-transferrin receptor (3F3) antibody (3F3 was identified and reported by Feng et al., 2020, Cell Reports, PMID 32160546).

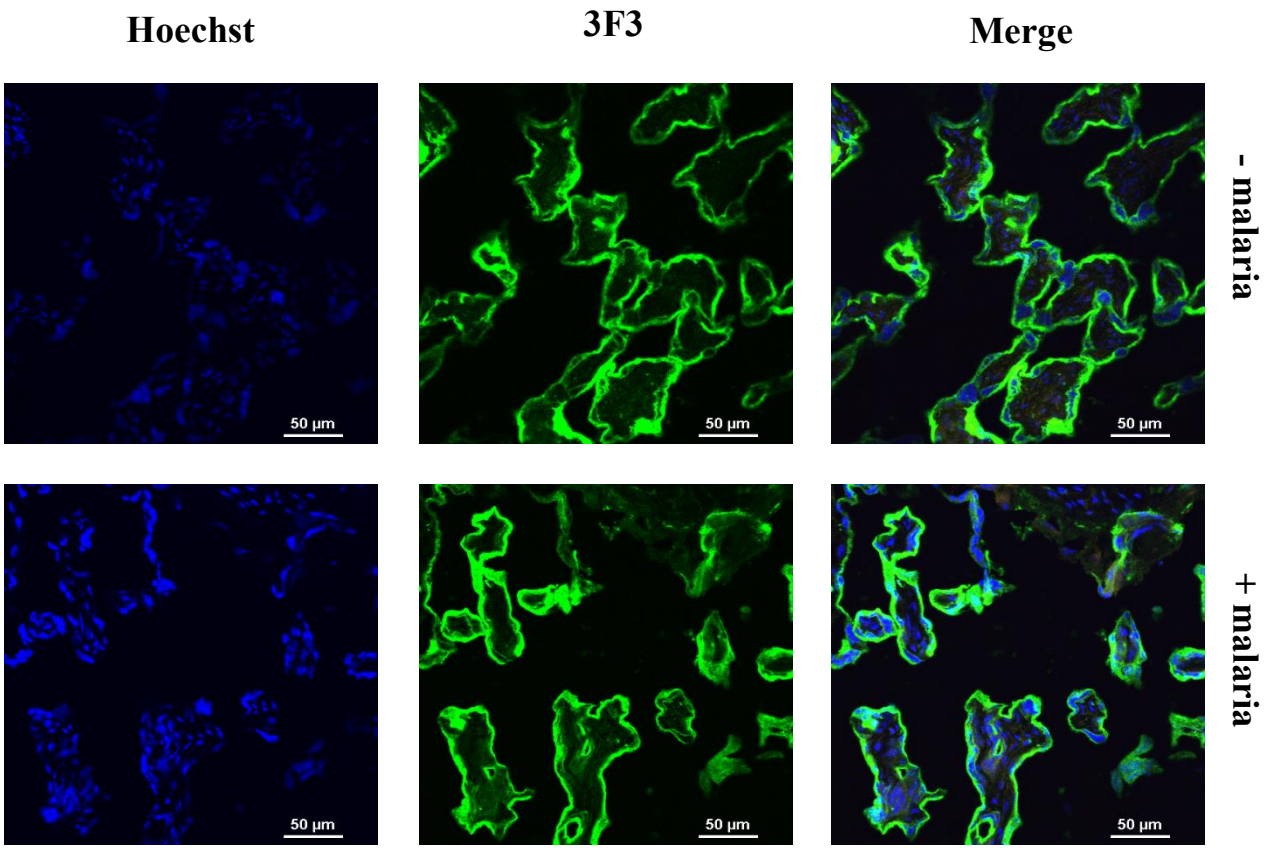

Appendix D. Glutathione peroxidase 4 (GPx4) protein detection in placental extracts by western blot from naturally exposed malaria-positive, HIV-positive, or co-infected women.

(A) GPx4 protein levels across placental samples. Beta-actin protein is shown as the loading control.
(B) Protein levels were quantified using densitometry. Group means are depicted.

Sample sizes: uninfected, *n* = 8; malaria positive, *n* = 3; HIV-positive, *n* = 2; coinfected, *n* = 5

A

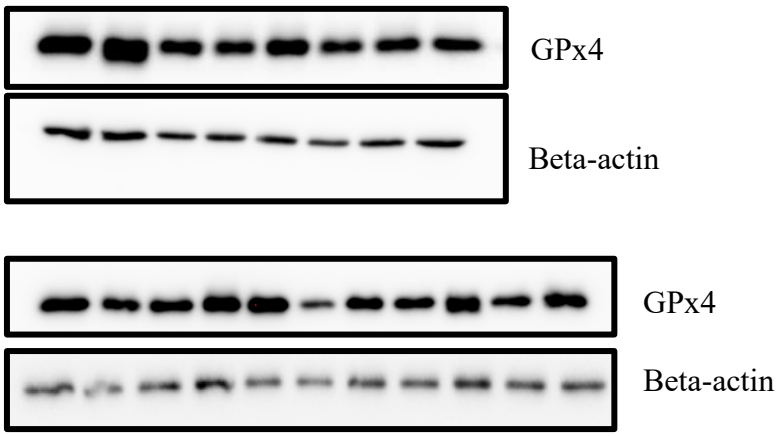

B

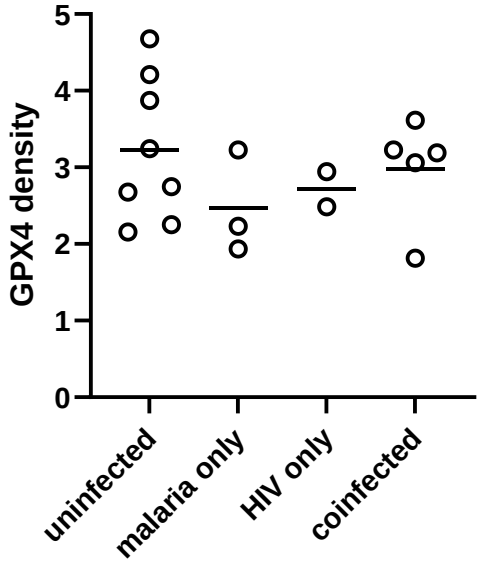

Appendix E. Correlation analyses between inflammation and oxidative stress-associated transcripts and parasitemia in placentae of mice infected on E6.5 and E10.5.

Mouse mRNA transcript abundance relative to peripheral parasitemia at the time of sacrifice or parasitemia area under the curve (AUC) in placenta collected one day before expected preterm birth. (A-B) *Tnf* transcripts tended to be correlated with parasitemia in the E10.5 infection group. (C-D) *Cat* and *Hmox1* transcripts tended to be positively correlated with parasitemia in the E6.5 infection group. (E) *Cox1* transcripts tended to have a positive correlation with parasitemia AUC.

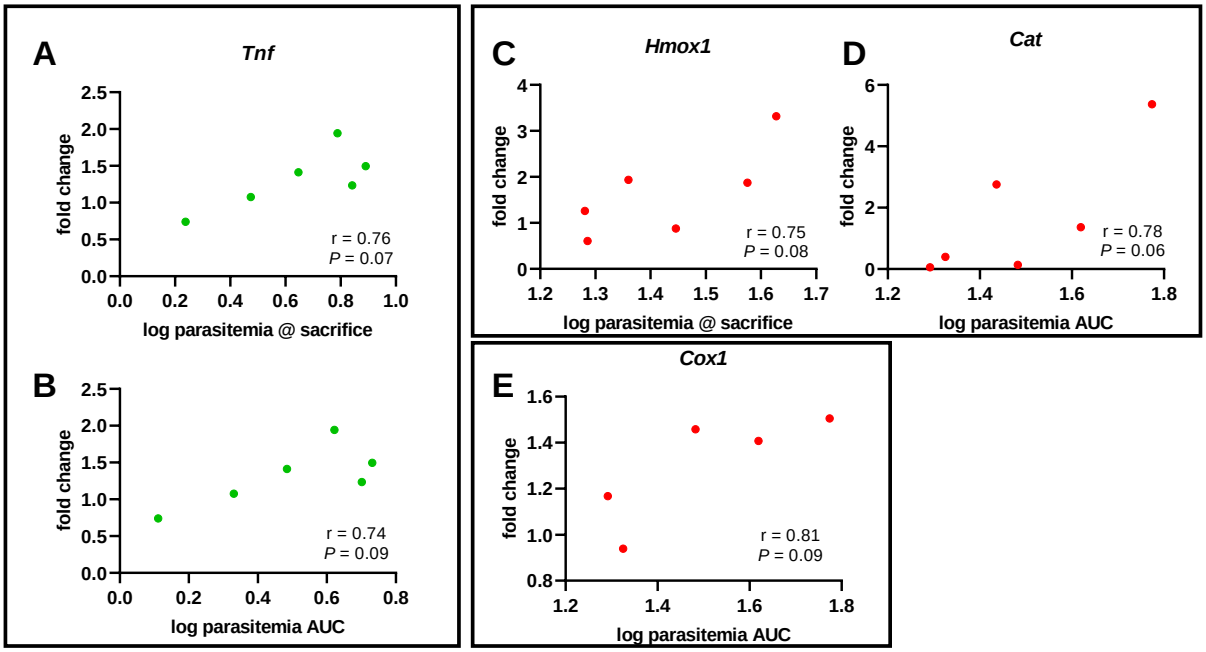

REFERENCES

[1] Clark IA, MacMicking JD, Gray KM, Rockett KA, Cowden WB. Malaria mimicry with tumor necrosis factor: Contrasts between species of murine malaria and Plasmodium falciparum. Am J Pathol 1992;140:325–36.

[2] Fried M, Muga RO, Misore AO, Duffy PE. Malaria elicits type 1 cytokines in the human placenta: IFN-gamma and TNF-alpha associated with pregnancy outcomes. J Immunol 1998;160:2523–30.

[3] Moormann AMM, Sullivan ADD, Rochford RAA, Chensue SWW, Bock PJJ, Nyirenda T, et al. Malaria and pregnancy: placental cytokine expression and its relationship to intrauterine growth retardation. J Infect Dis 1999;180:1987–93. https://doi.org/10.1086/315135.

[4] Rogerson SJ, Brown HC, Pollina E, Abrams ET, Tadesse E, Lema VM, et al. Placental tumor necrosis factor alpha but not gamma interferon is associated with placental malaria and low birth weight in Malawian women. Infect Immun 2003;71:267–70. https://doi.org/10.1128/IAI.71.1.267-270.2003.

[5] Poovassery JS, Sarr D, Smith G, Nagy T, Moore JM. Malaria-induced murine pregnancy failure: distinct roles for IFN-gamma and TNF. J Immunol 2009;183:5342–9. https://doi.org/10.4049/jimmunol.0901669.

[6] Sarr D, Smith GM, Poovassery JS, Nagy T, Moore JM. Plasmodium chabaudi AS induces pregnancy loss in association with systemic pro-inflammatory immune

responses in A/J and C57BL/6 mice. Parasite Immunol 2012;34:224–35. https://doi.org/10.1111/j.1365-3024.2012.01355.x.

[7] Sarr D, Bracken TC, Owino SO, Cooper CA, Smith GM, Nagy T, et al. Differential roles of inflammation and apoptosis in initiation of mid-gestational abortion in malaria-infected C57BL/6 and A/J mice. Placenta 2015;36:738–49. https://doi.org/10.1016/j.placenta.2015.04.007.

[8] Francischetti IMBB, Seydel KB, Monteiro RQ. Blood Coagulation, Inflammation, and Malaria. Microcirculation 2008;15:81–107. https://doi.org/10.1080/10739680701451516.

[9] Francischetti IMB. Does activation of the blood coagulation cascade have a role in malaria pathogenesis? Trends Parasitol 2008;24:258–63. https://doi.org/10.1016/j.pt.2008.03.009.

[10] Avery JW, Smith GM, Owino SO, Sarr D, Nagy T, Mwalimu S, et al. Maternal malaria induces a procoagulant and antifibrinolytic state that is embryotoxic but responsive to anticoagulant therapy. PLoS One 2012;7:1–15. https://doi.org/10.1371/journal.pone.0031090.

[11] O'Sullivan JM, Preston RJS, O'Regan N, O'Donnell JS. Emerging roles for hemostatic dysfunction in malaria pathogenesis. Blood 2016;127:2281–8. https://doi.org/10.1182/blood-2015-11-636464.

[12] Levi M, Keller TT, van Gorp E, ten Cate H. Infection and inflammation and the coagulation system. Cardiovasc Res 2003;60:26–39. https://doi.org/10.1016/S0008-6363(02)00857-X.

[13] Levi M, Van Der Poll T. Inflammation and coagulation Relevance of

Inflammation-Induced Coagulation Abnormalities n.d. https://doi.org/10.1097/CCM.0b013e3181c98d21.

[14] Esmon CT. The interactions between inflammation and coagulation. Br J Haematol 2005;131:417–30. https://doi.org/10.1111/j.1365-2141.2005.05753.x.

[15] Göbel K, Eichler S, Wiendl H, Chavakis T, Kleinschnitz C, Meuth SG. The coagulation factors fibrinogen, thrombin, and factor XII in inflammatory disorders-a systematic review. Front Immunol 2018;9. https://doi.org/10.3389/fimmu.2018.01731.

[16] Megnekou R, Djontu JC, Bigoga JD, Medou FM, Tenou S, Lissom A. Impact of Placental Plasmodium falciparum Malaria on the Profile of Some Oxidative Stress Biomarkers in Women Living in Yaoundé, Cameroon. PLoS One 2015;10:e0134633. https://doi.org/10.1371/journal.pone.0134633.

[17] Sharma L, Kaur J, Shukla G, Hviid L. Role of Oxidative Stress and Apoptosis in the Placental Pathology of Plasmodium berghei Infected Mice. PLoS One 2012;7. https://doi.org/10.1371/journal.pone.0032694.

[18] Sarr D, Cooper CA, Bracken TC, Martinez-Uribe O, Nagy T, Moore JM. Oxidative Stress: A Potential Therapeutic Target in Placental Malaria. ImmunoHorizons 2017;1:29–41. https://doi.org/10.4049/immunohorizons.1700002.

[19] Sharma L, Kaur J, Rishi P, Shukla G. Plasmodium berghei: Influence of infection on the oxidant and antioxidants levels in pregnant BALB/c mice. Exp Parasitol 2012;131:215–22. https://doi.org/10.1016/j.exppara.2012.04.005.

[20] Nigel Mackman. The many faces of tissue factor. J Thromb Haemost 2009;7:136–

9. https://doi.org/10.1111/j.1538-7836.2009.03368.x.The.

[21] Schoenmakers SHHF, Reitsma PH, Spek CA. Blood coagulation factors as inflammatory mediators. Blood Cells, Mol Dis 2005;34:30–7. https://doi.org/10.1016/j.bcmd.2004.09.001.

[22] WHO. Word Malaria Report 2021. 2021.

[23] Singh B, Daneshvar C. Human infections and detection of plasmodium knowlesi. Clin Microbiol Rev 2013. https://doi.org/10.1128/CMR.00079-12.

[24] Singh B, Sung LK, Matusop A, Radhakrishnan A, Shamsul SSG, Cox-singh J, et al. A large focus of naturally acquired Plasmodium knowlesi infections in human beings. Lancet 2003;362:1504. https://doi.org/10.1016/S0140-6736(03)14713-7.

[25] Anstey NM, Russell B, Yeo TW, Price RN. The pathophysiology of vivax malaria. Trends Parasitol 2009;25:220–7. https://doi.org/10.1016/J.PT.2009.02.003.

[26] Bartoloni A, Zammarchi L. Clinical Aspects of f Uncomplicated and Severe Malaria 2012. https://doi.org/10.4084/MJHID.2012.026.

[27] Brabin BJ, Romagosa C, Abdelgalil S, Menéndez C, Verhoeff FH, McGready R, et al. The Sick Placenta—The Role of Malaria. Placenta 2004;25:359–78. https://doi.org/10.1016/J.PLACENTA.2003.10.019.

[28] Bray RS, Garnham PCC. THE LIFE-CYCLE OF PRIMATE MALARIA PARASITES. Br Med Bull 1982;38:117–22.

[29] Tuteja R. Malaria - an overview. FEBS J 2007;274:4670–9. https://doi.org/10.1111/j.1742-4658.2007.05997.x.

[30] Garg S, Agarwal S, Dabral S, Kumar N, Sehrawat S, Singh S. Visualization and quantification of Plasmodium falciparum intraerythrocytic merozoites. Syst Synth

Biol 2015;9:23–6. https://doi.org/10.1007/s11693-015-9167-9.

[31] Gardiner DL, Trenholme KR. Plasmodium falciparum gametocytes: playing hide and seek. Ann Transl Med 2015;3:45. https://doi.org/10.3978/j.issn.2305-5839.2015.01.23.

[32] Blanford JI, Blanford S, Crane RG, Mann ME, Paaijmans KP, Schreiber K V., et al. Implications of temperature variation for malaria parasite development across Africa. Sci Rep 2013;3:1300. https://doi.org/10.1038/srep01300.

[33] Desai M, ter Kuile FO, Nosten F, McGready R, Asamoa K, Brabin B, et al. Epidemiology and burden of malaria in pregnancy. Lancet Infect Dis 2007;7:93–104. https://doi.org/10.1016/S1473-3099(07)70021-X.

[34] Ataíde R, Mayor A, Rogerson SJ. Malaria, primigravidae, and antibodies: knowledge gained and future perspectives. Trends Parasitol 2014;30:85–94. https://doi.org/10.1016/J.PT.2013.12.007.

[35] Walter PR, Garin Y, Blot P. Placental pathologic changes in malaria. A histologic and ultrastructural study. Am J Pathol 1982;109:330–42.

[36] Fried M, Duffy PE. Maternal malaria and parasite adhesion. J Mol Med 1998:162–71.

[37] Ordi J, Ismail MR, Ventura PJ, Kahigwa E, Hirt R, Cardesa A, et al. Massive Chronic Intervillositis of the Placenta Associated With Malaria Infection. Am J Surg Pathol 1998;22:1006–11.

[38] Ismail MR, Ordi J, Menendez C, Ventura PJ, Aponte JJ, Kahigwa E, et al. Placental pathology in malaria: A histological, immunohistochemical, and quantitative study. Hum Pathol 2000;31:85–93. https://doi.org/10.1016/S0046-

8177(00)80203-8.

[39] Olivier M, Van Den Ham K, Shio MT, Kassa FA, Fougeray S. Malarial Pigment Hemozoin and the Innate Inflammatory Response. Front Immunol 2014;5:25. https://doi.org/10.3389/fimmu.2014.00025.

[40] Achur RN, Valiyaveettil M, Alkhalil A, Ockenhouse CF, Gowda DC. Characterization of proteoglycans of human placenta and identification of unique chondroitin sulfate proteoglycans of the intervillous spaces that mediate the adherence of Plasmodium falciparum-infected erythrocytes to the placenta. J Biol Chem 2000;275:40344–56. https://doi.org/10.1074/jbc.M006398200.

[41] Muthusamy A, Achur RN, Bhavanandan VP, Fouda GG, Taylor DW, Gowda DC. Plasmodium falciparum-Infected Erythrocytes Adhere Both in the Intervillous Space and on the Villous Surface of Human Placenta by Binding to the Low-Sulfated Chondroitin Sulfate Proteoglycan Receptor. Am J Pathol 2004;164:2013–25. https://doi.org/10.1016/S0002-9440(10)63761-3.

[42] Fried M, Duffy PE. Adherence of Plasmodium falciparum to chondroitin sulfate A in the human placenta. Science 1996;272:1502–4. https://doi.org/10.1126/SCIENCE.272.5267.1502.

[43] Hviid L, Jensen AT. PfEMP1 - A Parasite Protein Family of Key Importance in Plasmodium falciparum Malaria Immunity and Pathogenesis. Adv Parasitol 2015;88:51–84. https://doi.org/10.1016/bs.apar.2015.02.004.

[44] Schantz-Dunn J, Nour NM. Malaria and Pregnancy: A Global Health Perspective. Rev Obstet Gynecol [Rev Obs Gynecol 2009;1862. https://doi.org/10.3909/riog0091.

[45] Feng G, Aitken E, Yosaatmadja F, Kalilani L, Meshnick SR, Jaworowski A, et al. Antibodies to Variant Surface Antigens of *Plasmodium falciparum* –Infected Erythrocytes Are Associated with Protection from Treatment Failure and the Development of Anemia in Pregnancy. J Infect Dis 2009;200:299–306. https://doi.org/10.1086/599841.

[46] Staalsoe T, Megnekou R, Fievét N, Ricke CH, Zornig HD, Leke R, et al. Acquisition and Decay of Antibodies to Pregnancy-Associated Variant Antigens on the Surface of *Plasmodium falciparum*– Infected Erythrocytes That Protect against Placental Parasitemia. J Infect Dis 2001;184:618–26. https://doi.org/10.1086/322809.

[47] Fried M, Nosten F, Brockman A, Brabin BJ, Duffy PE. Maternal antibodies block malaria. Nature 1998;395:851–2. https://doi.org/10.1038/27570.

[48] Duffy PE, Fried M. Antibodies that inhibit Plasmodium falciparum adhesion to chondroitin sulfate A are associated with increased birth weight and the gestational age of newborns. Infect Immun 2003;71:6620–3. https://doi.org/10.1128/IAI.71.11.6620-6623.2003.

[49] Gomes PS, Bhardwaj J, Rivera-Correa J, Freire-De-Lima CG, Morrot A. Immune escape strategies of malaria parasites. Front Microbiol 2016;7. https://doi.org/10.3389/fmicb.2016.01617.

[50] Hsieh F-L, Turner L, Bolla JR, Robinson C V., Lavstsen T, Higgins MK. The structural basis for CD36 binding by the malaria parasite. Nat Commun 2016;7:12837. https://doi.org/10.1038/ncomms12837.

[51] Beeson JG, Rogerson SJ, Cooke BM, Reeder JC, Chai W, Lawson AM, et al.

Adhesion of Plasmodium falciparum-infected erythrocytes to hyaluronicacid in placental malaria. Nat Med 2000;6:86–90. https://doi.org/10.1038/71582.

[52] Beeson JG, Brown G V. Plasmodium falciparum–Infected Erythrocytes Demonstrate Dual Specificity for Adhesion to Hyaluronic Acid and Chondroitin Sulfate A and Have Distinct Adhesive Properties. J INf 2004;189:169–79.

[53] WHO | Malaria in pregnant women. WHO 2018.

[54] Chen I, Clarke SE, Gosling R, Hamainza B, Killeen G, Magill A, et al. "Asymptomatic" Malaria: A Chronic and Debilitating Infection That Should Be Treated. PLOS Med 2016;13:e1001942. https://doi.org/10.1371/journal.pmed.1001942.

[55] Boudová S, Cohee LM, Kalilani-Phiri L, Thesing PC, Kamiza S, Muehlenbachs A, et al. Pregnant women are a reservoir of malaria transmission in Blantyre, Malawi. Malar J 2014;13:506. https://doi.org/10.1186/1475-2875-13-506.

[56] Gonçalves BP, Walker PG, Cairns M, Tiono AB, Bousema T, Drakeley C. Pregnant Women: An Overlooked Asset to Plasmodium falciparum Malaria Elimination Campaigns? Trends Parasitol 2017;33:510–8. https://doi.org/10.1016/j.pt.2017.03.001.

[57] Lindsay S, Ansell J, Selman C, Cox V, Hamilton K, Walraven G. Effect of pregnancy on exposure to malaria mosquitoes. Lancet 2000;355:1972. https://doi.org/10.1016/S0140-6736(00)02334-5.

[58] Ansell J, Hamilton KA, Pinder M, Walraven GEL, Lindsay SW. Short-range attractiveness of pregnant women to Anopheles gambiae mosquitoes. Trans R Soc Trop Med Hyg n.d.;96:113–6.

[59] Wilson NO, Ceesay FK, Obed SA, Adjei AA, Gyasi RK, Rodney P, et al. Intermittent preventive treatment with sulfadoxine-pyrimethamine against malaria and anemia in pregnant women. Am J Trop Med Hyg 2011. https://doi.org/10.4269/ajtmh.2011.10-0512.

[60] Thomsen EK, Koimbu G, Pulford J, Jamea-Maiasa S, Ura Y, Keven JB, et al. Mosquito Behavior Change After Distribution of Bednets Results in Decreased Protection Against Malaria Exposure. J Infect Dis n.d. https://doi.org/10.1093/infdis/jiw615.

[61] Mathanga DP, Mwandama DA, Bauleni A, Chisaka J, Shah MP, Landman KZ, et al. The effectiveness of long-lasting, insecticide-treated nets in a setting of pyrethroid resistance: a case–control study among febrile children 6 to 59 months of age in Machinga District, Malawi. Malar J 2015;14:457. https://doi.org/10.1186/s12936-015-0961-3.

[62] Ranson H, N'Guessan R, Lines J, Moiroux N, Nkuni Z, Corbel V. Pyrethroid resistance in African anopheline mosquitoes: What are the implications for malaria control? Trends Parasitol 2011;27:91–8. https://doi.org/10.1016/j.pt.2010.08.004.

[63] Okumu F. The fabric of life: What if mosquito nets were durable and widely available but insecticide-free? Malar J 2020;19:1–29. https://doi.org/10.1186/s12936-020-03321-6.

[64] Lindsay SW, Thomas MB, Kleinschmidt I. Threats to the effectiveness of insecticide-treated bednets for malaria control: thinking beyond insecticide resistance. Lancet Glob Heal 2021;9:e1325–31. https://doi.org/10.1016/S2214-109X(21)00216-3.

[65] Tokponnon FT, Sissinto Y, Ogouyémi AH, Adéothy AA, Adechoubou A, Houansou T, et al. Implications of insecticide resistance for malaria vector control with long-lasting insecticidal nets: Evidence from health facility data from Benin. Malar J 2019;18:1–9. https://doi.org/10.1186/s12936-019-2656-7.

[66] Conrad MD, Rosenthal PJ. Antimalarial drug resistance in Africa: the calm before the storm? Lancet Infect Dis 2019;19:e338–51. https://doi.org/10.1016/S1473-3099(19)30261-0.

[67] Mwendera CA, De Jager C, Longwe H, Phiri K, Hongoro C, Mutero CM. Changing the policy for intermittent preventive treatment with sulfadoxine-pyrimethamine during pregnancy in Malawi. Malar J 2017;16:1–13. https://doi.org/10.1186/s12936-017-1736-9.

[68] Desai M, Gutman J, Taylor SM, Wiegand RE, Khairallah C, Kayentao K, et al. Impact of Sulfadoxine-Pyrimethamine Resistance on Effectiveness of Intermittent Preventive Therapy for Malaria in Pregnancy at Clearing Infections and Preventing Low Birth Weight. Clin Infect Dis 2016;62:323–33. https://doi.org/10.1093/cid/civ881.

[69] van Eijk AM, Larsen DA, Kayentao K, Koshy G, Slaughter DEC, Roper C, et al. Effect of Plasmodium falciparum sulfadoxine-pyrimethamine resistance on the effectiveness of intermittent preventive therapy for malaria in pregnancy in Africa: a systematic review and meta-analysis. Lancet Infect Dis 2019. https://doi.org/10.1016/S1473-3099(18)30732-1.

[70] Chauvin P, Menard S, Iriart X, Nsango SE, Tchioffo MT, Abate L, et al. Prevalence of *Plasmodium falciparum* parasites resistant to

sulfadoxine/pyrimethamine in pregnant women in Yaoundé, Cameroon: emergence of highly resistant *pfdhfr* / *pfdhps* alleles. J Antimicrob Chemother 2015;70:2566–71. https://doi.org/10.1093/jac/dkv160.

[71] Edi CVA, Koudou BG, Jones CM, Weetman D, Ranson H. Multiple-insecticide resistance in Anopheles gambiae mosquitoes, Southern Côte d'Ivoire. Emerg Infect Dis 2012;18:1508–11. https://doi.org/10.3201/eid1809.120262.

[72] Hemingway J. Resistance: A problem without an easy solution. Pestic Biochem Physiol 2018;151:73–5. https://doi.org/10.1016/j.pestbp.2018.08.007.

[73] Dao A, Yaro AS, Diallo M, Timbine S, Huestis DL, Kassogue Y, et al. Signatures of aestivation and migration in Sahelian malaria mosquito populations. Nature 2014;516:387–90. https://doi.org/10.1038/nature13987.

[74] Huestis DL, Dao A, Diallo M, Sanogo ZL, Samake D, Yaro AS, et al. Windborne long-distance migration of malaria mosquitoes in the Sahel. Nature 2019;574:404–8. https://doi.org/10.1038/s41586-019-1622-4.

[75] Mordmüller B, Sulyok M, Egger-Adam D, Resende M, De Jongh WA, Jensen MH, et al. First-in-human, Randomized, Double-blind Clinical Trial of Differentially Adjuvanted PAMVAC, A Vaccine Candidate to Prevent Pregnancy-associated Malaria. Clin Infect Dis 2019;69:1509–16. https://doi.org/10.1093/cid/ciy1140.

[76] Sirima SB, Richert L, Chêne A, Konate AT, Campion C, Dechavanne S, et al. PRIMVAC vaccine adjuvanted with Alhydrogel or GLA-SE to prevent placental malaria: a first-in-human, randomised, double-blind, placebo-controlled study. Lancet Infect Dis 2020;20:585–97. https://doi.org/10.1016/S1473-3099(19)30739-

X.

[77] Gamain B, Chêne A, Viebig NK, Tuikue Ndam N, Nielsen MA. Progress and Insights Toward an Effective Placental Malaria Vaccine. Front Immunol 2021;12:1–8. https://doi.org/10.3389/fimmu.2021.634508.

[78] Chen Q, Fernandez V, Sundström A, Schlichtherle M, Datta S, Hagblom P, et al. Developmental selection of var gene expression in Plasmodium falciparum. Nature 1998;394:392–5. https://doi.org/10.1038/28660.

[79] Guizetti J, Scherf A. Silence, activate, poise and switch! Mechanisms of antigenic variation in Plasmodium falciparum. Cell Microbiol 2013;15:718–26. https://doi.org/10.1111/cmi.12115.

[80] Fastman Y, Noble R, Recker M, Dzikowski R. Erasing the epigenetic memory and beginning to switch-the onset of antigenic switching of var genes in plasmodium falciparum. PLoS One 2012;7. https://doi.org/10.1371/journal.pone.0034168.

[81] Duffy MF, Selvarajah SA, Josling GA, Petter M. Epigenetic regulation of the plasmodium falciparum genome. Brief Funct Genomics 2014;13:203–16. https://doi.org/10.1093/bfgp/elt047.

[82] Scherf A, Lopez-Rubio JJ, Riviere L. Antigenic Variation in Plasmodium falciparum. Annu Rev Microbiol 2008;62:445–70. https://doi.org/10.1146/annurev.micro.61.080706.093134.

[83] Frank M, Dzikowski R, Amulic B, Deitsch K. Variable switching rates of malaria virulence genes are associated with chromosomal position and gene subclass. Mol Microbiol 2007;64:1486–98. https://doi.org/10.1111/j.1365-2958.2007.05736.x.Variable.

[84] Nunes MC, Sterkers Y, Gamain B, Scherf A. Investigation of host factors possibly enhancing the emergence of the chondroitin sulfate A-binding phenotype in Plasmodium falciparum. Microbes Infect 2008;10:928–32. https://doi.org/10.1016/J.MICINF.2008.05.006.

[85] Georgiades P, Ferguson-Smith ACC, Burton GJJ. Comparative Developmental Anatomy of the Murine and Human Definitive Placentae. Placenta 2002;23:3–19. https://doi.org/10.1053/PLAC.2001.0738.

[86] Hviid L, Marinho CRF, Staalsoe T, Penha-Gonçalves C. Of mice and women: Rodent models of placental malaria. Trends Parasitol 2010;26:412–9. https://doi.org/10.1016/j.pt.2010.04.010.

[87] Barateiro A, Pereira MLM, Epiphanio S, Marinho CRF. Contribution of Murine Models to the Study of Malaria During Pregnancy. Front Microbiol 2019;10. https://doi.org/10.3389/fmicb.2019.01369.

[88] Neres R, Marinho CRF, Gonçalves LA, Catarino MB, Penha-Gonçalves C. Pregnancy Outcome and Placenta Pathology in Plasmodium berghei ANKA Infected Mice Reproduce the Pathogenesis of Severe Malaria in Pregnant Women. PLoS One 2008;3:e1608. https://doi.org/10.1371/journal.pone.0001608.

[89] Rodrigues-Duarte L, Vieira De Moraes L, Barboza R, Marinho CR, Franke-Fayard B, Janse CJ, et al. Distinct placental malaria pathology caused by different Plasmodium berghei lines that fail to induce cerebral malaria in the C57BL/6 mouse n.d. https://doi.org/10.1186/1475-2875-11-231.

[90] Timms R, Colegrave N, K Chan BH, Read AF. The effect of parasite dose on disease severity in the rodent malaria Plasmodium chabaudi 2018.

https://doi.org/10.1017/S0031182001008083.

[91] Van Zon AAJC, Eling WMC. Depressed Malarial Immunity in Pregnant Mice. Infect Immun 1980;28:630–2.

[92] de Moraes L V, Dechavanne S, Sousa PM, Barateiro A, Cunha SF, Nunes-Silva S, et al. Murine Model for Preclinical Studies of Var2CSA-Mediated Pathology Associated with Malaria in Pregnancy. Infect Immun 2016;84:1761–74. https://doi.org/10.1128/IAI.01207-15.

[93] Marinho CRF, Neres R, Epiphanio S, Gonçalves LA, Catarino MB, Penha-Gonçalves C. Recrudescent Plasmodium berghei from Pregnant Mice Displays Enhanced Binding to the Placenta and Induces Protection in Multigravida. PLoS One 2009;4:e5630. https://doi.org/10.1371/journal.pone.0005630.

[94] Megnekou R, Hviid L, Staalsoe T. Variant-specific immunity to Plasmodium berghei in pregnant mice. Infect Immun 2009;77:1827–34. https://doi.org/10.1128/IAI.01321-08.

[95] Stephens R, Culleton RL, Lamb TJ. The contribution of Plasmodium chabaudi to our understanding of malaria The rodent malarias: from the gallery forest to the lab 2015;28:73–82. https://doi.org/10.1016/j.pt.2011.10.006.

[96] Antia R, Yates A, De Roode JC. The dynamics of acute malaria infections. I. Effect of the parasite's red blood cell preference n.d. https://doi.org/10.1098/rspb.2008.0198.

[97] Cromer D, Evans KJ, Schofield L, Davenport MP. Preferential invasion of reticulocytes during late-stage Plasmodium berghei infection accounts for reduced circulating reticulocyte levels. Int J Parasitol 2006;36:1389–97.

https://doi.org/10.1016/J.IJPARA.2006.07.009.

[98] Mons B. Preferential invasion of malarial merozoites into young red blood cells. Blood Cells 1990;16:299–312.

[99] Stevenson MM, Lyanga JJ, Skamene E. Murine malaria: genetic control of resistance to Plasmodium chabaudi. Infect Immun 1982;38:80–8.

[100] Sharma A, Conteh S, Langhorne J, Duffy PE. Heterologous infection of pregnant mice induces low birth weight and modifies offspring susceptibility to malaria. PLoS One 2016;11:1–17. https://doi.org/10.1371/journal.pone.0160120.

[101] Poovassery J, Moore JM. Murine malaria infection induces fetal loss associated with accumulation of Plasmodium chabaudi AS-infected erythrocytes in the placenta. Infect Immun 2006;74:2839–48. https://doi.org/10.1128/IAI.74.5.2839-2848.2006.

[102] Poovassery J, Moore JM. Association of malaria-induced murine pregnancy failure with robust peripheral and placental cytokine responses. Infect Immun 2009;77:4998–5006. https://doi.org/10.1128/IAI.00617-09.

[103] Chua CLL, Brown G, Hamilton JA, Rogerson S, Boeuf P. Monocytes and macrophages in malaria: Protection or pathology? Trends Parasitol 2013;29:26–34. https://doi.org/10.1016/j.pt.2012.10.002.

[104] Rogerson SJ, Pollina E, Getachew A, Tadesse E, Lema VM, Molyneux ME. Placental monocyte infiltrates in response to Plasmodium falciparum malaria infection and their association with adverse pregnancy outcomes. Am J Trop Med Hyg 2003;68:115–9.

[105] Wegmann TG, Lin H, Guilbert L, Mosmann TR. Bidirectional cytokine

interactions in the maternal-fetal relationship: is successful pregnancy a Th2 phenomenon? Immunol Today 1993;14:353–6.

[106] Makhseed M, Raghupathy R, Azizieh F, Farhat R, Hassan N, Bandar A. Circulating cytokines and CD30 in normal human pregnancy and recurrent spontaneous abortions. Hum Reprod 2000;15:2011–7. https://doi.org/10.1093/humrep/15.9.2011.

[107] Redman CW., Sargent I. Pre-eclampsia, the Placenta and the Maternal System Inflammatory Response-A Review. Placenta 2003;17:S21–7.

[108] Suguitan, Jr. AL, Leke RGF, Fouda G, Zhou A, Thuita L, Metenou S, et al. Changes in the Levels of Chemokines and Cytokines in the Placentas of Women with *Plasmodium falciparum* Malaria. J Infect Dis 2003;188:1074–7082. https://doi.org/10.1086/378500.

[109] Suguitan Jr AL, Cadigan TJ, Nguyen TA, Zhou A, I Leke RJ, Metenou S, et al. Malaria-associated cytokine changes in the placenta of women with pre-term deliveries in Yaounde, Cameroon. Am J Trop Med Hyg 2003:574–81.

[110] Chua CLL, Brown G V., Hamilton JA, Molyneux ME, Rogerson SJ, Boeuf P. Soluble CD163, a Product of Monocyte/Macrophage Activation, Is Inversely Associated with Haemoglobin Levels in Placental Malaria. PLoS One 2013;8:e64127. https://doi.org/10.1371/journal.pone.0064127.

[111] Davison BBB, Kaack MBB, Rogers LBB, Rasmussen KKK, Rasmussen TAA, Henson EWW, et al. The role of soluble tumor necrosis factor receptor types I and II and tumor necrosis factor-alpha in malaria during pregnancy. J Infect Dis 2006;194:123–32. https://doi.org/10.1086/504694.

[112] Thevenon AD, Zhou JA, Megnekou R, Ako S, Leke RGF, Taylor DW. Elevated Levels of Soluble TNF Receptors 1 and 2 Correlate with Plasmodium falciparum Parasitemia in Pregnant Women: Potential Markers for Malaria-Associated Inflammation. J Immunol 2010;185:7115–22. https://doi.org/10.4049/jimmunol.1002293.

[113] Rogerson Malcolm E Molyneux SJ, Rochford R, Gareth D H Turner SR, Tadesse E, Lema VM, Abrams ET, et al. Expression Chemokine β Associated with Elevated Placental Monocyte Recruitment Is Host Response to Malaria During Pregnancy: Host Response to Malaria During Pregnancy: Placental Monocyte Recruitment Is Associated with Elevated ␣ Chemokine Expression. J Immunol Ref 2003;170:2759–64. https://doi.org/10.4049/jimmunol.170.5.2759.

[114] Kabyemela ER, Muehlenbachs A, Fried M, Kurtis JD, Mutabingwa TK, Duffy PE. Maternal peripheral blood level of IL-10 as a marker for inflammatory placental malaria. Malar J 2008;7:6–11. https://doi.org/10.1186/1475-2875-7-26.

[115] Nasr A, Allam G, Hamid O, Al-Ghamdi A. IFN-gamma and TNF associated with severe falciparum malaria infection in Saudi pregnant women. Malar J 2014;13:1–9. https://doi.org/10.1186/1475-2875-13-314.

[116] Chêne A, Briand V, Ibitokou S, Dechavanne S, Massougbodji A, Deloron P, et al. Placental Cytokine and Chemokine Profiles Reflect Pregnancy Outcomes in Women Exposed to Plasmodium falciparum Infection. Infect Immun 2014;82. https://doi.org/10.1128/IAI.01922-14.

[117] Moore JM, Chaisavaneeyakorn S, Perkins DJ, Othoro C, Otieno J, Nahlen BL, et al. Hemozoin Differentially Regulates Proinflammatory Cytokine Production in

Human Immunodeficiency Virus-Seropositive and -Seronegative Women with Placental Malaria. Infect Immun 2004;72:7022–9. https://doi.org/10.1128/IAI.72.12.7022–7029.2004.

[118] Lyke KE, Burges R, Cissoko Y, Sangare L, Dao M, Diarra I, et al. Serum levels of the proinflammatory cytokines interleukin-1 beta (IL-1beta), IL-6, IL-8, IL-10, tumor necrosis factor alpha, and IL-12(p70) in Malian children with severe Plasmodium falciparum malaria and matched uncomplicated malaria or healthy controls. Infect Immun 2004;72:5630–7. https://doi.org/10.1128/IAI.72.10.5630-5637.2004.

[119] Kumar R, Ng S, Engwerda C. The role of IL-10 in malaria: A double edged sword. Front Immunol 2019;10:1–10. https://doi.org/10.3389/fimmu.2019.00229.

[120] Othoro C, Lal AA, Nahlen B, Koech D, Orago ASS, Udhayakumar V. A Low Interleukin-10 Tumor Necrosis Factor-α Ratio Is Associated with Malaria Anemia in Children Residing in a Holoendemic Malaria Region in Western Kenya. J Infect Dis 1999;179:279–82. https://doi.org/10.1086/314548.

[121] Mahanta A, Kar SK, Kakati S, Baruah S. Heightened inflammation in severe malaria is associated with decreased IL-10 expression levels and neutrophils n.d. https://doi.org/10.1177/1753425914561277.

[122] Angulo I, Fresno M. Cytokines in the pathogenesis of and protection against malaria. Clin Diagn Lab Immunol 2002;9:1145–52. https://doi.org/10.1128/CDLI.9.6.1145-1152.2002.

[123] Li C, Sanni LA, Omer F, Riley E, Langhorne J. Pathology of Plasmodium chabaudi chabaudi infection and mortality in interleukin-10-deficient mice are

ameliorated by anti-tumor necrosis factor alpha and exacerbated by anti-transforming growth factor beta antibodies. Infect Immun 2003;71:4850–6. https://doi.org/10.1128/IAI.71.9.4850-4856.2003.

[124] Clark IA. Suggested importance of monokines in pathophysiology of endotoxin shock and malaria. Klin Wochenschr 1982;60:756–8. https://doi.org/10.1007/BF01716573.

[125] Clark IA, Alleva LM, Mills AC, Cowden WB. Pathogenesis of malaria and clinically similar conditions. Clin Microbiol Rev 2004;17:509–39, table of contents. https://doi.org/10.1128/CMR.17.3.509-539.2004.

[126] Clark IA, Budd AC, Alleva LM, Cowden WB. Human malarial disease: a consequence of inflammatory cytokine release. Malar J 2006;5:1–32. https://doi.org/10.1186/1475-2875-5-85.

[127] Michie HR, Manogue KR, Spriggs DR, Revhaug A, O'Dwyer S, Dinarello CA, et al. Detection of Circulating Tumor Necrosis Factor after Endotoxin Administration. N Engl J Med 1988;318:1481–6. https://doi.org/10.1056/NEJM198806093182301.

[128] Cannon JG, Tompkins RG, Gelfand JA, Michie HR, Stanford GG, van der Meer JW, et al. Circulating interleukin-1 and tumor necrosis factor in septic shock and experimental endotoxin fever. J Infect Dis 1990;161:79–84.

[129] Tracey KJ, Fong Y, Hesse DG, Manogue KR, Lee AT, Kuo GC, et al. Anti-cachectin/TNF monoclonal antibodies prevent septic shock during lethal bacteraemia. Nature 1987;330:662–4. https://doi.org/10.1038/330662a0.

[130] Hinshaw LB, Tekamp-Olson P, Chang AC, Lee PA, Taylor FB, Murray CK, et al.

Survival of primates in LD100 septic shock following therapy with antibody to tumor necrosis factor (TNF alpha). Circ Shock 1990;30:279–92.

[131] Fisher CJ, Agosti JM, Opal SM, Lowry SF, Balk RA, Sadoff JC, et al. Treatment of Septic Shock with the Tumor Necrosis Factor Receptor:Fc Fusion Protein. N Engl J Med 1996;334:1697–702. https://doi.org/10.1056/nejm199606273342603.

[132] Kwiatkowski D, Molyneux ME, Curtis N, Klein N, Pointaire P, Smit M, et al. Anti-TNF therapy inhibits fever in cerebral malaria. Q J Med 1993:91–8.

[133] King T, Lamb T. Interferon-γ: The Jekyll and Hyde of Malaria. PLOS Pathog 2015;11:e1005118. https://doi.org/10.1371/journal.ppat.1005118.

[134] Harmon AC, Cornelius DC, Amaral LM, Faulkner JL, Cunningham MW, Wallace K, et al. The role of inflammation in the pathology of preeclampsia. Clin Sci (Lond) 2016;130:409–19. https://doi.org/10.1042/CS20150702.

[135] Brabin BJ, Johnson PM. Placental malaria and pre-eclampsia through the looking glass backwards? J Reprod Immunol 2005;65:1–15.

[136] Conrad KP, Miles TM, Benyo DF. Circulating Levels of Immunoreactive Cytokines in Women with Preeclampsia. Am J Reprod Immunol 1998;40:102–11. https://doi.org/10.1111/j.1600-0897.1998.tb00398.x.

[137] Conrad KP, Benyo DF. Placental Cytokines and the Pathogenesis of Preeclampsia. Am J Reprod Immunol 1997;37:240–9. https://doi.org/10.1111/j.1600-0897.1997.tb00222.x.

[138] Souza MC, Padua TA, Henriques MG. Endothelial-Leukocyte Interaction in Severe Malaria: Beyond the Brain. Mediators Inflamm 2015;2015:1–10. https://doi.org/10.1155/2015/168937.

[139] Georg F, Holst E, Hemmer CJ, Foth C, Seitz R, Egbring R, et al. Low levels of fibrin-stabilizing factor (factor XIII) in human Plasmodium falciparum malaria: correlation with clinical severity. Am J Trop Med Hyg 1999;60:99–104.

[140] Horstmann RD, Dietrich M. Haemostatic alterations in malaria correlate to parasitaemia. Blut 1985;51:329–35. https://doi.org/10.1007/BF00320043.

[141] Ghosh K, Shetty S. Blood coagulation in falciparum malaria—a review. Parasitol Res 2008;102:571–6. https://doi.org/10.1007/s00436-007-0832-0.

[142] Steven M Opal CTE, Opal SM, Esmon CT. Bench-to-bedside review: Functional relationships between coagulation and the innate immune response and their respective roles in the pathogenesis of sepsis. Crit Care 2003;7:23–38. https://doi.org/10.1186/CC1854.

[143] Punyagupta S, Srichaikul T, Nitiyanant P, Petchclai B. Acute pulmonary insufficiency in Falciparum malaria: summary of 12 cases with evidence of disseminated intravascular coagulation. Am J Trop Med Hyg 1974;23.

[144] Jaroonvesama N. Intravascular coagulation in Falciparum malaria. Lancet 1972;299:221–3. https://doi.org/10.1016/S0140-6736(72)90621-6.

[145] Mostafa AG, Bilal NE, Abass A-E, Elhassan EM, Mohmmed AA, Adam I. Coagulation and Fibrinolysis Indicators and Placental Malaria Infection in an Area Characterized by Unstable Malaria Transmission in Central Sudan. Malar Res Treat 2015;2015:369237. https://doi.org/10.1155/2015/369237.

[146] Grover SP, Mackman N. Tissue Factor: An Essential Mediator of Hemostasis and Trigger of Thrombosis. Arterioscler Thromb Vasc Biol 2018. https://doi.org/10.1161/ATVBAHA.117.309846.

[147] Francischetti IMBB, Seydel KB, Monteiro RQ, Whitten RO, Erexson CR, Noronha ALLL, et al. Plasmodium falciparum-infected erythrocytes induce tissue factor expression in endothelial cells and support the assembly of multimolecular coagulation complexes. J Thromb Haemost 2007;5:155–65. https://doi.org/10.1111/j.1538-7836.2006.02232.x.

[148] Palta S, Saroa R, Palta A. Overview of the coagulation system. Indian J Anaesth 2014;58:515–23. https://doi.org/10.4103/0019-5049.144643.

[149] Bouwens EAM, Stavenuiter F, Mosnier LO. Mechanisms of anticoagulant and cytoprotective actions of the protein C pathway. J Thromb Haemost 2013;11:242–53. https://doi.org/10.1111/jth.12247.

[150] Dahlbäck B, Villoutreix BO. The anticoagulant protein C pathway. FEBS Lett 2005;579:3310–6. https://doi.org/10.1016/J.FEBSLET.2005.03.001.

[151] Isermann B, Sood R, Pawlinski R, Zogg M, Kalloway S, Degen JL, et al. The thrombomodulin–protein C system is essential for the maintenance of pregnancy. Nat Med 2003;9:331–7. https://doi.org/10.1038/nm825.

[152] Turner L, Lavstsen T, Berger SS, Wang CW, Petersen JE V., Avril M, et al. Severe malaria is associated with parasite binding to endothelial protein C receptor. Nature 2013;498:502–5. https://doi.org/10.1038/nature12216.

[153] Bernabeu M, Smith JD. EPCR and Malaria Severity: The Center of a Perfect Storm. Trends Parasitol 2017;33:295–308. https://doi.org/10.1016/j.pt.2016.11.004.

[154] Oduah EI, Linhardt RJ, Sharfstein ST, Pinto MMM, Emília De Sousa M. Heparin: Past, Present, and Future. Pharmaceuticals 2016;9.

https://doi.org/10.3390/ph9030038.

[155] Many A, Koren G. Low-molecular-weight heparins during pregnancy. Can Fam Physician 2005;51:199–201.

[156] Laskin CA, Spitzer KA, Clark CA, Crowther MR, Ginsberg JS, Hawker GA, et al. Low molecular weight heparin and aspirin for recurrent pregnancy loss: results from the randomized, controlled HepASA Trial. J Rheumatol 2009;36:279–87. https://doi.org/10.3899/jrheum.080763).

[157] Wood JP, Ellery PER, Maroney SA, Mast AE. Biology of tissue factor pathway inhibitor. Blood 2014;123:2934–43. https://doi.org/10.1182/blood-2013-11-512764.

[158] Lacerda MVGVG, Santos JBJB, Mourão MPG, Coelho HCC, Santos JBJB. Thrombocytopenia in malaria: who cares? Mem Inst Oswaldo Cruz Rio Janeiro 2011;106:52–63. https://doi.org/10.1590/S0074-02762011000900007.

[159] Pain A, Ferguson DJP, Kai O, Urban BC, Lowe B, Marsh K, et al. Platelet-mediated clumping of Plasmodium falciparum-infected erythrocytes is a common adhesive phenotype and is associated with severe malaria. PNAS 2001;98:1805–10.

[160] Mayor A, Hafiz A, Bassat Q, Rovira-Vallbona E, Sanz S, Nia Machevo S, et al. Association of Severe Malaria Outcomes with Platelet- Mediated Clumping and Adhesion to a Novel Host Receptor n.d. https://doi.org/10.1371/journal.pone.0019422.

[161] Morrell CN. Understanding platelets in malaria infection. Curr Opin Hematol 2014;21:445–9. https://doi.org/10.1097/MOH.0000000000000073.

[162] O'Sullivan JM, O'Donnell JS. Platelets in malaria pathogenesis. Platelets and Thrombopoiesis 2018;132:1220–2. https://doi.org/10.1182/blood-2018-07-859959.

[163] Wassmer SC, Taylor T, MacLennan CA, Kanjala M, Mukaka M, Molyneux ME, et al. Platelet-Induced Clumping of *Plasmodium falciparum* –Infected Erythrocytes from Malawian Patients with Cerebral Malaria—Possible Modulation In Vivo by Thrombocytopenia. J Infect Dis 2008;197:72–8. https://doi.org/10.1086/523761.

[164] van der Poll T, Levi M. Crosstalk between inflammation and coagulation: the lessons of sepsis. Curr Vasc Pharmacol 2012;10:632–8.

[165] Cicala C, Cirino G. Linkage between inflammation and coagulation: An update on the molecular basis of the crosstalk. Life Sci 1998. https://doi.org/10.1016/S0024-3205(97)01167-3.

[166] Cirino G, Napoli C, Bucci M, Cicala C. Inflammation-coagulation network: Are serine protease receptors the knot? Trends Pharmacol Sci 2000. https://doi.org/10.1016/S0165-6147(00)01469-3.

[167] Gieseler F, Ungefroren H, Settmacher U, Hollenberg MD, Kaufmann R. Proteinase-activated receptors (PARs) – focus on receptor-receptor-interactions and their physiological and pathophysiological impact. Cell Commun Signal 2013;11:86. https://doi.org/10.1186/1478-811X-11-86.

[168] Foley JH, Conway EM. Cross Talk Pathways between Coagulation and Inflammation. Circ Res 2016;118:1392–408. https://doi.org/10.1161/CIRCRESAHA.116.306853.

[169] Heuberger DM, Schuepbach RA. Protease-activated receptors (PARs):

mechanisms of action and potential therapeutic modulators in PAR-driven inflammatory diseases. Thromb J 2019;17:4. https://doi.org/10.1186/s12959-019-0194-8.

[170] Coughlin SR. Thrombin signalling and protease-activated receptors. Nature 2000;40.

[171] Macfarlane SR, Plevin R. Intracellular Signalling by the G-Protein Coupled Proteinase-Activated Receptor (PAR) Family. Drug Dev Res 2003;59:367–74. https://doi.org/10.1002/ddr.10305.

[172] COUGHLIN SR. Protease-activated receptors in hemostasis, thrombosis and vascular biology. J Thromb Haemost 2005;3:1800–14. https://doi.org/10.1111/j.1538-7836.2005.01377.x.

[173] Even-Ram SC, Grisaru-Granovsky S, Pruss D, Maoz M, Salah Z, Yong-Jun Y, et al. The pattern of expression of protease-activated receptors (PARs) during early trophoblast development. J Pathol 2003;200:47–52. https://doi.org/10.1002/path.1338.

[174] Renna SA, Michael J V., Kong X, Ma L, Ma P, Nieman MT, et al. Human and mouse PAR4 are functionally distinct receptors: Studies in novel humanized mice. J Thromb Haemost 2022;20:1236–47. https://doi.org/10.1111/jth.15669.

[175] Kahn ML, Nakanishi-Matsui M, Shapiro MJ, Ishihara H, Coughlin SR. Protease-activated receptors 1 and 4 mediate activation of human platelets by thrombin. J Clin Invest 1999;103:879–87. https://doi.org/10.1172/JCI6042.

[176] Zhao P, Metcalf M, Bunnett NW. Biased Signaling of Protease-Activated Receptors. Front Endocrinol (Lausanne) 2014;5:67.

https://doi.org/10.3389/fendo.2014.00067.

[177] Siefert SA, Sarkar R. Matrix metalloproteinases in vascular physiology and disease. Vascular 2012;20:210–6. https://doi.org/10.1258/vasc.2011.201202.

[178] Korkmaz B, Horwitz MS, Jenne DE, Gauthier F. Neutrophil elastase, proteinase 3, and cathepsin G as therapeutic targets in human diseases. Pharmacol Rev 2010;62:726–59. https://doi.org/10.1124/pr.110.002733.

[179] Estrada-Gutierrez G, Cappello RE, Mishra N, Romero R, Strauss Iii JF, Walsh SW. Increased Expression of Matrix Metalloproteinase-1 in Systemic Vessels of Preeclamptic Women A Critical Mediator of Vascular Dysfunction. AJPA 2011;178:451–60. https://doi.org/10.1016/j.ajpath.2010.11.003.

[180] Al-Ani B, Hewett PW, Cudmore MJ, Fujisawa T, Saifeddine M, Williams H, et al. Activation of proteinase-activated receptor 2 stimulates soluble vascular endothelial growth factor receptor 1 release via epidermal growth factor receptor transactivation in endothelial cells. Hypertens (Dallas, Tex 1979) 2010;55:689–97. https://doi.org/10.1161/HYPERTENSIONAHA.109.136333.

[181] Sies H, Berndt C, Jones DP. Oxidative Stress. Annu Rev Biochem 2017:715–48. https://doi.org/10.1007/978-3-540-69361-1_27.

[182] Sies H, Jones DP. Reactive oxygen species (ROS) as pleiotropic physiological signalling agents. Nat Rev Mol Cell Biol 2020;21:363–83. https://doi.org/10.1038/s41580-020-0230-3.

[183] Agarwal A, Gupta S, Sharma RK. Role of oxidative stress in female reproduction. Reprod Biol Endocrinol 2005;3:28. https://doi.org/10.1186/1477-7827-3-28.

[184] Sharma L, Shukla G. Placental Malaria: A New Insight into the Pathophysiology.

Front Med 2017;4:1–6. https://doi.org/10.3389/fmed.2017.00117.

[185] Poston L, Raijmakers MTM. Trophoblast Oxidative Stress, Antioxidants and Pregnancy Outcome—A Review. Placenta 2004;25:S72–8. https://doi.org/10.1016/J.PLACENTA.2004.01.003.

[186] Chiarello DI, Abad C, Rojas D, Toledo F, Vázquez CM, Mate A, et al. Oxidative stress: Normal pregnancy versus preeclampsia. Biochim Biophys Acta - Mol Basis Dis 2020;1866:165354. https://doi.org/10.1016/j.bbadis.2018.12.005.

[187] Sharma JB, Sharma A, Bahadur A, Vimala N, Satyam A, Mittal S. Oxidative stress markers and antioxidant levels in normal pregnancy and pre-eclampsia. Int J Gynecol Obstet 2006;94:23–7. https://doi.org/10.1016/j.ijgo.2006.03.025.

[188] Zejnullahu VA, Zejnullahu VA, Kosumi E. The role of oxidative stress in patients with recurrent pregnancy loss: a review. Reprod Health 2021;18:1–12. https://doi.org/10.1186/s12978-021-01257-x.

[189] Wang Y, Branicky R, Noë A, Hekimi S. Superoxide dismutases: Dual roles in controlling ROS damage and regulating ROS signaling. J Cell Biol 2018;217:1915–28. https://doi.org/10.1083/jcb.201708007.

[190] Winterbourn CC. Toxicity of iron and hydrogen peroxide: the Fenton reaction. Toxicol Lett 1995;82–83:969–74. https://doi.org/10.1016/0378-4274(95)03532-X.

[191] Thomas C, Mackey MM, Diaz AA, Cox DP. Hydroxyl radical is produced via the Fenton reaction in submitochondrial particles under oxidative stress: Implications for diseases associated with iron accumulation. Redox Rep 2009;14:102–8. https://doi.org/10.1179/135100009X392566.

[192] Lugrin J, Rosenblatt-Velin N, Parapanov R, Liaudet L. The role of oxidative stress

during inflammatory processes. Biol Chem 2014;395:203–30. https://doi.org/10.1515/hsz-2013-0241.

[193] Winterbourn CC, Kettle AJ, Hampton MB. Reactive Oxygen Species and Neutrophil Function. Annu Rev Biochem 2016;85:765–92. https://doi.org/10.1146/annurev-biochem-060815-014442.

[194] Lauridsen C. From oxidative stress to inflammation: Redox balance and immune system. Poult Sci 2019;98:4240–6. https://doi.org/10.3382/ps/pey407.

[195] Incalza MA, D'Oria R, Natalicchio A, Perrini S, Laviola L, Giorgino F. Oxidative stress and reactive oxygen species in endothelial dysfunction associated with cardiovascular and metabolic diseases. Vascul Pharmacol 2018;100:1–19. https://doi.org/10.1016/J.VPH.2017.05.005.

[196] Raijmakers MTM, Dechend R, Poston L. Oxidative stress and preeclampsia: rationale for antioxidant clinical trials. Hypertens (Dallas, Tex 1979) 2004;44:374–80. https://doi.org/10.1161/01.HYP.0000141085.98320.01.

[197] Percário S, Moreira DR, Gomes BAQ, Ferreira MES, Gonçalves A, Laurindo PSOC, et al. Oxidative Stress in Malaria. Int J Mol Sci Int J Mol Sci 2012;13:16346–72. https://doi.org/10.3390/ijms131216346.

[198] Francis SE, Sullivan DJ, Goldberg DE. Hemoglobin metabolism in the malaria parasite Plasmodium falciparium. Annu Rev Microbiol 1997;51:97–123. https://doi.org/10.1146/annurev.micro.51.1.97.

[199] Coronado LM, Nadovich CT, Spadafora C. Malarial hemozoin: from target to tool. Biochim Biophys Acta 2014;1840:2032–41. https://doi.org/10.1016/j.bbagen.2014.02.009.

[200] Ginsburg H. Some reflections concerning host erythrocyte-malarial parasite interrelationships. Blood Cells 1990:225–35.

[201] Schwarzer E, Alessio M, Ulliers D, Arese P. Phagocytosis of the malarial pigment, hemozoin, impairs expression of major histocompatibility complex class II antigen, CD54, and CD11c in human monocytes. Infect Immun 1998;66:1601–6.

[202] Márcia Boura, Frita R, Góis A, Carvalho T, Hänscheid T. The hemozoin conundrum: is malaria pigment immune-activating, inhibiting, or simply a bystander? Trends Parasitol 2013;29:469–76. https://doi.org/10.1016/j.pt.2013.07.005.

[203] Schwarzer E, Turrini F, Ulliers D, Giribaldi G, Ginsburg H, Arese P. Impairment of macrophage functions after ingestion of plasmodium falciparum-infected erythrocytes or isolated malarial pigment. J Exp Med 1992;176:1033–41. https://doi.org/10.1084/jem.176.4.1033.

[204] Mordmüller P, Arese E, Schwarzer OA, Skorokhod M, Alessio B, Skorokhod OA, et al. Monocyte-Derived Dendritic Cells: A Differentiation and Maturation of Human Hemozoin (Malarial Pigment) Inhibits Hemozoin (Malarial Pigment) Inhibits Differentiation and Maturation of Human Monocyte-Derived Dendritic Cells: A Peroxisome Proliferator-Activ. J Immunol Ref 2004;173:4066–74. https://doi.org/10.4049/jimmunol.173.6.4066.

[205] Skorokhod OA, Barrera V, Heller R, Carta F, Turrini F, Arese P, et al. Malarial pigment hemozoin impairs chemotactic motility and transendothelial migration of monocytes via 4-hydroxynonenal. Free Radic Biol Med 2014;75:210–21. https://doi.org/10.1016/J.FREERADBIOMED.2014.07.004.

[206] Skorokhod OA, Alessio M, Mordmüller B, Arese P, Schwarzer E. Hemozoin (Malarial Pigment) Inhibits Differentiation and Maturation of Human Monocyte-Derived Dendritic Cells: A Peroxisome Proliferator-Activated Receptor-γ-Mediated Effect. J Immunol 2004;173:4066–74. https://doi.org/10.4049/jimmunol.173.6.4066.

[207] Skorokhod O, Schwarzer E, Grune T, Arese P. Role of 4-hydroxynonenal in the hemozoin-mediated inhibition of differentiation of human monocytes to dendritic cells induced by GM-CSF/IL-4. BioFactors 2005;24:283–9. https://doi.org/10.1002/biof.5520240133.

[208] Schwarzer E, Arese P. Phagocytosis of malarial pigment hemozoin inhibits NADPH-oxidase activity in human monocyte-derived macrophages. Biochim Biophys Acta - Mol Basis Dis 1996;1316:169–75. https://doi.org/10.1016/0925-4439(96)00021-X.

[209] Fiori PL, Rappelli P, Mirkarimi SN, Ginsburg H, Cappuccinelli P, Turrini F. Reduced microbicidal and anti-tumour activities of human monocytes after ingestion of Plasmodium falciparum-infected red blood cells. Parasite Immunol 1993;15:647–55. https://doi.org/10.1111/j.1365-3024.1993.tb00579.x.

[210] Pichyangkul S, Saengkrai P, Webster HK, Pichyangkul S, Webster HK. Plasmodium falciparum pigment induces monocytes to release high levels of tumor necrosis factor-alpha and interleukin-1 beta. Am J Trop Med Hyg 1994;51:430–5. https://doi.org/10.4269/ajtmh.1994.51.430.

[211] Prada J, Malinowski J, Müller S, Bienzle U, Kremsner PG. Hemozoin differentially modulates the production of interleukin 6 and tumor necrosis factor

in murine malaria. Eur Cytokine Netw n.d.;6:109–12.

[212] Jaramillo M, Godbout M, Olivier M. Hemozoin induces macrophage chemokine expression through oxidative stress-dependent and -independent mechanisms. J Immunol 2005;174:475–84. https://doi.org/10.4049/JIMMUNOL.174.1.475.

[213] Keller CC, Kremsner PG, Hittner JB, Misukonis MA, Weinberg JB, Perkins DJ. Elevated nitric oxide production in children with malarial anemia: hemozoin-induced nitric oxide synthase type 2 transcripts and nitric oxide in blood mononuclear cells. Infect Immun 2004;72:4868–73. https://doi.org/10.1128/IAI.72.8.4868-4873.2004.

[214] Sherry BA, Alava G, Tracey KJ, Martiney J, Cerami A, Slater AF. Malaria-specific metabolite hemozoin mediates the release of several potent endogenous pyrogens (TNF, MIP-1 alpha, and MIP-1 beta) in vitro, and altered thermoregulation in vivo. J Inflamm 1995;45:85–96.

[215] Skorokhod OA, Schwarzer E, Ceretto M, Arese P. Malarial pigment haemozoin, IFN-gamma, TNF-alpha, IL-1beta and LPS do not stimulate expression of inducible nitric oxide synthase and production of nitric oxide in immuno-purified human monocytes. Malar J 2007;6:73. https://doi.org/10.1186/1475-2875-6-73.

[216] Dalapati T, Moore JM. Hemozoin: a Complex Molecule with Complex Activities. Curr Clin Microbiol Reports 2021;8:87–102. https://doi.org/10.1007/s40588-021-00166-8.

[217] Barrera V, Skorokhod OA, Baci D, Gremo G, Arese P, Schwarzer E. Host fibrinogen stably bound to hemozoin rapidly activates monocytes via TLR-4 and CD11b/CD18-integrin: a new paradigm of hemozoin action 2011;117:5674–82.

https://doi.org/10.1182/blood-2010-10-312413.

[218] Figueiredo RT, Fernandez PL, Mourao-Sa DS, Porto BN, Dutra FF, Alves LS, et al. Characterization of heme as activator of Toll-like receptor 4. J Biol Chem 2007;282:20221–9. https://doi.org/10.1074/jbc.M610737200.

[219] Coban C, Ishii KJ, Kawai T, Hemmi H, Sato S, Uematsu S, et al. Toll-like receptor 9 mediates innate immune activation by the malaria pigment hemozoin. J Exp Med JEM 2005;00:19–25. https://doi.org/10.1084/jem.20041836.

[220] Guleria I, Pollard JW. The trophoblast is a component of the innate immune system during pregnancy. Nat Med 2000;6:589–93. https://doi.org/10.1038/75074.

[221] Haider S, Knöfler M. Human Tumour Necrosis Factor: Physiological and Pathological Roles in Placenta and Endometrium. Placenta 2009;30:111–23.

[222] Barboza R, Lima FA, Reis AS, Murillo OJ, Paula E, Peixoto M, et al. TLR4-Mediated Placental Pathology and Pregnancy Outcome in Experimental Malaria. Sci Rep 2017;7:8623. https://doi.org/10.1038/s41598-017-08299-x.

[223] Dusse LM, Rios DRA, Pinheiro MB, Cooper AJ, Lwaleed BA. Pre-eclampsia: Relationship between coagulation, fibrinolysis and inflammation. Clin Chim Acta 2011;412:17–21. https://doi.org/10.1016/J.CCA.2010.09.030.

[224] Dugina TN, Kiseleva E V., Chistov I V., Umarova BA, Strukova SM. Receptors of the PAR family as a link between blood coagulation and inflammation. Biochemistry (Mosc) 2002;67:65–74. https://doi.org/10.1023/A:1013952114485.

[225] Varo R, Crowley VM, Sitoe A, Madrid L, Serghides L, Kain KC, et al. Adjunctive therapy for severe malaria: A review and critical appraisal. Malar J 2018;17:1–18. https://doi.org/10.1186/s12936-018-2195-7.

[226] Perri G Di, Monteiro GB, Bonora S, Henning C, Cassatella M, Micciolo R, et al. Pentoxifylline as a supportive agent in the treatment of cerebral malaria in children. J Infect Dis 1995:1317–22.

[227] Das BK, Mishra S, Padhi PK, Manish R, Tripathy R, Sahoo PK, et al. Pentoxifylline adjunct improves prognosis of human cerebral malaria in adults. Trop Med Int Heal 2003;8:680–4. https://doi.org/10.1046/j.1365-3156.2003.01087.x.

[228] Van Hensbroek MB, Palmer A, Onyiorah E, Schneider G, Jaffar S, Dolan G, et al. The effect of a monoclonal antibody to tumor necrosis factor on survival from childhood cerebral malaria. J Infect Dis 1996;174:1091–7. https://doi.org/10.1093/infdis/174.5.1091.

[229] Hemmer CJ, Hort G, Chiwakata CB, Seitz R, Egbring R, Gaus W, et al. Supportive pentoxifylline in falciparum malaria: no effect on tumor necrosis factor alpha levels or clinical outcome: a prospective, randomized, placebo-controlled study. Am J Trop Med Hyg 1997;56:349–403.

[230] Lell B, Köhler C, Wamola B, Olola CH, Kivaya E, Kokwaro G, et al. Pentoxifylline as an adjunct therapy in children with cerebral malaria. Malar J 2010;9:2–7. https://doi.org/10.1186/1475-2875-9-368.

[231] Hemmer CJ, Kern P, Holst P, Nawroth P, Dietrich M. Neither heparin nor acetylsalic acid influence the clinical course in human Plasmodium falciparum malaria: a prospective randomized study. Am J Tro 1991;5:608–12.

[232] Leitgeb AM, Charunwatthana P, Rueangveerayut R, Uthaisin C, Silamut K, Chotivanich K, et al. Inhibition of merozoite invasion and transient de-

sequestration by sevuparin in humans with Plasmodium falciparum malaria. PLoS One 2017;12:1–19. https://doi.org/10.1371/journal.pone.0188754.

[233] US Food & Drug Administration (FDA). FDA recommends avoiding use of NSAIDs in pregnancy at 20 weeks or later because they can result in low amniotic fluid 2022.

[234] Gibson PS, Powrie R. Anticoagulants and pregnancy : When are they safe ? Cleve Clin J Med 2009;76:113–27. https://doi.org/10.3949/ccjm.75a.072272.

[235] Mastrolia SA, Mazor M, Holcberg G, Leron E, Beharier O, Loverro G, et al. The physiologic anticoagulant and anti-inflammatory role of heparins and their utility in the prevention of pregnancy complications. Thromb Haemost 2015;113:1236–46. https://doi.org/10.1160/TH14-10-0848.

[236] Knol HM, Schultinge L, Erwich JJHM, Meijer K. Fondaparinux as an alternative anticoagulant therapy during pregnancy. J Thromb Haemost 2010;8:1876–9. https://doi.org/10.1111/j.1538-7836.2010.03926.x.

[237] Bracken T, Cooper C, Ali Z, Truong H, Moore J. Helicobacter Infection Significantly Alters Pregnancy Success in ...: Ingenta Connect. J Am Assoc Lab Anim Sci 2017. https://www.ingentaconnect.com/content/aalas/jaalas/2017/00000056/00000003/art00012%3Bjsessionid=3gpmr08k6rofx.x-ic-live-03# (accessed April 3, 2019).

[238] Jiménez-Díaz MB, Mulet T, Gómez V, Viera S, Alvarez A, Garuti H, et al. Quantitative measurement of plasmodium-infected erythrocytes in murine models of malaria by flow cytometry using bidimensional assessment of SYTO-16 fluorescence. Cytom Part A 2009;75:225–35. https://doi.org/10.1002/cyto.a.20647.

[239] Abatan OI, Welch KB, Nemzek JA. Evaluation of saphenous venipuncture and modified tail-clip blood collection in mice. J Am Assoc Lab Anim Sci 2008;47:8–15.

[240] Bae JS, Yang L, Rezaie AR. Factor X/Xa elicits protective signaling responses in endothelial cells directly via PAR-2 and indirectly via endothelial protein C receptor-dependent recruitment of PAR-1. J Biol Chem 2010;285:34803–12. https://doi.org/10.1074/jbc.M110.163642.

[241] Rao LVM, Esmon CT, Pendurthi UR. Endothelial cell protein C receptor: A multiliganded and multifunctional receptor. Blood 2014;124:1553–62. https://doi.org/10.1182/blood-2014-05-578328.

[242] Li C, Sanni L a, Omer FM, Riley EM, Langhorne J. Pathology and mortality of Plasmodium chabaudi chabaudi infection in IL-10-deficient mice is ameliorated by anti-TNF-[alpha] and exacerbated by anti-TGF-[beta] antibodies. Infect Immun 2003;71:4850–6. https://doi.org/10.1128/IAI.71.9.4850-4856.2003.

[243] Su Z, Stevenson MM. Central role of endogenous gamma interferon in protective immunity against blood-stage Plasmodium chabaudi AS infection. Infect Immun 2000;68:4399–406. https://doi.org/10.1128/IAI.68.8.4399-4406.2000.

[244] Sam H, Su Z, Stevenson MM. Deficiency in Tumor Necrosis Factor Alpha Activity Does Not Impair Early Protective Th1 Responses against Blood-Stage Malaria. Infect Immun 1999;67:2660–4.

[245] Mosnier LO, Zlokovic B V., Griffin JH. The cytoprotective protein C pathway. Blood 2007;109:3161–72. https://doi.org/10.1182/blood-2006-09-003004.

[246] López-Sagaseta J, Montes R, Puy C, Díez N, Fukudome K, Hermida J. Binding of

factor VIIa to the endothelial cell protein C receptor reduces its coagulant activity. J Thromb Haemost 2007;5:1817–24. https://doi.org/10.1111/j.1538-7836.2007.02648.x.

[247] Riewald M, Petrovan RJ, Donner A, Mueller BM, Ruf W. Activation of endothelial cell protease activated receptor 1 by the protein C pathway. Science (80-) 2002;296:1880–2. https://doi.org/10.1126/science.1071699.

[248] Posma JJ, Grover SP, Hisada Y, Iii APO, Antoniak S, Spronk HM, et al. Receptors in Mouse Models of Inflammatory Diseases 2020;39:13–24. https://doi.org/10.1161/ATVBAHA.118.311655.Roles.

[249] Russo G, Curcio F, Bulli G, Aran L, Della-morte D, Testa G, et al. Oxidative Stress and Diseases. Oxidative Stress Dis 2012:757–72. https://doi.org/10.5772/2535.

[250] Pereira AC, Martel F. Oxidative stress in pregnancy and fertility pathologies n.d. https://doi.org/10.1007/s10565-014-9285-2.

[251] Moore TA, Ahmad IM, Zimmerman MC. Oxidative Stress and Preterm Birth : An Integrative Review 2018;20:497–512. https://doi.org/10.1177/1099800418791028.

[252] Li HS, Zhou YN, Li L, Li SF, Long D, Chen XL, et al. HIF-1α protects against oxidative stress by directly targeting mitochondria. Redox Biol 2019;25. https://doi.org/10.1016/j.redox.2019.101109.

[253] Bonello S, Zähringer C, BelAiba RS, Djordjevic T, Hess J, Michiels C, et al. Reactive oxygen species activate the HIF-1α promoter via a functional NFκB site. Arterioscler Thromb Vasc Biol 2007;27:755–61. https://doi.org/10.1161/01.ATV.0000258979.92828.bc.

[254] Vomund S, Schäfer A, Parnham MJ, Brüne B, Von Knethen A. Nrf2, the master regulator of anti-oxidative responses. Int J Mol Sci 2017;18:1–19. https://doi.org/10.3390/ijms18122772.

[255] Cadet J, Ravanat JL, TavernaPorro M, Menoni H, Angelov D. Oxidatively generated complex DNA damage: Tandem and clustered lesions. Cancer Lett 2012;327:5–15. https://doi.org/10.1016/j.canlet.2012.04.005.

[256] Dixon SJ, Stockwell BR. The role of iron and reactive oxygen species in cell death. Nat Chem Biol 2014;10:9–17. https://doi.org/10.1038/nchembio.1416.

[257] Redza-Dutordoir M, Averill-Bates DA. Activation of apoptosis signalling pathways by reactive oxygen species. Biochim Biophys Acta - Mol Cell Res 2016;1863:2977–92. https://doi.org/10.1016/j.bbamcr.2016.09.012.

[258] Benhar M. Oxidants, Antioxidants and Thiol Redox Switches in the Control of Regulated Cell Death Pathways. Antioxidants 2020;9:309. https://doi.org/10.3390/antiox9040309.

[259] Banerjee R. Redox outside the box: Linking extracellular redox remodeling with intracellular redox metabolism. J Biol Chem 2012;287:4397–402. https://doi.org/10.1074/jbc.R111.287995.

[260] Tang D, Kang R, Berghe T Vanden, Vandenabeele P, Kroemer G. The molecular machinery of regulated cell death. Cell Res 2019;29:347–64. https://doi.org/10.1038/s41422-019-0164-5.

[261] Tang D, Chen X, Kang R, Kroemer G. Ferroptosis: molecular mechanisms and health implications. Cell Res 2020. https://doi.org/10.1038/s41422-020-00441-1.

[262] Murphy MP. How mitochondria produce reactive oxygen species. Biochem J

2009;417:1–13. https://doi.org/10.1042/BJ20081386.

[263] Palma FR, He C, Danes JM, Paviani V, Coelho DR, Gantner BN, et al. Mitochondrial Superoxide Dismutase: What the Established, the Intriguing, and the Novel Reveal about a Key Cellular Redox Switch. Antioxidants Redox Signal 2020;32:701–14. https://doi.org/10.1089/ars.2019.7962.

[264] Cho KJ, Seo JM, Kim JH. Bioactive lipoxygenase metabolites stimulation of NADPH oxidases and reactive oxygen species. Mol Cells 2011;32:1–5. https://doi.org/10.1007/s10059-011-1021-7.

[265] Smith WL, Murphy RC. The Eicosanoids: Cyclooxygenase, Lipoxygenase and Epoxygenase Pathways. Sixth Edit. Elsevier; 2015. https://doi.org/10.1016/B978-0-444-63438-2.00009-2.

[266] Yang WS, Stockwell BR. Ferroptosis: Death by Lipid Peroxidation. Trends Cell Biol 2016;26:165–76. https://doi.org/10.1016/j.tcb.2015.10.014.

[267] Gaschler MM, Stockwell BR. Lipid peroxidation in cell death. Biochem Biophys Res Commun 2017;482:419–25. https://doi.org/10.1016/j.bbrc.2016.10.086.

[268] Yang WS, Kim KJ, Gaschler MM, Patel M, Shchepinov MS, Stockwell BR. Peroxidation of polyunsaturated fatty acids by lipoxygenases drives ferroptosis. Proc Natl Acad Sci U S A 2016;113:E4966–75. https://doi.org/10.1073/pnas.1603244113.

[269] Kuang F, Liu J, Tang D, Kang R. Oxidative Damage and Antioxidant Defense in Ferroptosis. Front Cell Dev Biol 2020;8:1–10. https://doi.org/10.3389/fcell.2020.586578.

[270] Kajiwara K, Beharier O, Chng C-P, Goff JP, Ouyang Y, St Croix CM, et al.

Ferroptosis induces membrane blebbing in placental trophoblasts. J Cell Sci 2021;135. https://doi.org/10.1242/jcs.255737.

[271] Zhang Y, Hu M, Zhang Y, Hu M, Jia W, Liu G, et al. Hyperandrogenism and insulin resistance modulate gravid uterine and placental ferroptosis in PCOS-like rats n.d.

[272] Wang H, An P, Xie E, Wu Q, Fang X, Gao H, et al. Characterization of ferroptosis in murine models of hemochromatosis. Hepatology 2017;66:449–65. https://doi.org/10.1002/hep.29117.

[273] Beharier O, Tyurin VA, Goff JP, Guerrero-Santoro J, Kajiwara K, Chu T, et al. PLA2G6 guards placental trophoblasts against ferroptotic injury. Proc Natl Acad Sci U S A 2020;117:27319–28. https://doi.org/10.1073/pnas.2009201117.

[274] Ng SW, Norwitz SG, Norwitz ER. The impact of iron overload and ferroptosis on reproductive disorders in humans: Implications for preeclampsia. Int J Mol Sci 2019;20. https://doi.org/10.3390/ijms20133283.

[275] Zhang H, He Y, Wang J xia, Chen M hua, Xu J juan, Jiang M hui, et al. miR-30-5p-mediated ferroptosis of trophoblasts is implicated in the pathogenesis of preeclampsia. Redox Biol 2020;29:101402. https://doi.org/10.1016/j.redox.2019.101402.

[276] Toldi G, Stenczer B, Molvarec A, Takáts Z, Beko G, Rigó J, et al. Hepcidin concentrations and iron homeostasis in preeclampsia. Clin Chem Lab Med 2010;48:1423–6. https://doi.org/10.1515/CCLM.2010.290.

[277] Erlandsson L, Masoumi Z, Hansson LR, Hansson SR, Toldi G, Stenczer B, et al. The roles of free iron, heme, haemoglobin, and the scavenger proteins haemopexin

and alpha-1-microglobulin in preeclampsia and fetal growth restriction. J Intern Med 2021;48:1423–6. https://doi.org/10.1515/CCLM.2010.290.

[278] Nti AM, Botchway F, Salifu H, Cespedes JC, Harbuzariu A, Onyekaba J, et al. Effects of iron supplements on heme scavengers in pregnancy. Am J Trop Med Hyg 2021;105:1163–72. https://doi.org/10.4269/ajtmh.20-0413.

[279] Mégier C, Peoc'h K, Puy V, Cordier AG. Iron Metabolism in Normal and Pathological Pregnancies and Fetal Consequences. Metabolites 2022;12. https://doi.org/10.3390/metabo12020129.

[280] Liu M, Hassana S, Stiles JK. Heme-mediated apoptosis and fusion damage in BeWo trophoblast cells. Sci Rep 2016;6:1–12. https://doi.org/10.1038/srep36193.

[281] Ferreira A, Balla J, Jeney V, Balla G, Soares MP. A central role for free heme in the pathogenesis of severe malaria: The missing link? J Mol Med 2008;86:1097–111. https://doi.org/10.1007/s00109-008-0368-5.

[282] Naveenkumar SK, Sharathbabu BN, Hemshekhar M, Kemparaju K, Girish KS, Mugesh G. The Role of Reactive Oxygen Species and Ferroptosis in Heme-Mediated Activation of Human Platelets. ACS Chem Biol 2018;13:1996–2002. https://doi.org/10.1021/acschembio.8b00458.

[283] McGready R, Brockman A, Cho T, Levesque MA, Tkachuk AN, Meshnick SR, et al. Haemozoin as a marker of placental parasitization. Trans R Soc Trop Med Hyg 2002;96:644–6. https://doi.org/10.1016/S0035-9203(02)90339-1.

[284] Sullivan AD, Nyirenda T, Cullinan T, Taylor T, Lau A, Meshnick SR. Placental haemozoin and malaria in pregnancy. Placenta 2000;21:417–21. https://doi.org/10.1053/plac.1999.0479.

[285] McGready R, Lee SJ, Wiladphaingern J, Ashley EA, Rijken MJ, Boel M, et al. Adverse effects of falciparum and vivax malaria and the safety of antimalarial treatment in early pregnancy: A population-based study. Lancet Infect Dis 2012;12:388–96. https://doi.org/10.1016/S1473-3099(11)70339-5.

[286] Morffy Smith CD, Russ BN, Andrew AK, Cooper CA, Moore JM. A novel murine model for assessing fetal and birth outcomes following transgestational maternal malaria infection. Sci Rep 2019;9:1–16. https://doi.org/10.1038/s41598-019-55588-8.

[287] O'Donnell AJ, Mideo N, Reece SE. Disrupting rhythms in Plasmodium chabaudi: Costs accrue quickly and independently of how infections are initiated. Malar J 2014;13:1–9. https://doi.org/10.1186/1475-2875-13-503.

[288] O'Donnell AJ, Schneider P, McWatters HG, Reece SE. Fitness costs of disrupting circadian rhythms in malaria parasites. Proc R Soc B Biol Sci 2011;278:2429–36. https://doi.org/10.1098/rspb.2010.2457.

[289] Drewlo S, Levytska K, Kingdom J. Revisiting the housekeeping genes of human placental development and insufficiency syndromes. Placenta 2012;33:952–4. https://doi.org/10.1016/j.placenta.2012.09.007.

[290] Lanoix D, Lacasse A, St-Pierre J, Taylor SC, Ethier-Chiasson M, Lafond J, et al. Quantitative PCR Pitfalls: The case of the human placenta. Mol Biotechnol 2012;52:234–43. https://doi.org/10.1007/s12033-012-9539-2.

[291] Sarr D, Oliveira LJ, Russ BN, Owino SO, Middii JD, Mwalimu S, et al. Myeloperoxidase and Other Markers of Neutrophil Activation Associate With Malaria and Malaria/HIV Coinfection in the Human Placenta. Front Immunol

2021;12:1–19. https://doi.org/10.3389/fimmu.2021.682668.

[292] Holden P, Nair LS. Deferoxamine: An Angiogenic and Antioxidant Molecule for Tissue Regeneration. Tissue Eng - Part B Rev 2019;25:461–70. https://doi.org/10.1089/ten.teb.2019.0111.

[293] Hershko C, Konijn AM, Nick HP, Breuer W, Cabantchik ZI, Link G. ICL670A: A new synthetic oral chelator: Evaluation in hypertransfused rats with selective radioiron probes of hepatocellular and reticuloendothelial iron stores and in iron-loaded rat heart cells in culture. Blood 2001;97:1115–22. https://doi.org/10.1182/blood.V97.4.1115.

[294] Xu J, Sun T, Zhong R, You C, Tian M. PEGylation of Deferoxamine for Improving the Stability, Cytotoxicity, and Iron-Overload in an Experimental Stroke Model in Rats. Front Bioeng Biotechnol 2020;8:1–13. https://doi.org/10.3389/fbioe.2020.592294.

[295] White NJ. Anaemia and Malaria. Malar J 2018;17:1–17. https://doi.org/10.1186/s12936-018-2509-9.

[296] Linkermann A, Skouta R, Himmerkus N, Mulay SR, Dewitz C, De Zen F, et al. Synchronized renal tubular cell death involves ferroptosis. Proc Natl Acad Sci U S A 2014;111:16836–41. https://doi.org/10.1073/pnas.1415518111.

[297] Zhang Y, Sun C, Zhao C, Hao J, Zhang Y, Fan B, et al. Ferroptosis inhibitor SRS 16-86 attenuates ferroptosis and promotes functional recovery in contusion spinal cord injury. Brain Res 2019;1706:48–57. https://doi.org/10.1016/j.brainres.2018.10.023.

[298] Tait WGS, Douglas RG. Mitochondrial Regulation of Cell Death. Cold Spring

Harb Perspect Biol 2013.

[299] Wu H, Wang F, Ta N, Zhang T, Gao W. The multifaceted regulation of mitochondria in ferroptosis. Life 2021;11:1–24. https://doi.org/10.3390/life11030222.

[300] Gao M, Yi J, Zhu J, Minikes AM, Monian P, Thompson CB, et al. Role of Mitochondria in Ferroptosis. Mol Cell 2019;73:354-363.e3. https://doi.org/10.1016/j.molcel.2018.10.042.

[301] Gan B. Mitochondrial regulation of ferroptosis. J Cell Biol 2021;220:1–10. https://doi.org/10.1083/jcb.202105043.

[302] Fisher JJ, Vanderpeet CL, Bartho LA, McKeating DR, Cuffe JSM, Holland OJ, et al. Mitochondrial dysfunction in placental trophoblast cells experiencing gestational diabetes mellitus. J Physiol 2021;599:1291–305. https://doi.org/10.1113/JP280593.

[303] Fisher JJ, Bartho LA, Perkins A V., Holland OJ. Placental mitochondria and reactive oxygen species in the physiology and pathophysiology of pregnancy. Clin Exp Pharmacol Physiol 2020;47:176–84. https://doi.org/10.1111/1440-1681.13172.

[304] Trnka J, Blaikie FH, Smith RAJ, Murphy MP. A mitochondria-targeted nitroxide is reduced to its hydroxylamine by ubiquinol in mitochondria. Free Radic Biol Med 2008;44:1406–19. https://doi.org/10.1016/j.freeradbiomed.2007.12.036.

[305] Tsafack A, Loyevsky M, Ponka P, Cabantchik ZI. Mode of action of iron (III) chelators as antimalarials. IV. Potentiation of desferal action by benzoyl and isonicotinoyl hydrazone derivatives. J Lab Clin Med 1996;127:574–82.

https://doi.org/10.1016/S0022-2143(96)90148-1.

[306] Loyevsky M, Lytton SD, Mester B, Libman J, Shanzer A, Cabantchik ZI. The antimalarial action of desferal involves a direct access route to erythrocytic (Plasmodium falciparum) parasites. J Clin Invest 1993;91:218–24. https://doi.org/10.1172/JCI116174.

[307] Hershko C, Peto TEA. Deferoxamine inhibition of malaria is independent of host iron status. J Exp Med 1988;168:375–87. https://doi.org/10.1084/jem.168.1.375.

[308] Reeder BJ, Wilson MT. Desferrioxamine inhibits production of cytotoxic heme to protein cross-linked myoglobin: A mechanism to protect against oxidative stress without iron chelation. Chem Res Toxicol 2005;18:1004–11. https://doi.org/10.1021/tx049660y.

[309] Hartley A, Davies M, Rice-Evans C. Desferrioxamine as a lipid chain-breaking antioxidant in sickle erythrocyte membranes. FEBS Lett 1990;264:145–8. https://doi.org/10.1016/0014-5793(90)80786-I.

[310] Vippagunta SR, Dorn A, Bubendorf A, Ridley RG, Vennerstrom JL. Deferoxamine: Stimulation of hematin polymerization and antagonism of its inhibition by chloroquine. Biochem Pharmacol 1999;58:817–24. https://doi.org/10.1016/S0006-2952(99)00161-6.

[311] Beeson JG, Amin N, Kanjala M, Rogerson SJ. Selective accumulation of mature asexual stages of Plasmodium falciparum-infected erythrocytes in the placenta. Infect Immun 2002;70:5412–5. https://doi.org/10.1128/IAI.70.10.5412-5415.2002.

[312] Ismail MR, Ordi J, Menendez C, Ventura PJ, Aponte JJ, Kahigwa E, et al. Placental Pathology in Malara: A Histological, Immunohistochemical, and

Quantitative Study 2000;31:85–93. https://doi.org/10.1016/S0046-8177(00)80203-8.

[313] WHO. World Malaria Report. https://www.who.int/malaria. 2019.

[314] Fried M, Kurtis JD, Swihart B, Pond-tor S, Barry A, Gaoussou S, et al. Systemic inflammatory response to malaria during pregnancy is associated with pregnancy loss and preterm delivery. Clin Infect Dis 2017;65. https://doi.org/10.1093/cid/cix623/3980252/Systemic-inflammatory-response-to-malaria-during.

[315] Rogerson SJ, Hviid L, Duffy PE, Leke RF, Taylor DW. Malaria in pregnancy: pathogenesis and immunity. Lancet Infect Dis 2007;7:105–17. https://doi.org/10.1016/S1473-3099(07)70022-1.

[316] Tiyong Ifoue SH, Teugwa Mofor C, Gouado I, Teto G, Asonganyi T, Amvam Zollo PH. Evaluation of oxidative stress and antioxidant status of pregnant women suffering from malaria in Cameroon. Indian J Clin Biochem 2009;24:288–93. https://doi.org/10.1007/s12291-009-0054-6.

[317] Reis AS, Barboza R, Murillo O, Barateiro A, Peixoto EPM, Lima FA, et al. Inflammasome activation and IL-1 signaling during placental malaria induce poor pregnancy outcomes. Sci Adv 2020;6:eaax6346. https://doi.org/10.1126/sciadv.aax6346.

[318] Sharma L, Shukla G. Treatment of pregnant BALB/c mice with sulphadoxine pyrimethamine or chloroquine abrogates Plasmodium berghei induced placental pathology. Parasitol Int 2014;63:49–56. https://doi.org/10.1016/j.parint.2013.08.016.

[319] Cottrell G, Mary JY, Barro D, Cot M. The importance of the period of malarial infection during pregnancy on birth weight in tropical Africa. Am J Trop Med Hyg 2007;76:849–54. https://doi.org/10.4269/ajtmh.2007.76.849.

[320] Huynh B, Fievet N, Gbaguidi G, Dechavanne S, Borgella S, Guézo-mévo B, et al. Influence of the Timing of Malaria Infection during Pregnancy on Birth Weight and on Maternal Anemia in Benin 2011;85:214–20. https://doi.org/10.4269/ajtmh.2011.11-0103.

[321] Kalilani-Phiri L, Thesing PC, Nyirenda OM, Mawindo P, Madanitsa M, Membe G, et al. Timing of Malaria Infection during Pregnancy Has Characteristic Maternal, Infant and Placental Outcomes. PLoS One 2013;8:1–8. https://doi.org/10.1371/journal.pone.0074643.

[322] Kalilani L, Mofolo I, Chaponda M, Rogerson SJ, Meshnick SR. The effect of timing and frequency of Plasmodium falciparum infection during pregnancy on the risk of low birth weight and maternal anemia. Trans R Soc Trop Med Hyg 2010;104:416–22. https://doi.org/10.1016/j.trstmh.2010.01.013.

[323] Valea I, Tinto H, Drabo MK, Huybregts L, Sorgho H, Ouedraogo J, et al. An analysis of timing and frequency of malaria infection during pregnancy in relation to the risk of low birth weight , anaemia and perinatal mortality in Burkina Faso 2012:1–7.

[324] Moore KA, Simpson JA, Wiladphaingern J, Min AM, Pimanpanarak M, Paw MK, et al. Influence of the number and timing of malaria episodes during pregnancy on prematurity and small-for-gestational-age in an area of low transmission. BMC Med 2017;15. https://doi.org/10.1186/s12916-017-0877-6.

[325] Rijken MJ, Papageorghiou AT, Thiptharakun S, Kiricharoen S, Dwell SLM, Wiladphaingern J, et al. Ultrasound evidence of early fetal growth restriction after maternal malaria infection. PLoS One 2012;7:1–8. https://doi.org/10.1371/journal.pone.0031411.

[326] Gutman J, Kalilani L, Taylor S, Zhou Z, Wiegand RE, Thwai KL, et al. The A581G mutation in the gene encoding plasmodium falciparum dihydropteroate synthetase reduces the effectiveness of sulfadoxine-pyrimethamine preventive therapy in malawian pregnant women. J Infect Dis 2015;211:1997–2005. https://doi.org/10.1093/infdis/jiu836.

[327] Soncin F, Khater M, To C, Pizzo D, Farah O, Wakeland A, et al. Comparative analysis of mouse and human placentae across gestation reveals species-specific regulators of placental development. Dev 2018;145. https://doi.org/10.1242/dev.156273.

[328] Doritchamou J, Bertin G, Moussiliou A, Bigey P, Viwami F, Ezinmegnon S, et al. First-trimester plasmodium falciparum infections display a typical placental phenotype. J Infect Dis 2012;206:1911–9. https://doi.org/10.1093/infdis/jis629.

[329] Doritchamou J, Sossou-tchatcha S, Cottrell G, Moussiliou A, Hounton Houngbeme C, Massougbodji A, et al. Dynamics in the cytoadherence phenotypes of Plasmodium falciparum infected erythrocytes isolated during pregnancy. PLoS One 2014;9. https://doi.org/10.1371/journal.pone.0098577.

[330] Ishikawa H, Seki R, Yokonishi S, Yamauchi T, Yokoyama K. Relationship between fetal weight, placental growth and litter size in mice from mid- to late-gestation. Reprod Toxicol 2006;21:267–70.

https://doi.org/10.1016/j.reprotox.2005.08.002.

[331] Romero R, Dey SK, Fisher SJ. Preterm labor: one syndrome, many causes. Science 2014;345:760–5. https://doi.org/10.1126/science.1251816.

[332] Argik JM, Carb6 N, L6pez-Soriano FJ. TNF and Pregnancy: the Paradigm of a Complex Interaction n.d.:181–7.

[333] Romero R, Mazor M, Sepulveda W, Avila C, Copeland D, Williams J. Tumor necrosis factor in preterm and term labor. Am J Obstet Gynecol 1992;166:1576–87.

[334] WHO. Updated WHO policy recommendation: intermittent preventive treatment of malaria in pregnancy using sulfadoxine-pyrimethamine (IPTp-SP). 2012.

[335] Rogerson SJ, Desai M, Mayor A, Sicuri E, Taylor SM, Van Eijk AM, et al. Burden, pathology, and costs of malaria in pregnancy: new developments for an old problem. Lancet Infect Dis 2018;18:e107–18. https://doi.org/10.1016/S1473-3099(18)30066-5.

[336] Loftin CD, Tiano HF, Langenbach R. Phenotypes of the COX-deficient mice indicate physiological and pathophysiological roles for COX-1 and COX-2. Prostaglandins Other Lipid Mediat 2002;68–69:177–85. https://doi.org/10.1016/S0090-6980(02)00028-X.

[337] Loudon JAZ, Groom KM, Bennett PR. Prostaglandin inhibitors in preterm labour. Best Pract Res Clin Obstet Gynaecol 2003;17:731–44. https://doi.org/10.1016/S1521-6934(03)00047-6.

[338] Sena-Dos-Santos C, Braga-da-Silva C, Marques D, Azevedo Dos Santos Pinheiro J, Ribeiro-Dos-Santos Â, Cavalcante GC. Unraveling Cell Death Pathways during

Malaria Infection: What Do We Know So Far? Cells 2021;10:1–29. https://doi.org/10.3390/cells10020479.

[339] Salifu H, Wilson NO, Liu M, Dickinson-copeland C, Keenan J, Turpin C, et al. (HO-1) Levels In Pregnant Women in Ghana 2017;4.

[340] Penha-GonÃ§alves C, Gozzelino R, de Moraes L V. Iron overload in Plasmodium berghei-infected placenta as a pathogenesis mechanism of fetal death. Front Pharmacol 2014;5:155. https://doi.org/10.3389/fphar.2014.00155.

[341] Ngai M, Weckman AM, Erice C, McDonald CR, Cahill LS, Sled JG, et al. Malaria in Pregnancy and Adverse Birth Outcomes: New Mechanisms and Therapeutic Opportunities. Trends Parasitol 2020;36:127–37. https://doi.org/10.1016/j.pt.2019.12.005.

[342] George EM, Granger JP. Heme oxygenase in pregnancy and preeclampsia. Curr Opin Nephrol Hypertens 2013;22:156–62. https://doi.org/10.1097/MNH.0b013e32835d19f7.

[343] McDonald CR, Tran V, Kain KC. Complement activation in placental malaria. Front Microbiol 2015;6:1–9. https://doi.org/10.3389/fmicb.2015.01460.

[344] Mcdonald CR, Cahill LS, Gamble JR, Elphinstone R, Gazdzinski LM, Zhong KJY, et al. Malaria in pregnancy alters L -arginine bioavailability and placental vascular development n.d.:1–14.

[345] Megnekou R, Tenou S, Bigoga JD, Djontu JC, Medou FM, Lissom A. Placental malaria and modulation of immune and hormonal responses in Cameroonian women. Acta Trop 2015;147:23–30. https://doi.org/10.1016/j.actatropica.2015.04.001.

[346] Fontes KN, Reginatto MW, Silva NL, Andrade CB V, Bloise FF. Dysregulation of placental ABC transporters in a murine model of malaria-induced preterm labor. Sci Rep 2019:1–13. https://doi.org/10.1038/s41598-019-47865-3.

[347] Singh PP, Bhandari S, Sharma RK, Singh N, Bharti PK. Association of angiopoietin dysregulation in placental malaria with adverse birth outcomes. Dis Markers 2020;2020. https://doi.org/10.1155/2020/6163487.

[348] Lima FA, Barateiro A, Dombrowski JG, de Souza RM, de Sousa Costa D, Murillo O, et al. Plasmodium falciparum infection dysregulates placental autophagy. PLoS One 2019;14:1–15. https://doi.org/10.1371/journal.pone.0226117.

[349] Dimasuay KG, Gong L, Rosario F, McBryde E, Spelman T, Glazier J, et al. Impaired placental autophagy in placental malaria. PLoS One 2017;12. https://doi.org/10.1371/journal.pone.0187291.

[350] Elphinstone RE, Weckman AM, McDonald CR, Tran V, Zhong K, Madanitsa M, et al. Early malaria infection, dysregulation of angiogenesis, metabolism and inflammation across pregnancy, and risk of preterm birth in Malawi: A cohort study. PLoS Med 2019;16:1–21. https://doi.org/10.1371/journal.pmed.1002914.

[351] Schmidt A, Morales-Prieto DM, Pastuschek J, Fröhlich K. Only humans have human placentas: molecular differences between mice and humans. J Reprod Immunol 2015;108:65–71. https://doi.org/10.1016/J.JRI.2015.03.001.

[352] Hemberger M, Hanna CW, Dean W. Mechanisms of early placental development in mouse and humans. Nat Rev Genet 2020;21:27–43. https://doi.org/10.1038/s41576-019-0169-4.

[353] Carter AM. Alternatives To the Mouse. Reproduction 2021;160:1470–626.

[354] Dorman EK, Shulman CE, Kingdom J, Bulmer JN, Mwendwa J, Peshu N, et al. Impaired uteroplacental blood flow in pregnancies complicated by falciparum malaria. Ultrasound Obstet Gynecol 2002;19:165–70. https://doi.org/10.1046/j.0960-7692.2001.00545.x.

[355] Chen X, Li J, Kang R, Klionsky DJ, Tang D. Ferroptosis: machinery and regulation. Autophagy 2021;17:2054–81. https://doi.org/10.1080/15548627.2020.1810918.